MASARYK UNIVERSITY

FACULTY OF SCIENCE

DEVELOPMENT OF NON-THERMAL PLASMA SOURCES FOR FAST PLASMA TREATMENT OF MATERIALS: DIAGNOSTICS AND APPLICATIONS

HABILITATION THESIS

JAN ČECH

DEPARTMENT OF PLASMA PHYSICS AND TECHNOLOGY

BRNO 2025

MUNI
SCI

Bibliographic record

Author: Jan Čech
Faculty of Science
Masaryk University
Department of Plasma Physics and Technology

Title of Thesis: Development of Non-thermal Plasma Sources for Fast Plasma Treatment of Materials: Diagnostics and Applications

Year: 2025

Number of Pages: x+71

Keywords: DCSBD, dielectric barrier discharge, CaviPlasma, cavitation, water, diagnostics, ICCD, phase-resolved, spatially resolved, optical emission spectroscopy, applications

Abstract

The habilitation thesis presents nearly 20 years of the author's research focused on the development, diagnostics, and applications of non-equilibrium discharges at the Department of Plasma Physics and Technology at Masaryk University (DPPT). The thesis is designed as a commentary on annotated scientific papers. The thesis addresses two technologically significant plasma sources developed for fast and efficient treatment of materials. It is divided into two major parts: the first part commenting on the Diffuse Coplanar Surface Barrier Discharge (DCSBD) used for surface modification of temperature-sensitive materials, and the second part addressing the novel CaviPlasma® technology for large-volume plasma treatment of liquids. The commentary to the selected scientific papers presents the author's contribution to the research and development of DCSBD (and generally coplanar dielectric barrier discharges) and CaviPlasma. The presented discharge diagnostics are based primarily on optical emission diagnostics utilising CCD, intensified gated CCD cameras, and correlated current-voltage measurements. In the commentary, the diagnostic articles are also complemented by the applications of DCSBD and CaviPlasma that the author investigated.

Acknowledgements

I want to express my gratitude to my family and especially to my wife Petra for her support, which accompanied my professional effort presented in this thesis.

I want to thank all the people from our department and all the institutions with whom I have had the chance to collaborate throughout my career so far.

My special thanks go to my supervisors and consultants for their invaluable help, advice and support: Prof. Mirko Černák, Prof. David Trunec, and Assoc. Prof. Pavel Sťahel, Assoc. Prof. Jozef Ráheľ and Assoc. Prof. Zdeněk Navrátil. My very personal thanks go to Assoc. Prof. Antonín Brablec, an eternal optimist, colleague, office mate and friend, who passed away unexpectedly in June 2022. Thanks to them, I spent a fruitful 15 years of barrier discharges research touching many aspects of plasma research – the construction and development of plasma sources, which includes design iterations, dielectric barrier influence, electric insulation challenges, and many more practical aspects of applied research wizardry. In this way, I could learn from the best atmospheric pressure plasma treatment practice, follow the evolution of discharge design and acquire the skills in discharge diagnostics.

The last 7 years of my professional career were associated with CaviPlasma research, and my warm thanks go to colleagues from the CaviPlasma team at Brno University of Technology, led by Assoc. Prof. Pavel Rudolf, Institute of Botany of the Czech Academy of Sciences, led by Prof. Blahoslav Maršálek and the members of the Applied Plasmachemistry group at Masaryk University, for outstanding collaboration on this fascinating topic. Being part of the CaviPlasma discovery and development has probably been a once-in-a-lifetime experience.

And above all, I thank God for everything He has given me.

Table of Contents

List of Annotated Papers

For the habilitation thesis, I have selected two sets of research articles dedicated to the research of Diffuse Coplanar Surface Barrier Discharge (DCSBD) and coplanar barrier discharges, respectively and CaviPlasma. The list of publications is ordered according to their appearance in the thesis, and citations of the annotated papers in the text are distinguished by **blue boldface type**. The annotated papers were selected and sorted to comprehensively overview the author's involvement in the DCSBD/coplanar barrier discharge and CaviPlasma research and development at the Department of Plasma Physics and Technology (former Department of Physical Electronics), Masaryk University.

The author's contribution to annotated papers is estimated in terms of content and quality in the respective tables and the list below.

i) DCSBD-related papers:

[1] CECH, Jan*(corresponding author)*, Pavel STAHEL, Zdenek NAVRATIL and Mirko CERNAK, 2008. Space and Time Resolved Optical Emission Spectroscopy of Diffuse Coplanar Barrier Discharge in Nitrogen. *Chemicke Listy*. **102**(S4), S1348-S1351. ISSN 1213-7103.

Experimental work (%)	Supervision[1] (%)	Manuscript (%)	Research direction (%)
30	--	30	25

[2] CECH, J.*(corresponding author)*, P. STAHEL and Z. NAVRATIL, 2009. The influence of electrode gap width on plasma properties of diffuse coplanar surface barrier discharge in nitrogen. *European Physical Journal D* [online]. **54**(2), 259–264. ISSN 1434-6079. Available at: doi:10.1140/epjd/e2009-00013-1

Experimental work (%)	Supervision (%)	Manuscript (%)	Research direction (%)
60	--	50	35

[3] CECH, Jan*(corresponding author)*, Jana HANUSOVA, Pavel ST'AHEL and Mirko CERNAK, 2015. Diffuse Coplanar Surface Barrier Discharge in Artificial Air: Statistical Behaviour of Microdischarges. *Open Chemistry* [online]. **13**(1), 528–540. ISSN 2391-5420. Available at: doi:10.1515/chem-2015-0062

Experimental work (%)	Supervision (%)	Manuscript (%)	Research direction (%)
60	75	75	70

[1] The category ‚Supervision' represents the supervision of students and is enumerated, where applicable.

[4] RAHEL, Jozef, Zsolt SZALAY, **Jan CECH** and Tomas MORAVEK, 2016. On spatial stabilization of dielectric barrier discharge microfilaments by residual heat build-up in air. *European Physical Journal D* [online]. **70**(4, Article 92). ISSN 1434-6079. Available at: doi:10.1140/epjd/e2016-70061-5

Experimental work (%)	Supervision (%)	Manuscript (%)	Research direction (%)
25	--	15	15

[5] MORAVEK, Tomas, **Jan CECH**, Zdenek NAVRATIL and Jozef RAHEL, 2016. Pre-breakdown phase of coplanar dielectric barrier discharge in helium. *European Physical Journal-Applied Physics* [online]. **75**(2, Article 24706). ISSN 1286-0050. Available at: doi:10.1051/epjap/2016150538

Experimental work (%)	Supervision (%)	Manuscript (%)	Research direction (%)
30	25	25	30

[6] NAVRATIL, Zdenek, Tomas MORAVEK, Jozef RAHEL, **Jan CECH**, Ondrej LALINSKY and David TRUNEC, 2017. Diagnostics of pre-breakdown light emission in a helium coplanar barrier discharge: the presence of neutral bremsstrahlung. *Plasma Sources Science & Technology* [online]. **26**(5, Article 055025). ISSN 1361-6595. Available at: doi:10.1088/1361-6595/aa66b5

Experimental work (%)	Supervision (%)	Manuscript (%)	Research direction (%)
15	15	15	15

[7] **CECH, Jan*(corresponding author)***, Zdenek NAVRATIL, Michal STIPL, Tomas MORAVEK and Jozef RAHEL, 2018. 2D-resolved electric field development in helium coplanar DBD: spectrally filtered ICCD camera approach. *Plasma Sources Science & Technology* [online]. **27**(10, Article 105002). ISSN 1361-6595. Available at: doi:10.1088/1361-6595/aade41

Experimental work (%)	Supervision (%)	Manuscript (%)	Research direction (%)
50	75	50	50

[8] PRYSIAZHNYI, V., A. BRABLEC, **J. CECH**, M. STUPAVSKA and M. CERNAK, 2014. Generation of Large-Area Highly-Nonequlibrium Plasma in Pure Hydrogen at Atmospheric Pressure. *Contributions to Plasma Physics* [online]. **54**(2), 138–144. ISSN 1521-3986. Available at: doi:10.1002/ctpp.201310060

Experimental work (%)	Supervision (%)	Manuscript (%)	Research direction (%)
15	--	20	15

[9] KROMKA, Alexander, **Jan CECH**, Halyna KOZAK, Anna ARTEMENKO, Tibor IZAK, Jan CERMAK, Bohuslav REZEK and Mirko CERNAK, 2015. Low-temperature hydrogenation of diamond nanoparticles using diffuse coplanar surface barrier discharge at atmospheric pressure. *Physica Status Solidi B-Basic Solid State Physics* [online]. **252**(11), 2602–2607. ISSN 1521-3951. Available at: doi:10.1002/pssb.201552232

Experimental work (%)	Supervision (%)	Manuscript (%)	Research direction (%)
15	--	20	15

[10] **CECH, J.*(corresponding author)***, Z. BONAVENTURA, P. STAHEL, M. ZEMANEK, H. DVORAKOVA and M. CERNAK, 2017. Wide-pressure-range coplanar dielectric barrier discharge: Operational characterisation of a versatile plasma source. *Physics of Plasmas* [online]. **24**(1, Article 013504). ISSN 1089-7674. Available at: doi:10.1063/1.4973442

Experimental work (%)	Supervision (%)	Manuscript (%)	Research direction (%)
50	40	50	30

ii) CaviPlasma-related papers:

[11] MARSALEK, Blahoslav, Eliska MARSALKOVA, Klara ODEHNALOVA, Frantisek POCHYLY, Pavel RUDOLF, Pavel STAHEL, Jozef RAHEL, **Jan CECH**, Simona FIALOVA and Stepan ZEZULKA, 2020. Removal of Microcystis aeruginosa through the Combined Effect of Plasma Discharge and Hydrodynamic Cavitation. *Water* [online]. **12**(1, Article 8). ISSN 2073-4441. Available at: doi:10.3390/w12010008

Experimental work (%)	Supervision (%)	Manuscript (%)	Research direction (%)
10	--	10	10

[12] **CECH, Jan*(corresponding author)***, Pavel STAHEL, Jozef RAHEL, Lubomir PROKES, Pavel RUDOLF, Eliska MARSALKOVA and Blahoslav MARSALEK, 2020. Mass Production of Plasma Activated Water: Case Studies of Its Biocidal Effect on Algae and Cyanobacteria. *Water* [online]. **12**(11, Article 3167). ISSN 2073-4441. Available at: doi:10.3390/w12113167

Experimental work (%)	Supervision (%)	Manuscript (%)	Research direction (%)
15	--	40	15

[13] **CECH, J.*(corresponding author)***, P. STAHEL, L. PROKES, D. TRUNEC, R. HORNAK, P. RUDOLF, B. MARSALEK, E. MARSALKOVA, P. LUKES, A. LAVRIKOVA and Z. MACHALA, 2024. CaviPlasma: parametric study of discharge parameters of high-throughput water plasma treatment technology in glow-like discharge regime. *Plasma Sources Science & Technology* [online]. **33**(11, Article 115005). ISSN 1361-6595. Available at: doi:10.1088/1361-6595/ad7e4e

Experimental work (%)	Supervision (%)	Manuscript (%)	Research direction (%)
30	25	50	30

[14] **CECH, J.**, P. STAHEL, L. PROKES, D. TRUNEC, R. HORNAK, P. RUDOLF, B. MARSALEK, E. MARSALKOVA and P. LUKES, 2025. Glow discharge in water cavitation cloud with improved efficiency for hydrogen peroxide production. *Plasma Sources Science & Technology* [online]. **34**(6, Article 065009). ISSN 1361-6595. Available at: doi:10.1088/1361-6595/addf79

Experimental work (%)	Supervision (%)	Manuscript (%)	Research direction (%)
30	75	50	40

[15] HORNAK, Radek, **Jan CECH*(corresponding author)***, Pavel ST'AHEL, Lubomir PROKES, David TRUNEC, Pavel RUDOLF and Blahoslav MARSALEK, 2025. Spatial Mapping of OH Radicals Produced by Electric Discharge in Hydrodynamic Cavitation Cloud. *Journal of Physical Chemistry Letters* [online]. **16**(25), 6279–6285. ISSN 1948-7185. Available at: doi:10.1021/acs.jpclett.5c00979

Experimental work (%)	Supervision (%)	Manuscript (%)	Research direction (%)
30	75	40	60

The author's qualitative contribution to the annotated papers (where appropriate (significant), the co-authors are indicated):

- [1] Design and construction of the 'The Box' experimental apparatus (with P.S.), conduction of experiment – electrical measurements, optical emission spectroscopy (with Z.N.) and imaging, data analysis (with Z.N.), responsible for the writing of the manuscript
- [2] Design (with P.S. and Z.N.) and conduction of experiment – electrical measurements, optical emission spectroscopy and imaging, data analysis, responsible for the writing of the manuscript
- [3] Design (with P.S.) and conduction (with J.H.) of experiment – electrical measurements, optical emission spectroscopy and imaging, data analysis, responsible for the writing of the manuscript
- [4] Numerical model and analysis of residual heat build-up, joint interpretation of results with J.R., comments on the manuscript
- [5,6] Discovery of investigated phenomenon, design and conduction (with T.M.) of ICCD-related measurements and analysis, preparation of the respective part of the manuscript, comments on the manuscript

- [7] Design (with Z.N.) and conduction of ICCD-related measurements (with Z.N., T.M. and M.S.) and analysis (with Z.N.), responsible for the writing of the manuscript
- [8] Design and conduction of ICCD-related measurements and analysis, optical emission spectroscopy (with A.B.), preparation of the respective part of the manuscript, co-editing of the manuscript (with A.B. and M.C.)
- [9] Design and conduction of plasma treatment experiment, design and conduction of plasma diagnostics and data analysis; writing of respective parts of the manuscript, comments on the manuscript
- [10] Design (with P.S. and M.Z.) and conduction of experiment (with P.S., H.D.), (phase-resolved) imaging and electrical characterisation and analysis, responsible for the writing of the manuscript (Z.B. was responsible for the development and application of the modified Paschen law part of the manuscript)
- [11] Co-inventor of the CaviPlasma technology, optical emission spectroscopy (with P.S. and J.R.) and related part of the manuscript, comments on the manuscript
- [12] Design and conduction of the diagnostics experiment (with P.S., J.R. and L.P.), electrical measurements (with P.S.), optical emission spectroscopy and imaging, data analysis, and responsible for the writing of the manuscript
- [13] Design and conduction of the experiment (diagnostics – with P.S., parametric study – with L.P., R.H., E.M.), electrical measurements (with R.H.), optical emission spectroscopy and imaging, data analysis, responsible for the writing of the manuscript (co-editing with D.T.); phenol and colourimetric measurement of peroxide with P.L., OH analysis A.L. and Z.M.
- [14] Design and conduction of the experiment (diagnostics – with P.S. and R.H., parametric study – with P.L, P.S. and L.P.), electrical measurements and optical emission spectroscopy and imaging (with R.H.), data analysis (with R.H.), responsible for the writing of the manuscript (co-editing with D.T.)
- [15] Design and conduction of experiment (with L.P. and R.H.), electrical measurements (with L.P.) and analysis, optical emission spectroscopy (with R.H.), (spectrally resolved) imaging and analysis, data analysis with numerical model (with D.T. and P.R.), responsible for the writing of the manuscript (co-editing with D.T. and R.H.)

1 Introduction

The habilitation thesis deals with the development, diagnostics and application of non-equilibrium discharges, specifically the so-called Diffuse Coplanar Surface Barrier Discharge (DCSBD), including its model development unit, and the CaviPlasma® technology[2], in which the author was involved during his career at the Department of Plasma Physics and Technology (DPPT), formerly the Department of Physical Electronics, at Masaryk University. These plasma sources were invented for the fast treatment of solid surfaces (DCSBD) and liquids (CaviPlasma). In this thesis, the fundamental diagnostics of these discharges, as well as selected examples of their applications, will be presented.

The author spent about 2/3 of his scientific career at Masaryk University researching the coplanar barrier discharges and the Diffuse Coplanar Surface Barrier Discharge, respectively. This unique low-temperature, high-density and macroscopically uniform atmospheric pressure discharge was invented by Prof. Mirko Cernak and his team at Comenius University (Slovakia) and developed into an industrially mature technology under his supervision at DPPT. Since 2018, the author's primary research interest has focused on plasma treatment of liquids, particularly the development, diagnostics and application of the multiple-awarded CaviPlasma technology. The CaviPlasma technology was invented by the researchers at Brno University of Technology (BUT), Masaryk University (MUNI) and the Institute of Botany of the Czech Academy of Sciences (IBOT). CaviPlasma has been patent-protected since 2019 and internationally patent-protected since 2023. The author has been a co-inventor of CaviPlasma technology and a member of the core team exploiting its application and commercial potential.

This thesis is therefore divided into two principal parts. The first part covers the research on the coplanar dielectric barrier discharges (CDBDs). The second part is focused on the CaviPlasma.

This thesis is a collection of previously published scholarly works with commentary. The full texts of the annotated articles are attached in the Appendix.

[2] The label CaviPlasma is an internationally registered trademark of patent holders, BUT, MUNI and IBOT.

2 Motivation and Objectives of the Work

Both commented plasma sources have a lot in common. The DCSBD, as well as CaviPlasma, represented technologies with clear application potential. However, none of them had been studied in detail when the author became familiar with them, and the mechanisms governing the properties of these discharges had not been investigated to a large extent. The level of technological readiness was low at these early stages of development, which allowed for the broad tests of substantial modifications to their physical implementation. This situation hindered the development and adaptation of these plasma technologies for intended applications. However, the same situation fostered the discharge diagnostics and set the direction for application-oriented fundamental research on these sources. The commentary on the set of annotated papers evidences the author's involvement in this process and progress.

The studied plasma sources, the DCSBD or generally coplanar barrier discharges (CDBD), and the CaviPlasma, are both highly transient phenomena. Moreover, their behaviour is sensitive to the presence of extrinsic electrodes, which prevents the use of probe measurements common in low-pressure plasma diagnostics. Therefore, the study of discharge development and related phenomena requires non-invasive diagnostic techniques enabling temporal resolution on the μs timescale or better. Moreover, the spatial distribution of discharge properties or their constituents further restrains the diagnostic techniques. These requirements were met by adopting optical diagnostics techniques, such as discharge pattern imaging and optical emission spectroscopy, supplemented with electrical measurements.

The author specialised in optical diagnostics with spatial, temporal, and/or spectral resolution. He utilised the newly acquired diagnostics equipment, namely the intensified gated CCD camera[3] (ICCD) for the space and phase-resolved imaging and the optical emission spectroscopy, respectively. This type of diagnostics also brings several challenges that the author had to overcome. The precise image registration was necessary for dual-wavelength imaging. The temporal resolution resulted in low signal intensity and the necessity of an accumulated, time-averaged acquisition. The sensitivity of instruments, or detectors, and the repeatability and jitter of studied phenomena (discharge stabilisation) become important parameters for such studies. For these measurements, the semi-autonomous and correlated electric-optical measurements were established. The author then developed processing codes for (large) datasets import and subsequent analysis, such as image registration or electric measurements analysis. In some cases, physical (numerical) models were also developed to support interpreting the results. The author was also actively involved in the design of the plasma sources, e.g., the model CDBD configuration simplifies the complex DCSBD structure and enables broad parametric studies.

[3] The author was responsible for the ICCD camera selection process at DPPT and subsequent experiments using this camera.

The author's contribution to the investigated phenomena can be briefly summarised in the following list:

i) DCSBD-related contribution

- The parametric study on electrode geometry **(Čech et al. 2009)**, temperature and overvoltage **(Čech et al. 2008)** using model CDBD configuration revealed their substantial influence on the magnitude and spatial distribution of rotational temperature in the CDBD. These results served as the input data for tailored DCSBD electrode geometry optimisation, optimising the treatment of temperature-sensitive materials.
- The author designed and performed the correlated electric and optical measurements to study, e.g. the statistical behaviour of microdischarges in CDBD. The study revealed the influence of electrode geometry and overvoltage on the probability of reusing the single, common discharge path by subsequent microdischarges **(Čech et al. 2015)**. When combined with the temperature influence experiment on CDBD with annular electrodes **(Ráheľ et al. 2016)** and the related numerical model by the author, the new mechanism of memory effect in barrier discharges was proposed – the role of residual heat build-up on microdischarges stabilisation **(Ráheľ et al. 2016)**.
- The study of the homogeneous regime of CDBD in helium resulted in the author's discovery of an ultra-low emission event preceding the Townsend avalanching phase **(Morávek et al. 2016)**. The follow-up study **(Navrátil et al. 2017)** disclosed its origin as a bremsstrahlung of released surface charges, giving this phenomenon the designation 'charge relaxation event'. Even the single-photon sensitivity and registration become essential for successfully resolving the studied phenomena.
- The homogeneous regime of helium CDBD also enabled the study of the dynamics of ionising waves and the 2D-resolved development of the electric field in these waves, studied using an intensified CCD camera imaging, with spectral resolution (dual-wavelength imaging) **(Čech et al. 2018)**.
- The potential of DCSBD for niche applications was investigated under special discharge conditions. The reduction of surface metal-oxide layers in a hydrogen atmosphere was studied **(Prysiazhnyi et al. 2014)**. The author performed a characterisation of H_2-DCSBD behaviour in this paper. The experience with H_2-DCSBD was also utilised for the functionalisation of nanoparticles (nanodiamonds) in **(Kromka et al. 2016)**. The author was responsible for the plasma treatment experiment and the treatment process characterisation in this research. The author also studied also the behaviour of coplanar discharge in wide pressure range conditions **(Čech et al. 2017)** using a compact laminated electrode setup developed at DPPT. This study was performed within the research on the CDBD-based plasma decontaminator.

ii) CaviPlasma related contribution

- The novel plasma-liquid treatment technology was developed, and the intellectual property rights of MUNI, VUT and IBOT were protected by the (international) patents. In the first public disclosure of the technology, we have presented the direct cyanobacteria decontamination in fast-flowing liquid **(Maršálek et al. 2020)**. The follow-up paper presented the indirect decontamination potential utilising the CaviPlasma-treated water **(Čech et al. 2020)**.
- The author then performed the discharge diagnostics of CaviPlasma. The correlated electric and ICCD measurements were performed to characterise the electric discharge development in the hydrodynamic cavitation cloud. We have revealed two distinct operation regimes of the CaviPlasma, the spark/glow discharges depending on the electrode configuration. The thorough parametric study revealed the influence of, e.g., the cavitation cloud parameters, electrode geometry, electrode composition, input power, or water conductivity on the energy efficiency and production rate of reactive oxygen species and the results of this complex CaviPlasma characterisation were published in **(Čech et al. 2024, Čech et al. 2025, Horňák et al. 2025)**. The results achieved in this fundamental research enabled the optimisation of CaviPlasma for large-volume water treatment applications.

The application-oriented research is the unifying line of the author's effort at Masaryk University, presented in this thesis. Understanding the influence of discharge configuration and physical conditions on the properties of the discharge, or the phenomena that govern the development of the discharge, provided a tool for tailored development of industrially oriented plasma sources. Nevertheless, not only were the diagnostics performed. The application potential of DCSBD and CaviPlasma discharges was also investigated, and the author was also involved in these processes.

3 Part I: Research and Development of the DCSBD

Plasma technologies[4] offer unique possibilities in material science as the sources of reactive species that promote non-equilibrium chemistry processes (Bogaerts et al. 2002, Eliasson and Kogelschatz 1991). The broad classes of products for everyday life are manufactured from materials that offer intended bulk properties, but lack the surface properties or compatibility for further industrial processing. Plasma technologies have high application potential in the processing of these materials, e.g., natural or synthetic fibres, nonwovens, polymers, paper, or glass, where surface cleaning, functionalisation or coating is often required to improve wettability, printability, adhesion of layered materials, or barrier properties, i.e., the modification of physical, and/or chemical surface properties (Weltmann et al. 2019, Cvelbar et al. 2019). However, meeting the industrial demands on scale-up, high-speed and low cost represents a challenging task (Weltmann et al. 2019, Cvelbar et al. 2019). This task has been under investigation at DPPT MUNI for over two decades.

The potential of plasma technologies has been recognised for a broad spectrum of applications, including those benefiting from the atmospheric pressure conditions (Adamovich et al. 2022, Weltmann et al. 2019, Cvelbar et al. 2019, Samukawa et al. 2012). However, the potential for high processing speed and engineering simplicity of atmospheric pressure plasma technologies comes along with the high rate of collisional processes. While being beneficial for the desired plasma chemistry, the collisions result in a positive-feedback mechanism of energy transfer to neutral processing gas (thermalisation) and enhanced tendency to instability development (constriction) (Bruggeman et al. 2017). These effects negatively affect atmospheric pressure plasma treatment of thermally sensitive materials.

Several strategies for sustaining discharges out of the thermal equilibrium were developed (Bruggeman et al. 2017), e.g. the generation in noble gases, the limitation of transferred charge, and/or limitation of temporal evolution of the discharge. In common processing gases, as ambient air, nitrogen, or oxygen, the non-equilibrium, or non-thermal discharges can be secured through the pulsed operation (Fridman et al. 2005, Janda et al. 2011, Dvonc and Janda 2015), e.g., using nanosecond high-voltage switching, or the self-induced pulsing of the discharge resulting from the design of high voltage power supply, as for the spark or transient-spark discharge.

[4] This thesis will cover the research on electric discharges with a highly transient nature. In these cases, the strict conditions imposed in the definition of *plasma* are not always fulfilled. However, for better text readability, the term '*plasma*' will be consciously adopted according to the general usage of this term in the literature, despite the known interference with the scientific rigor in particular cases.

Dielectric Barrier Discharges – Design and Application Challenges

The first group of the annotated papers focus on the class of non-equilibrium discharges, where the transported charge and discharge duration are limited using a dielectric barrier between the electrodes. These are the dielectric barrier discharges[5] (DBD) (Kogelschatz et al. 1997, Kogelschatz 2003, Brandenburg 2017). The inherently non-thermal nature of DBDs resolves the thermalisation issue of atmospheric pressure processing of materials. The constriction problem, however, persists.

Dielectric barrier discharges typically consist of individual microdischarges, each representing a microplasma reactor (Kogelschatz 2003, Eliasson and Kogelschatz 1991). This resulted in utilisation of DBD induced plasma-chemical reactions in a broad range of applications from the ozone production (Eliasson et al. 1987), surface engineering (Hegemann and Gaiser 2022), bio-medical applications (Graves 2012, Weltmann et al. 2010), growing field of plasma treatment of liquids (Montalbetti et al. 2025), or plasma-induced airflow control (Moreau 2007), For the details on the properties of individual microdischarges and the characterisation of DBDs, please consult, e.g., the review of Brandenburg (2017) and the references there in.

The discharge breakdown in DBDs generally starts as the Townsend (avalanching) phase, followed by the spatially constricted fast ionising waves bridging the gas gap between electrodes in the so-called streamer mechanism (Kogelschatz 2003, Brandenburg 2017, Gibalov and Pietsch 2012). Finally, the filament, a thin luminous channel, is formed with a width of tens of μm in the air at atmospheric pressure (Šimek et al. 2011). A structured overview of the highly spatially and temporally resolved optical diagnostics of the microdischarges can be found, e.g., in the habilitation thesis of Hoder (2017).

The temporal occurrence of individual microdischarges has a stochastic nature (Akishev et al. 2011). However, the spatial occurrence of microdischarges is strongly influenced by the mutual interaction of preceding and concurrent microdischarges. These collective effects were attributed to UV photons and remnant, memory, surface charges (Tschiersch et al. 2017, Kogelschatz 2010), and result in spatial recurrence of microdischarges and therefore non-random localisation of filaments (Chirokov et al. 2006), even the formation of regular patterns (Kogelschatz 2010). This ‚memory effect' places technological burdens on the uniformity of plasma treatment using DBDs and the propensity of the (localised) thermal damage of treated materials.

However, the truly diffuse and unconstricted DBDs can be achieved only in narrow discharge conditions (Massines et al. 2009, Brandenburg et al. 2009, Kozlov et al. 2005, Ráheľ and Sherman 2005). Two homogeneous regimes can be sustained, when the transition to the streamer breakdown is suppressed, the ionisation is slow and the discharge

[5] The temporal evolution of DBDs is, in fact, limited by the transferred charge that is deposited on the surface of the dielectric barrier in DBDs.

mechanism is the Townsend breakdown (Massines et al. 2009): (i) the Atmospheric Pressure Townsend Discharge (APTD) in, e.g., nitrogen gas, where the discharge development stops before the cathode fall formation; or (ii) the Atmospheric Pressure Glow Discharge (APGD) in, e.g., helium, where the cathode fall and positive column develops. However, the reported conditions for APTD in air gaps are quite limiting (Ran et al. 2018), which probably prevents the utilisation of APTD in industrial conditions of ambient air inline treatment.

The level of the homogeneity of material treatment in filamentary discharges then depends on the implementation of a particular DBD geometry. The author's closing remarks to this section will therefore be devoted to the influence of DBD configuration on practical aspects of plasma (surface) treatment. Designs of DBD electrode and barrier arrangements can be divided into three main groups: volume, surface, and coplanar dielectric barrier discharges (Brandenburg 2017), each with specific implications for plasma processing applications.

In the volume DBD configuration (VDBD), the discharge is generated in the free space (volume) between the electrodes. At least a single dielectric barrier separates the electrodes. The treatment is affected by the density of filaments bridging the electrode gap and their spatio-temporal localisation. Filaments strike the surface of the treated material nearly perpendicularly, and the microdischarges tend to recur at the same spot on the treated surface due to the mentioned memory effect (Kogelschatz 2010). This imposes a high risk of localised thermal load on the material, causing its localised damage. The small gas gaps and high voltage amplitude help in 'homogenization' of the discharge (Wagner et al. 2003). There is also a principal technological limitation of material treatment in VDBD – the treated specimen thickness is limited by the gas gap width between electrodes, which ranges from 0.1 mm to 10 mm for moderate high voltage amplitude (Brandenburg 2017).

The VDBD technical limitations can be overcome through surface and coplanar arrangements. The electrodes are positioned along the surface(s) of a single thin dielectric barrier, forming a strongly tangential electric field along the dielectric, and the generated microdischarges are 'sliding' along the dielectric surface (Gibalov and Pietsch 2012). The microdischarges' principal orientation enhances the contact area of the treated material and also lowers the risk of perforation or pinhole in the treated material. There is also no limitation on the gas gap, and the only condition placed on the treated material is that the surface curvature follows the surface geometry of the electrode arrangement (dielectric plate). The typical configuration of surface DBD (SDBD) consists of a system of surface electrodes deposited on the dielectric plate with the counter-electrode(s) situated at the opposite surface of the barrier (Gibalov and Pietsch 2012). The so-called plasma actuator studied for plasma aerodynamics applications could be achieved using an asymmetric electrode configuration (Boeuf and Pitchford 2005). However, the advantage of the SDBD electrode configuration is redeemed by the risk of the surface electrode's erosion. The exposed surface electrode could suffer from mechanical abrasion caused by the movement of the treated material or by the action of microdischarges

alone, imposing thermal and oxidative[6] stress on the electrode in direct contact with the discharge. Therefore, the SDBD electrode lifetime should be expected to be limited.

This disadvantage is not present in a coplanar electrode arrangement called the coplanar DBD (CDBD), where no bare electrode is exposed to the discharge, discharge atmosphere or treated material; the dielectric barrier covers both electrodes, or systems of electrodes (Gibalov and Pietsch 2004a, Gibalov and Pietsch 2004b; Šimor et al. 2002). However, this comes at the cost of the complexity of the design and assembly of the coplanar discharge units. In a typical configuration, the electrodes are positioned along a common plane, buried into the dielectrics, or deposited at the barrier's common surface and electrically isolated, typically using oil (Brandenburg 2017, Hoder et al. 2017). This imposes high demands on the quality of the insulation, which has to have low dielectric losses, withstand the thermal load during high-power discharge operation, and ideally, have a high mechanical strength and abrasion resistance.

The invention of a specific CDBD arrangement called Diffuse Coplanar Surface Barrier Discharge (DCSBD) (Šimor et al. 2002) enabled the development of a non-thermal, low-temperature plasma source operating at atmospheric pressure and offering a high degree of spatial uniformity at high power density. On the way towards an industrially robust plasma unit, the discharge physics and engineering challenges of CDBD have to be resolved at DPPT to achieve the possibility of continuous generation of approx. 0.3 mm thin surface layer of dense plasma (exceeding 100 W/cm^3), making DCSBD highly beneficial for fast surface modifications (Černák et al. 2009).

This first section of this thesis is therefore focused on the DCSBD research. It consists of annotated original scientific papers co-authored by the author of this thesis, who was privy to the DCSBD story in the research team led by Prof. Mirko Černák at DPPT.

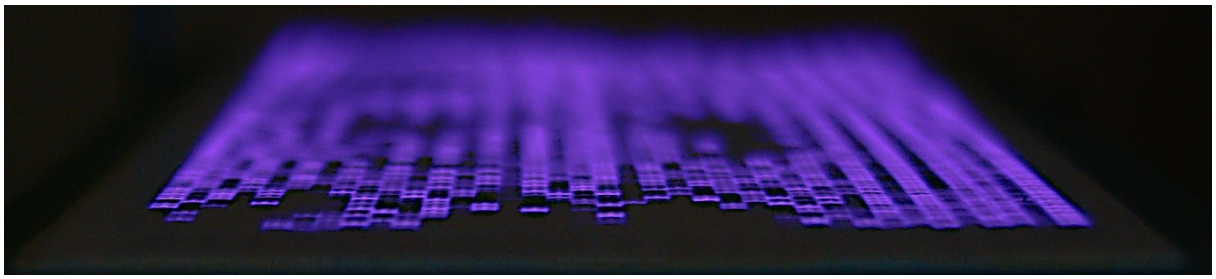

Figure 1: DCSBD in ambient air, side view with partial coverage by a treated glass plate. The DCSBD electrode design has narrow stripes and grooved ceramic. The nominal input power was derated to make the individual microdischarges and their bow-like protrusion above the ceramic plate distinguishable. Source: Author

[6] In ambient air or oxygen containing gas mixtures.

3.1 Commentary on the Annotated Scientific Papers: CDBD/DCSBD

Due to the complexity of the manufacturing process of the DCSBD discharge unit, the model coplanar DBD units were developed to discover CDBD properties and implement them in the design of DCSBD. Two width parameters are involved in the DCSBD geometry: the width of strip electrodes and the width of interelectrode gaps. Both have substantial effects on the discharge parameters of DCSBD. The discharge structure of CDBD consists of (a) thin discharge channels (filaments) in between electrodes that protrude to the half-space above the dielectric barrier, forming a bow-like structure and (b) surface discharges evolving above the electrodes after contact of the microdischarge with the dielectrics. The ongoing research on CDBD brings knowledge on the influence of discharge configuration and discharge conditions on microdischarges properties. The knowledge of the spatially resolved properties of microdischarges, in terms of their appearance, intensity, temperature, or statistics, supported the tailored DCSBD development by the team of researchers at DPPT.

3.1.1 The Study of the Fundamental Parameters of DCBD for DCSBD Development

For the study of the fundamental parameters of DCBD and the influence of different physical and geometrical conditions, the unique design called 'The Box' was developed by the author, his mentor associate Prof. Pavel Stahel and technician Petr Saul. This unique device was successfully used for over 12 years of DCBD research at DPPT. It enabled the fast exchange of dielectric barrier plates, changes in electrodes' distance, intentional heating/cooling of the grounded electrode, and exchangeable electrode geometry (pattern). The electrode setup, forming a rectangular gap of 30 mm length, was studied as the reference model for DCSBD development. This multi-microdischarge configuration enabled the studies of discharge parameters under the influence of interacting adjacent microdischarges. In addition, the controlled discharge atmosphere was easily achievable, allowing the survey of CDBD in rare gases, electronegative and electropositive gases and their mixtures.

The first results on extended electrode configuration achieved on the 'The Box' reactor, see Fig. 2, were published in **(Čech et al. 2008)**. The study was performed in pure nitrogen (99.996% purity) for a fixed interelectrode gap width of 0.7 mm. The influence of discharge overvoltage and the temperature of the grounded electrode were studied, see Fig. 2. At high overvoltage, the intense discharge channels could be identified, which probably results from the repetitive breakdown at close paths within the single half-period of the input voltage (see also **(Čech et al. 2015)** for the extended CDBD geometry and (Hoder et al. 2017) for the single-filament CDBD electrode geometry).

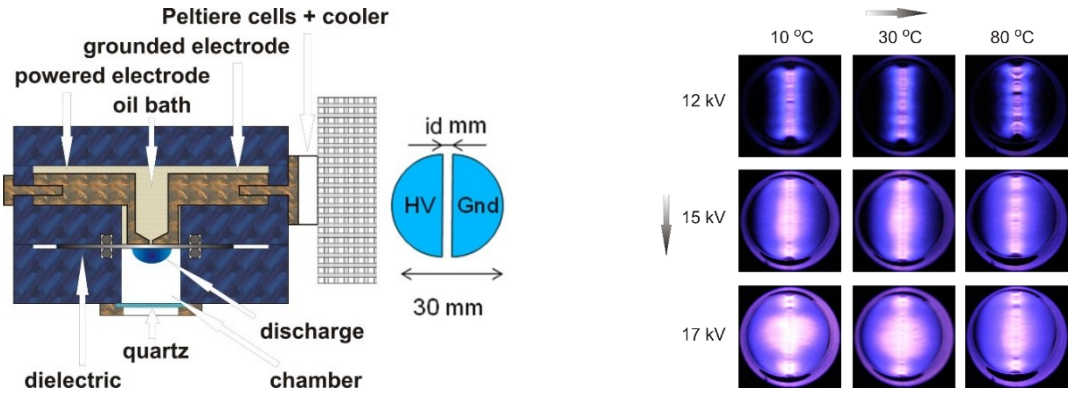

Figure 2: Cross-section of The Box reactor (left) and the influence of overvoltage and ground electrode temperature on CDBD appearance (right). Source: Author (Čech et al. 2008)

Spatial profiles of discharge intensities as well as rotational and vibrational temperatures from the second positive system of nitrogen (SPS N_2) were gained, see Fig. 3, using a space-resolved optical emission spectroscopy on the high-resolution spectrometer Horiba Jobin-Yvon FHR 1000 equipped with 1200 gr/mm and 3600 gr/mm gratings and a pair of CCD and ICCD detectors. The spatiotemporal development of emission of first negative (FNS) and second positive (SPS) systems of nitrogen was also investigated using highly time-demanding spatially and phase-resolved emission spectroscopy. We have obtained the first results on time-averaged SPS/FNS development in an extended, multi-filamentary CDBD configuration, see Fig. 5 and the comments to the next annotated paper **(Čech et al. 2009)**.

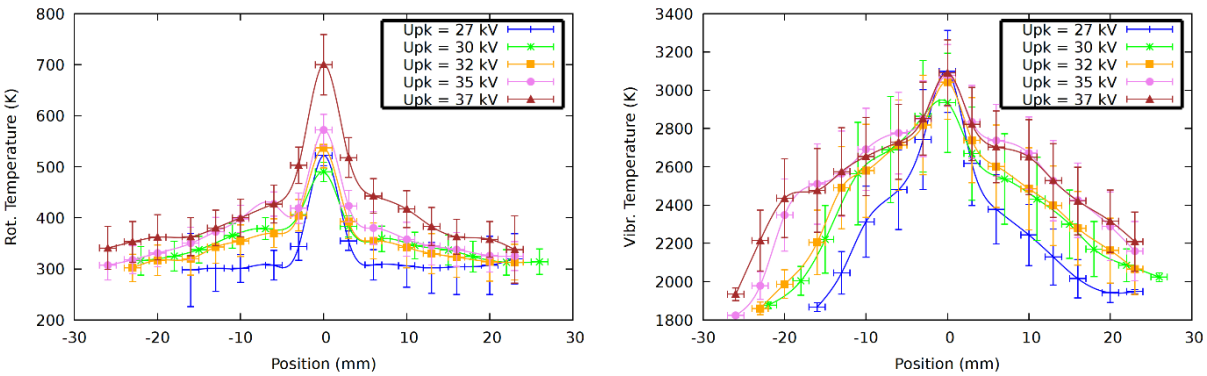

Figure 3: Dependence of SPS N_2 rotational temperature (left) and vibrational temperature (right) on voltage amplitude in CDBD; '*d*' denotes the distance from the centre of the interelectrode gap. Source: Author

The next logical step was to systematically investigate the influence of the interelectrode gap width. The first paper on this topic was published in **(Čech et al. 2009)**. The electrode gap width was changed in the range of 0.6 to 2.2 mm, given by the dielectric strength of the insulating oil on the narrow side of the interval and the range of high voltage (HV) amplitude of the power supply on the broad side. It was found that the electrode gap width is a crucial geometrical parameter influencing the discharge pattern in terms of filamentary and diffusive parts of the discharge. The electrode gap width also determines the operating parameters of the HV generator (range of amplitude). The channels of microdischarges develop in a highly non-homogeneous electric field above the dielectric barrier and form a bow-like structure above the electrode gap following the electric field geometry. The length of the microdischarge channel is not restricted by the electrode gap width in coplanar DBD, as it is in the volume DBD (by the width of the gas gap). The observed CDBD microdischarge channels were not completely squeezed by the narrow electrode gap and bridged a longer distance than the gap width, see also the results in the annotated paper **(Čech et al. 2017)**. The linear increase of ignition voltage with the gap width was observed in the studied gap width range. The voltage increases by nearly 30 % with a 4-fold increase in the gap width, see Fig. 4.

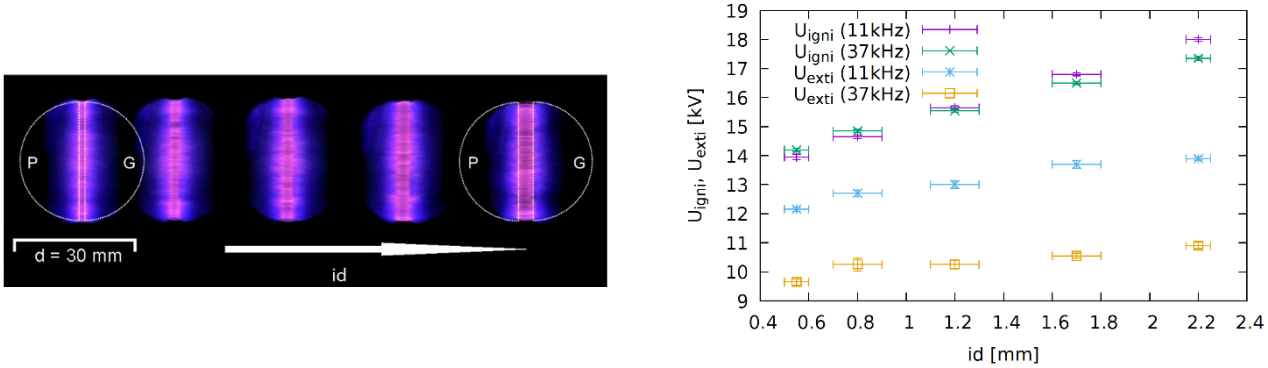

Figure 4: Influence of interelectrode gap width on CDBD pattern (left) and ignition and extinction voltage for two frequencies (right); '*id*' denotes the interelectrode gap width. Source: Author, (Čech et al. 2009)

The ignition voltage was only slightly reduced with the increase in the frequency of the HV (within the studied acoustic frequency range). However, the voltage needed to sustain the discharge is considerably lower, because of the electric field distortion caused by the surface charges deposited on the dielectric barrier, see, e.g., (Abolmasov et al. 2006, Brandenburg 2017) and our study of charge relaxation event **(Navrátil et al. 2017)**.

While the HV frequency did not influence the ignition voltages, the sustained discharge voltage decreased by 20-30 % when the HV frequency was tripled, and a higher amount of residual surface charges on the dielectrics and excited/ionised species in the gas were preserved from the previous half-cycle of the discharge.

From the point of view of the applications, the significant results provided the spatially resolved spectroscopy. The rotational and vibrational temperatures of SPS N_2 analysis revealed that the hottest part of the discharge is the filamentary part above the electrode gap, with rotational temperature ranging from 450 K for the 0.6 mm gap width to 650 K for the 2.2 mm gap width at the same HV amplitude. The above electrode rotational temperature was slightly above the room temperature, i.e., around 300-330 K, see Fig. 5. The vibrational temperature also shows a significant difference between filamentary and above electrode parts (over 3,000 K vs 2,200 K), with a clear trend of temperature increase with increasing gap width. The measured accumulated spatiotemporal development of SPS N_2 in extended CDBD geometry could be qualitatively compared to the cross-correlation spectroscopy measurements performed in the single-filament configuration (Hoder et al. 2009), see the map in Fig. 5. Although the individual ionisation waves could not be identified due to highly averaged multi-microdischarge measurement, the collective dynamics of microdischarges propagating from the interelectrode area across the dielectrics could be identified.

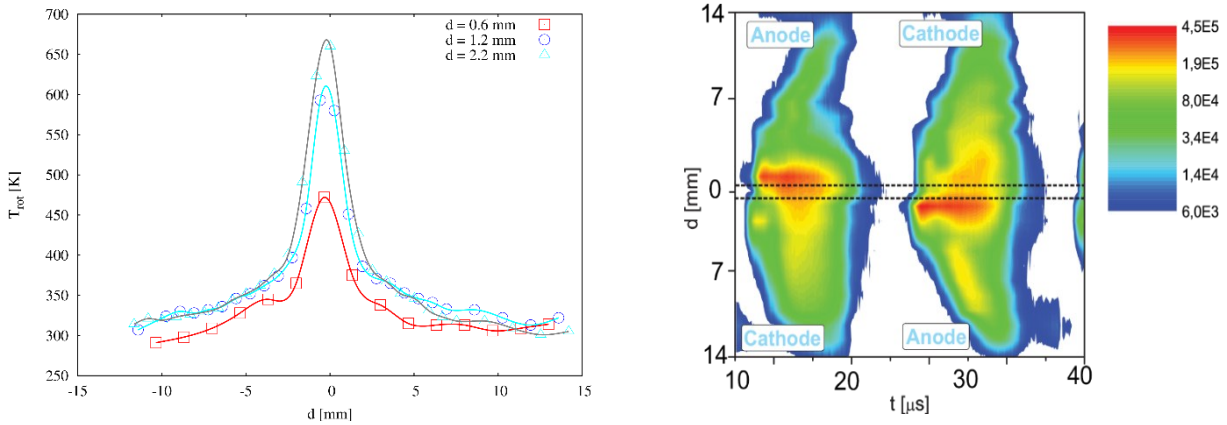

Figure 5: Dependence of SPS N_2 rotational temperature (left) and phase-resolved emission of SPS N_2 in logscale (right) on interelectrode distance of CDBD; '*d*' denotes the distance from the centre of the interelectrode gap. Source: Author (Čech et al. 2009)

These results supported the optimisation of DCSBD geometry concerning the interelectrode gap width and electrode strip thickness, as the development of DCSBD technology was explicitly focused on treating temperature-sensitive materials like nonwoven textiles. This results in adopting a narrow gap width configuration of the DCSBD electrode design. This way, the filamentary part of the discharge can be suppressed, and the rotational temperature can be lowered substantially. The results of optical diagnos-

tics also prove that the visually diffuse and luminous regions above electrodes generate a highly non-equilibrium plasma with low rotational temperature.

⁂

The following annotated paper was focused on the spatially and phase-resolved time-correlated diagnostics of DCBD. The results of a statistical study on DCBD microdischarges were published in **(Čech et al. 2015)**. In this paper, the correlated signal acquisition was used to reveal the statistical behaviour of CDBD microdischarges in extended, multi-filamentary geometry. The ICCD camera was capturing a phase-resolved discharge pattern, see Fig. 6, and a fast multi-channel digital storage oscilloscope was recording the respective voltage and current waveforms and also the ICCD camera gate monitor signal. The unique feature of the Princeton Instruments PI-MAX3 ICCD camera at DPPT enabled the sequential acquisition of the discharge pattern from two consecutive half-periods. The custom scripts for numerical image and waveform analysis were then developed to discriminate the number and position of individual filaments crossing the discharge (electrode) gap in respective half-periods of the excitation HV, together with the correlated current peaks of respective half-periods.

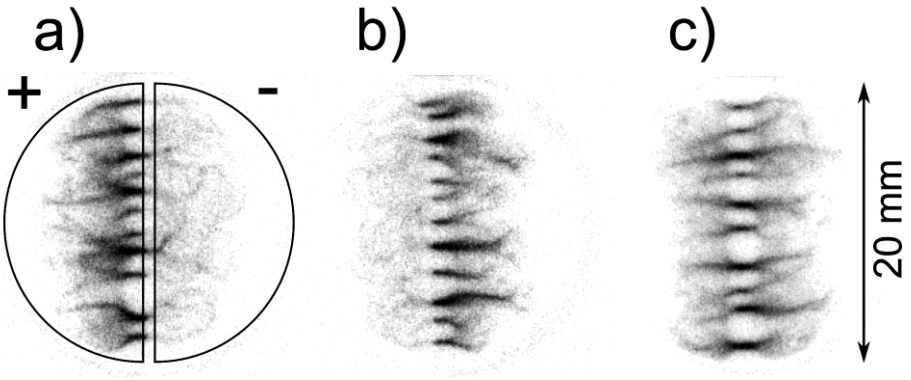

Figure 6: CDBD discharge pattern resolved for positive (left), negative (middle) half-periods (non-accumulated), and a single period (right). Polarity concerning the left of a pair of electrodes, depicted as semicircles. Source: Author (Čech et al. 2015)

The extended discharge geometry enabled the study of microdischarges that were geometrically unconstricted in selecting their discharge paths. The analysis of the steady-state discharge conditions revealed the influence of the so-called memory effect using the relation matrices of incidence. Matrix of incidence relates the number of observed unique discharge paths to the derived number of current pulses representing individual microdischarge events, see Fig. 7. Reusing pre-existing discharge paths by the following microdischarges manifests this memory effect. This phenomenon was statistically more pronounced when the discharge gap was widened.

For the short discharge gap, there was a significantly higher number of individual discharge paths (identified filaments) compared to the wide discharge gap (approx. by a factor of 2 for the 0.6 mm gap compared to the 2.2 mm gap).

Moreover, this study revealed that the discharge path could be reused by following microdischarges even within a single, identical discharge half-period, a behaviour previously not considered in CDBD dynamics interpretations. This behaviour was infrequent for slight overvoltage, where microdischarges preferred the unique paths within single half-periods. However, this effect was highly significant for high overvoltage, when most microdischarges reuse the same discharge path or prolong the existing path within the same half-period of the excitation HV. This effect cannot be satisfactorily explained by the charge deposition at the dielectric surface or reduced electric field distortion by residual charged species in the gas along the discharge path, i.e. the commonly accepted memory effect mechanisms at the time of the study.

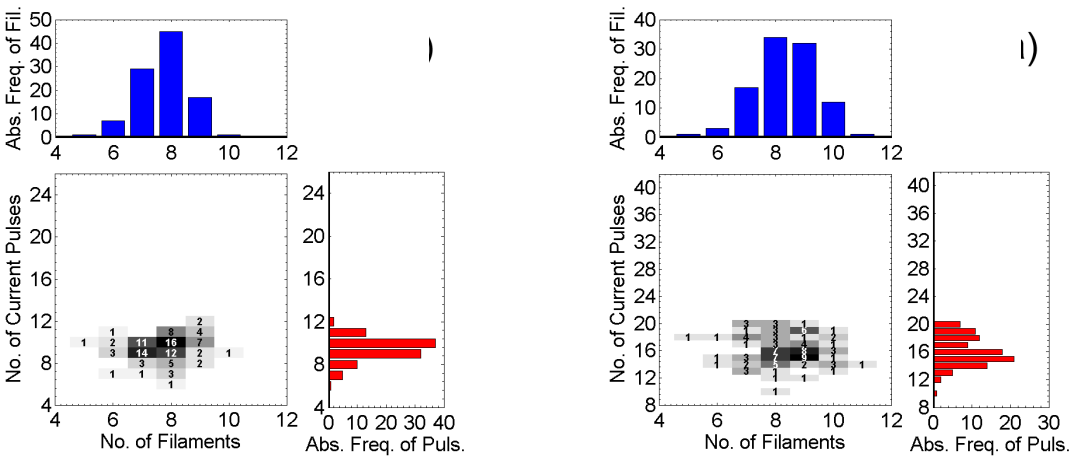

Figure 7: Relation matrix of incidence of current pulses and number of filaments in the positive half-period of CDBD operated at artificial air at interelectrode gap distance 2.0 mm and voltage amplitude 16 kV (left) and 18 kV (right). The number of unique discharge paths (filaments) is comparable for both conditions. However, the number of microdischarges is considerably higher for high overvoltage. Source: Author (Čech et al. 2015)

⁂⁂⁂⁂⁂

3.1.2 New Findings on CDBD Phenomena

Based on **(Čech et al. 2015)** results, the author, together with Assoc. Prof. Jozef Ráheľ proposed a hypothesis on a new mechanism involved in the current interpretation of the memory effect, i.e., that the thermal effects will be responsible for the observed behaviour of microdischarges. To verify this hypothesis, Dr. Zsolt Szalay, the PhD student of Assoc. Prof. Ráheľ, at the time of the research, conducted a series of experiments on CDBD in a temperature range of 20 to 180 °C. The corresponding numerical model on the microdischarge channel temperature build-up was assembled by the author, and the

common investigations resulted in the publication **(Ráheľ et al. 2016)**. The annular discharge gap was used with ring-shaped electrodes to minimise the influence of the finite-length discharge gap. The phase-resolved discharge imaging using an ICCD camera revealed the temporal stabilisation of the discharge pattern on the time scale of 40-60 periods. The simple thermodynamic estimation suggests that the single microdischarge event could result in the rise of a microdischarge channel temperature by approximately 100 K, and the previous spectroscopic measurements indicate that restriking microdischarges will reach the quasi-stationary channel temperature around 600 K for given conditions.

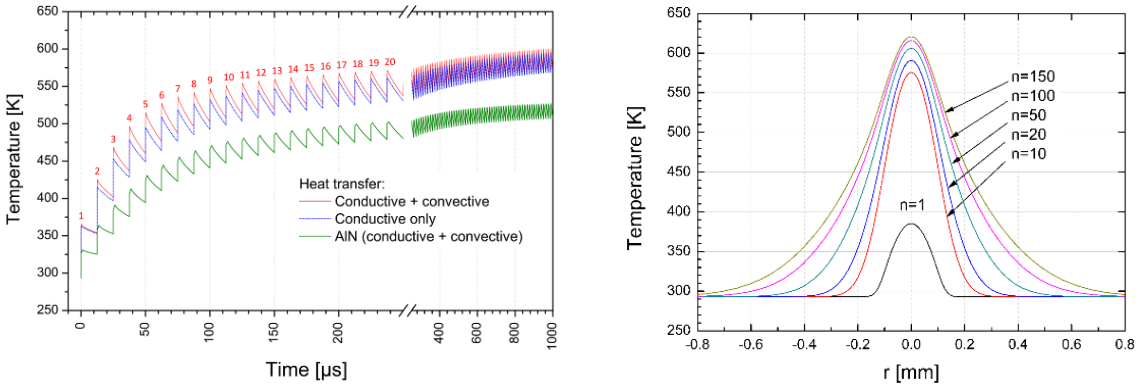

Figure 8: Simulation of average temperature inside the microfilament's column volume, built by the train of recurring localised breakdowns (left). Radial temperature profile resulting from the train of recurring microfilaments, immediately before the (n+1)th breakdown (right). Source: Author and Jozef Ráheľ (Ráheľ et al. 2016)

To investigate this behaviour, the simulation in COMSOL Multiphysics® SW was assessed. The temperature influence on breakdown voltage and system capacitance was experimentally investigated to determine the energy per pulse dependence in the studied temperature range. These estimations serve as the input parameters in the numerical model that follows the residual heat build-up in the discharge channel by the train of restriking microdischarges. The quasi-stationary steady-state conditions were achieved after 20 microdischarge events, and the simulated channel temperature around 550 K showed very good agreement with the previous results of the DCBD diagnostics described in annotated papers, see Fig. 8. Paradoxically, this phenomenon is also responsible for the observed lateral drift of microdischarges on the temporal scale longer than 40-60 consecutive discharge half-periods. There is a radial expansion of the elevated-temperature volume of gas during the quasi-stationary state build-up. The spreading of the 'high-temperature channel' creates favourable conditions for microdischarge development besides the quasi-stationary position, according to the stochastic nature of streamer breakdown. The results of our investigation pointed clearly to the link between residual heat build-up and the spatial stabilisation of the microdischarges on a sub-ms time scale. The residual heat phenomenon was proposed to be included in the memory effect, explaining the spatiotemporal reoccurrence of individual microdischarges.

⁂⁂⁂⁂⁂

The common knowledge on CDBD dynamics was broadened by the author's discovery of the very faint luminous event in the so-far considered dark phase of the discharge at electrode polarity reversal. During our spectroscopic studies of surface charge recombination in dielectric barrier discharges, we have realised that in helium and/or neon working gas, the highly repeatable diffuse discharge regime can be stabilised even for a coplanar barrier discharge configuration. This enabled highly accumulated optical diagnostics of the discharge. As we followed the Townsend avalanching initiation of the discharge, a very faint light was observed prior to this phase. This transient luminous event was approximately three orders of magnitude less luminous than the main discharge phase, and the discovery opens numerous questions on the mechanisms governing this phenomenon, which have been solved within the underlying fundamental research project aimed at studying the surface charges induced 'memory effects' in barrier discharges.

The basic description of the discovery was published in **(Morávek et al. 2016)**. This annotated paper was the first in which we reported on a newly discovered CDBD phenomenon. The helium diffuse mode of CDBD was stabilised in a single-pair semi-circular electrode configuration (the Box reactor). The temporal repeatability of this regime was around 50 ns, which perfectly matches the requirements of a highly accumulated phase-resolved ICCD study used to investigate the pre-breakdown phase of the discharge development. The highly accumulated acquisition of the Townsend breakdown was surprisingly accompanied by the unexpected transient luminous event heading in the opposite direction from the expected Townsend avalanches.

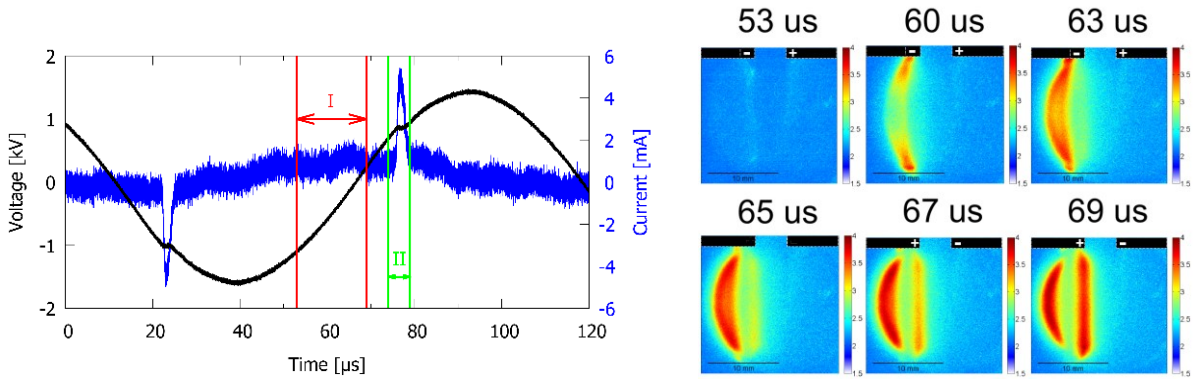

Figure 9: Pre-breakdown phase of DCBD in helium, alumina with high-permittivity coating; (left) Current-voltage waveforms, with labelled temporal window of pre-Townsend luminous event (label 'I') and ionising waves (label 'II'); (right) phase-resolved pre-Townsend luminous event, the Townsend avalanching phase visible from 65 μs. Source: Author

Further investigations were carried out to shed light on the nature of this event. The studied luminous event started at the edge of the cathode approximately 20 μs before the electrode polarity reversal point (discharge period was 106 μs). A weak luminous wave was formed, propagating from the cathode edge above the surface of the dielectric and moving towards the area of the 'cathode' electrode (away from the interelectrode gap). As this luminous event decays, the Townsend avalanche phase starts at the edge of the (so far) cathode, see Fig. 9. We suspect the charges deposited during the preceding discharge on the surface of the dielectrics and the corresponding induced electric field will be responsible for the pre-Townsend luminous event. Therefore, we have modified the dielectrics by the high-permittivity coating deposited on the alumina surface to enhance the observed phenomenon. The coating has more than one order of magnitude higher permittivity than the bare alumina, and the change in the permittivity substantially affected the observed phenomena, delaying the pre-Townsend luminous event by several μs. The emission from this event increased by approximately an order of magnitude using a high permittivity coating. The well-defined bow-shaped luminous wave was found to be propagating along the dielectric covering the instantaneous cathode. The emission was observed first above the edge of the cathode adjacent to the interelectrode gap. The luminous event was then travelling away from the interelectrode gap. Approx. 7 μs after the first emission was observed, the Townsend avalanching started at the edge of the former cathode (instantaneous anode), and both phenomena – Townsend phase and pre-Townsend luminous event – coexisted for about 10 μs. Then the studied luminous event decays and the discharge evolution continues as the Townsend avalanches and the (accelerating) ionising wave heading towards the instantaneous cathode, i.e. in the opposite direction from the pre-Townsend luminous event. During the spatiotemporal evolution the discharge lightens considerably at the halfway point from the anode edge to the cathode edge, and the discharge development continues as the cathode-directed and anode-directed ionising waves (CDIW/ADIW). The velocities of the Townsend avalanching phase and ionising waves above dielectrics were relatively low for the streamer mechanism (7 km/s for CDIW, 4 km/s for ADIW), and our further analysis indicated that the drifting electrons should be fully capable of mediating the CDIW propagation.

Our conclusion on the pre-Townsend event origin was that the weakly adsorbed electrons were released from the surface of dielectrics above the anode and were accelerated towards the oppositely charged dielectrics above the cathode at the temporal window, when the electric field from applied voltage decays. However, due to the very faint photon flux, we lack the spectral information from the pre-Townsend event.

The follow-up experiments revealed that with the increase of the HV frequency, the onset of the discovered pre-Townsend phase is shifted from the edge of the instantaneous cathode towards the instantaneous anode, and its emission was stronger. We took advantage of these findings for further investigations of the origin of the discovered low-light phenomenon.

The author conducted a thorough and experimentally challenging spectral investigation of pre-Townsend emission in collaboration with Assoc. Profs. Rahel, Navratil, and Dr. Tomas Moravek. Following the disclosure of the nature of the discovered phenomenon, the name CRE – charge relaxation event was given to it. Several attempts were made to resolve the CRE emission spectrally. The best-performing spectrometer with ICCD camera at DPPT (Andor Shamrock 750 + iStar ICCD detector) and the ICCD camera imaging using optical interference filters gave only clues for further investigation due to the insufficient signal-to-noise ratio of the obtained signals[7]. Only after the adoption of the single photon counting detection (SPC) using a photomultiplier tube mounted on a low-dispersion monochromator, the signal-to-noise ratio and spectral resolution were sufficient to disclose the mechanisms of this phenomenon, with the details published in **(Navrátil et al. 2017)**.

The discharge setup developed for the first systematic CDBD tests at DPPT ('the Box') again proved to be a valuable tool, this time for the phase-resolved and spectrally resolved analysis of CDBD with a focus on the CRE event. The complex experiment was performed to investigate the spatiotemporal behaviour of CRE and its spectral signature in a helium discharge atmosphere. The observed CRE occurs at the same temporal window as the Townsend avalanching phase of the consequent cathode-directed ionising wave. As the two phenomena overlap in time and space depending on the driving HV frequency, the favourable experimental conditions were found when CRE could be temporally discriminated from the Townsend phase. Under these conditions, adopting spatially unresolved spectroscopy was possible.

The highly customised phase-resolved SPC technique was developed by Assoc. Prof. Navratil, which definitively resolved the CRE temporal and spectral development at the required single-photon sensitivity. The CRE signal was as low as units of photons per second×nm, considering the spectral resolution of 4 nm and a 0.2 μs long temporal window. To better understand how faint the CRE is, we can point out that it took 100 seconds of accumulation at a single wavelength to detect about 100 photons of CRE emission. The acquisition of a single spectrum of the discharge period took around 4 hours after thorough optimisation and automation of the experiment.

[7] This motivated the author to further exploration of ICCD spectroscopy, supervising the bachelor's thesis of Vozárová (2020). In the thesis, the single photon counting technique that the Andor ICCD camera SW offers was adopted, and more than 6x SNR increase was achieved using such a technique.

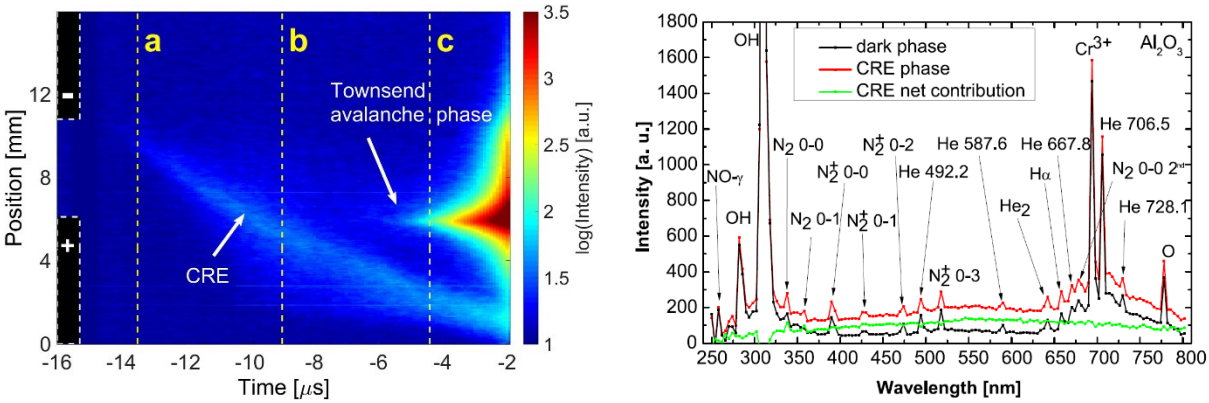

Figure 10: Charge relaxation event (CRE) in helium CDBD, formerly called pre-Townsend luminous event; (left) Streak-camera representation of ICCD phase-resolved imaging (integrated perpendicularly to electrode gap, polarity valid after -8 μs), (right) emission spectrum of CRE – dark-phase spectrum with/without CRE and CRE net contribution. Source: Author, Zdeněk Navrátil (Navrátil et al. 2017)

The CRE event was studied at two CDBD configurations differing in dielectric plate composition – alumina, see Fig. 10, and AlN. The careful discrimination of the spectral signal of the CRE phase revealed that the spectra from the CRE phase for both dielectrics consist of a very broad and weak continuum above 400 nm. However, significant spectral differences occurred in the 300-400 nm window. Both dielectrics' photoluminescence and cathodoluminescence spectra were measured to disclose the material-dependent and material-independent spectral components. The spectra comparison revealed that the radiation during the CRE phase consists of material-dependent luminescence of the dielectrics and material-independent broad continuous radiation to be identified. Several hypotheses were proposed, including molecular continua, recombination spectra and bremsstrahlung of electron collisions with neutral atoms and ions. Careful analysis of temporally unresolved and temporally resolved spectra with a small admixture of neon confirmed that the CRE event light emission is of a bremsstrahlung nature.

Finally, the CRE description was completed using the spatially averaged estimation of electric fields obtained using the numerical model by Assoc. Prof. Navratil. During the CRE, the peak electric field of 1 kV/cm was estimated together with the memory field of 0.5-0.7 kV/cm caused by the deposited electric charge on the surface of dielectrics from the preceding discharge phase. Our investigation completed the picture of the development of CDBD by lighting up the CRE in the previously dark phase of the discharge.

The last paper concerning CDBD's physics utilises the experimental technique developed with Assoc. Prof. Jozef Ráhel', we have called the 'bino-box'. The principle of this optical diagnostic technique stands in the simultaneous dual-beam spectrally filtered imaging of the discharge, when only a single ICCD camera with high spatiotemporal resolution is available. After months of iterations, we have obtained spectrally resolved image stacks that were spatially and temporally registered using the bino-box technique and were suitable for further analysis using spectral methods.

We have utilised the described method in **(Čech et al. 2018)** to follow the fully 2D resolved temporal evolution of the electric field in the ionisation waves in coplanar DBD generated in helium, see Fig. 11. The experimental method follows the spatiotemporal evolution of helium atomic emission lines, 667.8 nm (HeI $2^1P–3^1D$) and 728.1 nm (HeI $2^1P–3^1S$) using a pair of interference spectral filters providing satisfactory isolation of the studied emission lines. After careful spectral calibration, we could use a polynomial fit formula to calculate the electric field using the helium lines ratio method developed by our colleagues in Belgrade (Ivković et al. 2014), based on the collisional-radiative model, which they have validated through the Stark polarisation spectroscopy.

For the experimental success, the repetitive discharge conditions were crucial. After systematic testing, the highly stabilised diffuse discharge regime was obtained for a discharge geometry with a 4.75 mm electrode gap, using a sinusoidal HV of 10 kHz frequency and 1.5 kV amplitude and 550 sccm of Helium flow rate. The discharge breakdown jitter, as low as 50 ns (3σ of discharge jitter), enables the adoption of highly accumulated ICCD measurement of the discharge emission and sets the temporal resolution. The macrophotography setup enabled the spatial resolution up to 20 μm (lens aberrations and ICCD spatial resolution).

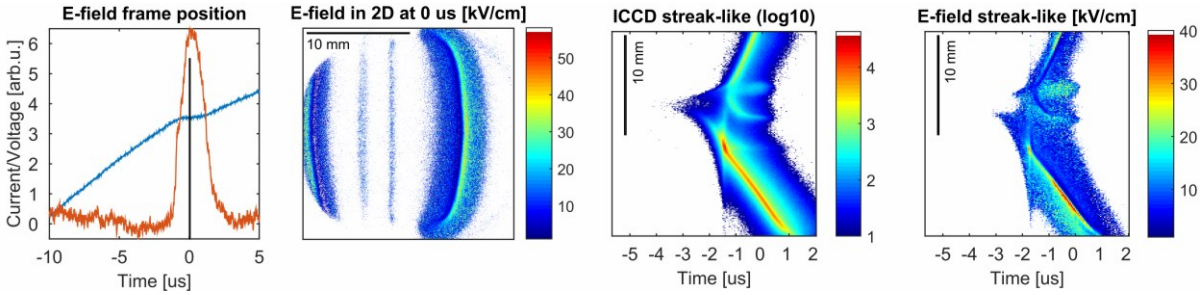

Figure 11 The result of 2D-resolved temporal evolution of electric field determined using helium lines ratio; (left part): 2D map of electric field at current peak maximum (0 μs) with corresponding current (orange) and voltage (blue) waveforms; (right part): Streak-camera representation of 1D temporal development of total discharge intensity and electric field, the spatial axis corresponds to central horizontal cross-section of depicted 2D frame. Source: Author

The peak reduced electric field was registered at the cathode-directed ionising wave, and its values were 60-130 Td with the maximum at the edge of the cathode. At the moment of the electric field maxima, we also observed a local peak on the discharge current waveform. At this moment, the rate of current increase changes to a lower rate. Considering the shape of electric field lines and the behaviour of CDBD (bow-like shape of discharge protruding above the dielectrics at the interelectrode gap), we can attribute the moment of the local maxima of the electric field to the moment when the first ionising wave bridging the electrode gap touches the dielectrics. The ionising waves then travel along the dielectric as a strong cathode-directed ionising wave (velocity of 3.7 km/s) and anode-directed ionising wave (velocity of 4.4 km/s), respectively, which was about an order of magnitude weaker (in emission). ADIW reduced electric field peaked at approximately 60 Td, i.e. only half of that of the CDIW. Interestingly, the ionising waves' velocities were lower than the electron drift velocity at the measured electric field (around 300 km/s at 100 Td). The discrepancy could be explained by the fact that the electric field determined using the emission lines ratio is the magnitude of the field. However, the electric field, being a vector quantity, has, besides its magnitude, also a certain direction. In the case of CDBD, the major component of the electric field is the normal component perpendicular to the dielectrics (plane defined by the dielectric plate). The tangential component along the dielectric plate responsible for the discharge propagation is the smaller one. The cathode-directed ionising wave's propagation can also be viewed as a slow displacement of the formed cathode fall.

An important note regarding the spatially resolved helium lines ratio method must be added. During the experiments, we have realized that an exact spatiotemporal calibration will be necessary due to high sensitivity of the line-ratio model in studied range of electric field of 3-40 kV at temperature of 310 K. Using the synthetic test on the acquired image stacks we have realized that the electric field estimation is extremely sensitive to the temporal and (to a slightly lesser extent) also spatial alignment of acquired image stacks. Even a single frame temporal misalignment led to significant distortion of the derived electric field – the estimated field values increased considerably, with maximum values being an order of magnitude higher. This sensitivity is expected due to the high velocity of the ionising waves we have studied. The pixel shift of the image stack also resulted in a deviation of estimated electric field values. However, the single pixel misalignment did not significantly distort the spatiotemporal evolution of ionising waves but shifted the highest electric field values within a 10% margin. Artificial decimation of spatial or temporal resolution led to systematic underestimation of electric field values, and for temporal resolution, also to a rapid loss of temporal details. These findings forced us to do several iterations to improve the experimental procedure. Despite their lower spatial resolution, the bino-box measurements enabled us to correlate the temporal evolution of image stacks. Image stacks of the respective spectral windows were acquired independently due to the chromatic aberration of a professional macro lens, preventing a common focus for both spectral windows. The four registration marks were made on the dielectric plate for precise image stack alignment and used for programmatic image reg-

istration and affine transform of the spatial coordinates of image stacks. Using all the mentioned calibration procedures, we have finally obtained well-aligned image stacks representing the spatiotemporal development of each helium line intensity. And finally, the 2D resolved and temporally resolved electric field development.

3.1.3 Applications of DCSBD

The fundamental research during the DCSBD development phase was accompanied by application-oriented research, as the applications have been the cornerstone of this technology. The large-scale, fast and efficient surface treatment of temperature-sensitive materials was the utmost goal of the DCSBD research effort (Černák et al. 2009). The author selected two annotated papers focused on the niche topic of material treatment in a reducing atmosphere containing hydrogen gas.

⁂

The first paper utilising DCSBD in a reduction atmosphere is **(Prysiazhnyi et al. 2014)**. This research paper, authored by Dr. Vadym Prysiazhnyi, his colleagues and the author, represents the proof-of-concept of the plasma-induced metal-oxide reduction using DCSBD operated in a reduction atmosphere of pure hydrogen. The thin Cu_2O layer was prepared by oxidation of the PVD-deposited Cu film on a silicon wafer. The same DCSBD discharge configuration was used for oxidation and subsequent reduction of the copper layer. The oxidation was done in ambient air, while the plasma-induced reduction was done in pure hydrogen atmosphere.

The surface analyses were used to follow the plasma-induced surface modifications. The XPS analysis confirmed the successful plasma reduction of copper oxides. The plasma-induced reduction process results in more than doubling the percentage of copper atoms in the surface layer, while simultaneously reducing oxygen, carbon and nitrogen atoms in the surface layer.

The phase-resolved optical imaging revealed interesting properties of H_2-DCSBD, favourable for uniform large-scale plasma treatment of surfaces. The behaviour of microdischarges constituting DCSBD discharge changed considerably when generated in a hydrogen atmosphere. Unlike in ambient air or nitrogen atmosphere, we could not stabilise restriking microdischarges in a particular position above the surface of the dielectric barrier. Localisation of microdischarges for many discharge periods leads to local temperature buildup and/or overtreatment, resulting in surface damage. The microdischarges in H_2-DCSDB displace fast along the electrode strips, further supporting the treatment homogeneity. One of the possible causes of this phenomenon could be found in the considerably higher thermal conductivity of hydrogen gas to nitrogen or oxygen (approximately 7x), which prevents the hot gas channel buildup that stabilises the microdischarge (see the annotated paper **(Ráheľ et al. 2016)** above). The second interest-

ing phenomenon of H_2-DCSBD was the highly diffuse nature of the surface part of microdischarges, contrary to air or nitrogen, where the highly branched, distinct structures were observed, see Fig. 12 and the regular pattern observed above instantaneous cathode. This further supports the even surface treatment in H_2-DCSDB.

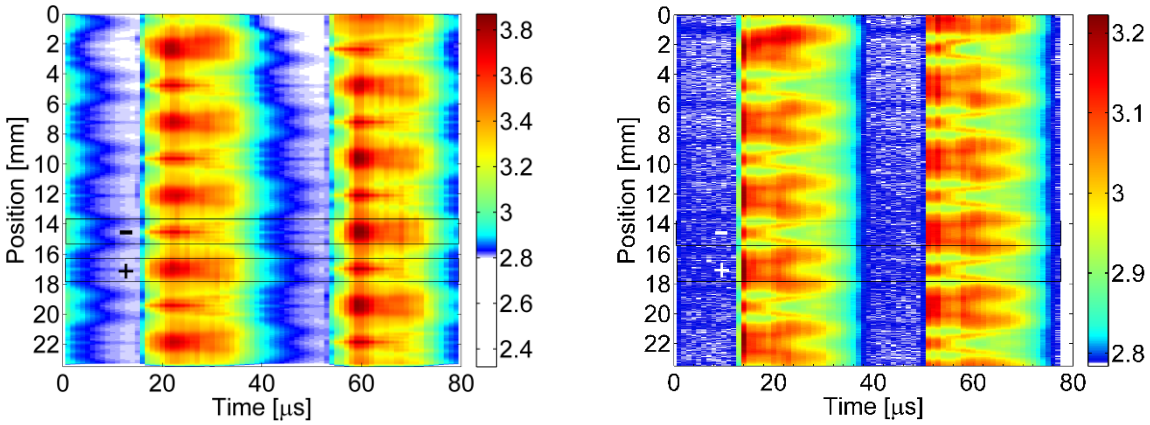

Figure 12: Collective behaviour of DCSBD microdischarges visualised using accumulated phase-space intensity maps: DCSBD in pure N_2 (left) and pure H_2 (right); colour scale represents $\log_{10}$ of emission intensity. One electrode pair position is given with the indication of instantaneous polarity during the first half-period. Source: Author and Antonín Brablec

After the first hydrogen experiment, research on hydrogen-nitrogen gas mixtures followed, and microdischarge behaviour and plasma-induced surface modifications were studied. The experience gained in the research of DCSBD in a hydrogen-nitrogen atmosphere was utilised in dry etching of silicon oxide[8] (Krumpolec et al. 2017), achieving a promising etching rate of 1.5 nm/min. The functionalisation of nanodiamond nanoparticles using DCSBD in hydrogen-nitrogen gas mixtures was investigated in collaboration with the team led by Dr. Alexander Kromka from the Institute of Physics of the Czech Academy of Sciences. The results were published in the two research papers (**Kromka et al. 2015,** Jirásek et al. 2016). The first, annotated paper **(Kromka et al. 2015)** proved the concept of DCSBD-induced nanodiamonds hydrogenation, and the second paper (Jirásek et al. 2016) investigated the surface amination of the nanodiamonds.

The study (**Kromka et al. 2015**) explores the low-temperature plasma-induced hydrogenation of nanodiamonds using DCSBD. The DCSBD reaction cell was developed to enable controlled operation in pure hydrogen at atmospheric pressure. Its modular de-

[8] The author was involved in the plasma treatment design and experiment and interpretation of results concerning the H_2-DCSBD properties.

sign enabled batch processing of nanoparticles and optical diagnostics through a sapphire glass window. The thermally annealed detonation nanodiamonds were subjected to plasma treatment at 1.8 and 3.1 W/cm^2 power levels. We have observed strong and dynamic interaction of the microdischarges with the nanoparticles. After the discharge ignition, the discharge-induced transport of the nanoparticles occurs. Part of the nanodiamonds was pushed outside the discharge; however, the remaining nanoparticles were immobilised at the active discharge zone above the dielectrics and aligned along the microdischarges. This behaviour was probably caused by the combination of the charging of the particles and the plasma-induced momentum utilised in plasma actuators.

The FTIR spectroscopy confirmed the presence of CH_2 and CH_3 surface groups on hydrogen plasma-treated nanodiamonds at simultaneous reduction of C=O and C-O-C groups. The OES of the discharge with nanodiamonds confirmed the expected molecular and atomic hydrogen emission; however, no OH emission was observed. The traces of nitrogen and oxygen, found in the discharge emission spectrum, could result from processing gas impurities and air desorption from the treated nanoparticle surface. Another supportive evidence of the plasma-induced processes was found using the OES of the effluent gas, which was combusted as a pre-emptive safety measure. The flame properties changed considerably after the treatment onset and gradually returned to the original state with the ongoing treatment time. The blackbody radiation model was used to estimate the flame temperature (a small amount of nanodiamond particles was carried in the effluent gas), which increased from 1500 K to 2200 K after the treatment onset. The flame appearance was used to determine the combustion stoichiometry – the diffusive plum shape rapidly evolved into a very bright jet structure, indicating a rapid combustion stoichiometry change from lean combustion towards oxygen-rich fuel mixture. Both results support the estimated dynamics of the plasma hydrogenation process – the rapid outgassing of the nanodiamond particles' surface at simultaneous replacement of oxygen atoms by hydrogen ones. The treatment was done at a moderate temperature of 70 °C. Even the short treatment time of 5 minutes was sufficient for creating detectable --CH_x functional groups, which was a promising result considering the processing throughput compared to standard microwave plasma treatment at vacuum conditions. Another interesting result was that the hydrogen was predominantly accumulated in the amorphous detonation nanodiamond shell, which could be interesting for hydrogen-storage applications.

The H_2-DCSDB research continued further. Before the author's scientific effort was refocused towards plasma treatment of liquids, he was involved in the pilot experiments of PTFE surface functionalization and polymer etching experiments, which were further investigated by the team of Prof. Černák. The author was also supervising a Master thesis of Michal Štipl (2019), which deepened our understanding of CDBD behaviour in binary mixtures containing hydrogen gas. There, the dedicated ring electrode setup was adopted to study the memory effect causing the discharge pattern (de)stabilisation and the influence of H_2 admixture on the behaviour of microdischarges. The binary mixtures

of argon or nitrogen with an admixture of 1 to 8 % hydrogen and a mixture of argon and nitrogen were studied. The mobility of microdischarges was investigated using a special feature of the interline ICCD camera, enabling the acquisition of a second image with incremental delay from 1 μs. This enabled the programmatic acquisition of the discharge pattern evolution on the time scale from the half-period to 100 of the HV periods, i.e. more than milliseconds. More than 100 experimental conditions were measured and evaluated, including HV frequency, amplitude and composition of discharge atmosphere. Focussing only on the influence of hydrogen admixture (units of percent), we can conclude that in the case of nitrogen as the carrier gas, the hydrogen admixture led to lower displacement of the discharge pattern, i.e., higher spatial stability. On the contrary, the increase of HV frequency from 16 to 57 kHz led to the destabilisation of the discharge pattern, i.e. higher mobility of microdischarges. When the argon was used as the carrier gas, the amplitude of HV necessary to sustain the discharge was approximately 3 × lower, and the microdischarges' density along the circumference of the ring-shaped electrodes was also lower. Hydrogen admixture led to discharge pattern stabilisation, i.e., lower microdischarge mobility, also for the argon carrier gas. The effect was substantial even for a 1% hydrogen admixture. In 8% hydrogen mixture and at a 30 kHz frequency, the angular displacement of the discharge pattern was even less than a milliradian during a 4-ms wide temporal window, which could be beneficial for further spatiotemporal studies of the microdischarges in highly accumulated experiments.

ⱾⱾⱩⱾⱾ

The results of coplanar discharge diagnostics, summarised in this thesis, and an increasing number of comments from the research community on the term ‘diffuse’ in the nomenclature of DCSBD discharge led us to further investigations. The key dispute was whether the term ‘diffuse’ could also be used for macroscopically uniform CDBD, despite its inherent nature of spatiotemporally constricted individual microdischarges. The author, together with Assoc. Prof. Rahel investigated the diffusiveness of DCSBD under various conditions, and the results were presented at the HAKONE XV conference in 2016 (Ráhel’ et al. 2016). The truly diffusive regime of coplanar barrier discharge without constricted filaments crossing the interelectrode gap was achieved in helium and neon, and only in a specific parametric window (HV frequency, amplitude and power, respectively). This diffuse regime was utilised for charge relaxation event discovery and 2D resolved electric field measurements of helium CDBD (see the annotated papers **(Morávek et al. 2016, Navrátil et al. 2017, Čech et al. 2018)**). Nonetheless, the DCSBD discharge was primarily developed for fast and homogeneous treatment of various, temperature-sensitive materials, such as nonwovens, textiles, polymeric foils, etc. From that perspective, the DCSBD discharge consists of many individual microdischarges that interact with each other along the electrodes (adjacent microdischarges) and across the electrodes (opposite microdischarges). The microdischarges interact, e.g., through the photons (significantly in the UV range), space charge, surface charge, or residual heat. These effects are commonly referred to as the ‘memory effect’.

The individual microdischarges consist of spatially constricted hot filaments crossing the interelectrode gap and surface discharges along the dielectrics above the electrode footprints. While the filamentary part could reach more than 300 °C for wide electrode gaps, the surface part of the discharge follows the dielectric surface temperature, usually between 50 and 70 °C. The unique feature of DCSBD generated in the ambient atmosphere lies in enhancing the surface part of the discharge with the increasing gap voltage. This surface part is macroscopically, i.e. visually, homogeneous, or let's call it 'a diffusive'. However, when investigated using a high-speed camera, e.g., ICCD, even this visually homogeneous part could break down into a complex system of fibrous surface discharges in, e.g., air, argon, or nitrogen working gas. The collective interactions among surface discharges, e.g. in nitrogen, could even result in complex surface discharge patterns. We have observed the system of three equidistant parallel strips of luminous channels above electrodes in nitrogen DCSBD. From this point of view, only in a hydrogen and oxygen atmosphere at atmospheric pressure, we have observed that the surface part of the DCSBD lacks a distinct structure or branching and is visually diffusive on a microscopical, single microdischarge level. Moreover, the microdischarges in a hydrogen atmosphere are highly mobile, contributing to the visually homogeneous/diffuse character of DCSBD. But we must note here that the DCSBD / CDBD discharge diagnostics were and still are dominantly performed without the treated surface. This is understandable, as the dominant discharge information is acquired through discharge light emission. However, the completely different situation represents the discharge behaviour and its appearance when the treated surface is brought into the near vicinity of the discharge. And this is the use case of DCSBD. We used a transparent glass plate and spacers to cover the dielectric plate of DCSBD. Then we investigated the structure of DCSBD in contact with the additional nonconductive surface above the ceramic plate, see Fig. 13. The narrow gas gap of 0.1 mm thickness was chosen to be lower than the uncovered DCSBD plasma layer thickness of 0.3 mm in the ambient atmosphere[9].

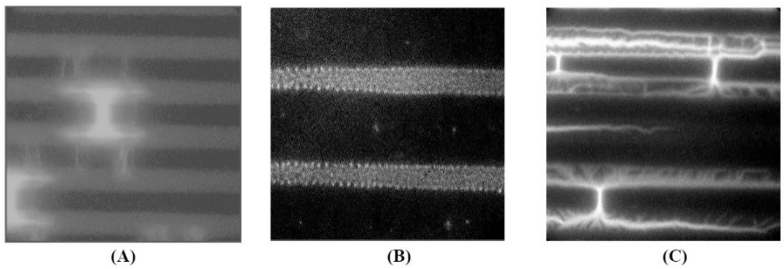

Figure 13: Single period ICCD acquisition (exp. time 100 µs) on DCSBD formed in narrow gaps: (A) nitrogen; (B) air – magnified 2.5×; (C) argon. Source: Author and Jozef Ráheľ (Ráheľ et al. 2016b)

[9] This value resulted from spatially resolved emission spectroscopy probing the vertical profile of DCSBD plasma layer. The experiment was conducted by the author and Dr. Andrej Buček at DPPT (former DPE).

We have imaged the discharge pattern using an ICCD camera with a single period resolution. In the case of argon gas, the filamentary microdischarges crossing the interelectrode gap were still present. Compared to the uncovered DCSBD, the density of observed filaments was lower, and the surface part of microdischarges was slightly diffusive, but still highly fibrous and branched. In nitrogen, the typical H-shaped microdischarges crossing the electrode gap could still be observed; however, a uniformly glowing strip was observed above the electrode footprints, i.e. places where the highly structured surface discharges were observed in the uncovered DCSBD configuration. The most interesting discharge pattern change was observed in ambient air DCSBD. When generated in a narrow gas gap, the microdischarges pattern disappears. Instead of filaments crossing the interelectrode gap, the fine-spotted, luminous strips were observed above the electrode footprints. The discharge probably transitions into some hybrid CDBD-VDBD regime, considering the electric field distortion resulting from the surface charging of the glass surface brought into contact with the DCSBD. Our high-speed camera investigation gave us compelling evidence that even a microscopically uniform diffuse plasma can be routinely formed in narrow gaps at conditions similar to those used in plasma treatment setups.

⁂⁂⁂⁂⁂

The last annotated paper, closing the DCSBD chapter of the thesis, will be devoted to the niche study of CDBD generated under low-pressure conditions. The DCSBD unit was developed to produce a plasma layer[10] of high energy density intended for the high-speed inline industrial processing of flat materials like glass, foils or textiles. And this inherently required atmospheric pressure operation conditions. However, the passively cooled laminated small-scale coplanar DBD electrode system was developed by the team led by Assoc. Prof. Pavel Sťahel in 2014, and it was later found suitable also for the vacuum operations. In the same year, 2014, another team led by Assoc. Prof. Pavel Sťahel patented a unique way of vacuum chamber cleaning method based on photocatalysis principles[11]. In the follow-up research, the plasma decontaminator based on the newly developed laminated CDBD system was successfully tested for an electron microscope vacuum chamber.

To better understand the behaviour of CDBD under low-pressure working conditions, a series of experiments on the characterisation of the discharge under wide pressure-range conditions was performed, resulting in the publication **(Čech et al. 2017)**. The studied plasma source was based on the coplanar DBD electrode arrangement and could operate at sub-Pa to super-atmospheric conditions.

[10] Though the DCSBD probably does not fulfil the strict 'plasma' definition.

[11] Czech patent CZ 305097 *Method of reducing or removing organic and/or inorganic contamination of vacuum system of display and analytic devices and apparatus for making the same*

Temporally unresolved orthogonal imaging and phase-resolved ICCD imaging were adopted to follow plasma geometry and microdischarge behaviour. Together with breakdown voltage measurements, the discharge diagnostics revealed three operational regimes of the discharge: 'high-pressure,' 'transitional', and 'low-pressure' with fuzzy boundaries at pressures of approximately 10 kPa and 1 kPa, when operated in a nitrogen atmosphere, see Fig. 14 depicting microdischarge structure changes with the pressure.

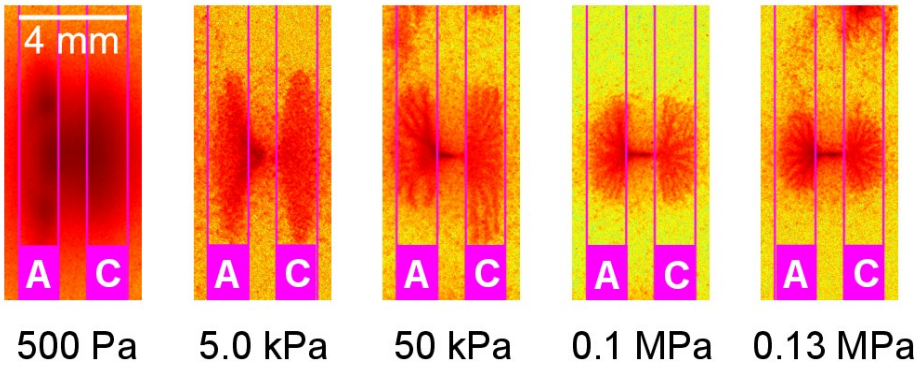

Figure 14: ICCD images of individual microdischarges concerning the working gas pressure. Pictures taken in a single half-period of the discharge. Polarity and edges of electrodes are labelled A (anode) and C (cathode). Source: Author (Čech et al. 2017)

The 'high-pressure' regime is a typical regime of CDBD operation. The discharge consists of numerous nanosecond microdischarges that form a 10-100 μm thin filament bridging the interelectrode gap and creating a highly branched structure of surface discharges above the electrodes. The shape of the microdischarges resembles a bow-like protrusion above the dielectrics, resulting in a sub-millimetre-thin plasma layer formation. In the photography of the discharge, the distinct and sharp images of microdischarges are visible, indicating the low mobility of individual microdischarges.

When the gas pressure is gradually reduced, the filament diameter increases, the surface part of the microdischarge starts spreading wider along the electrodes, and its branched structure gradually transforms into the diffusive spots. This 'transitional' regime occurred at a 10-20 kPa pressure. The plasma layer is, however, still sub-millimetre thin until the pressure is reduced to approximately 1 kPa. Below this boundary pressure, the discharge enters the 'low-pressure' regime.

With further pressure decrease, the so-far thin plasma layer gradually spreads into the half-space above the dielectric plate. The microdischarges became blurry, and with power increase, a continuous luminous layer is formed at the dielectric surface above the electrodes. We have found that the thickness of the plasma layer (forming finally a plasma plume at a low-pressure regime) scales inversely proportional to the gas pressure. In contrast, the width of the microdischarge channel scales inversely proportional to the square root of the gas pressure.

We have also found that the breakdown voltage rapidly decreased from approximately 8 kV at atmospheric pressure conditions to less than 1 kV below a gas pressure of 1 kPa. The canonical form of the Paschen law cannot fit the experimental data. We have realised that the microdischarge channel length deviates considerably from the distance between the electrodes (the interelectrode gap), as the arched 'bow-like' structure of the microdischarges channel is protruding higher above the dielectric plate with pressure decrease. Dr. Zdenek Bonaventura proposed modifying the canonical form of the Paschen law, introducing an effective electrode distance based on a parabolic approximation of the microdischarge channel shape. The measured pressure dependence of the breakdown voltage follows the proposed modified Paschen law.

The measured data can support the tailored design of the low-pressure plasma units based on a coplanar DBD arrangement.

3.2 Conclusion to the DCSBD Part

The broad discharge conditions were investigated during the development of DCSBD on a dedicated simplified electrode arrangement as well as on a full-scale electrode arrangement. The results of the diagnostics on model CDBD served the DCSBD development team at MUNI for evidence-based evolution of DCSBD electrode and dielectrics configuration. During this research, two novel phenomena were described – the role of residual heat on the spatial stabilisation of filaments (memory effect) and the ultra-low intensity process preceding the Townsend avalanching phase – the Charge Relaxation Event discovered in the dark phase of diffuse CDBD in helium. From the broad spectrum of DCSBD applications, the niche research utilising DCSBD in a hydrogen atmosphere was commented on.

The first part of the thesis comments on the discharges in contact with solids, more precisely with solid surfaces. However, the presented dielectric barrier discharges and numerous other discharge systems were also utilised for the plasma treatment of liquids, which is the topic of the second part of the thesis.

4 Part II: Plasma Treatment of Liquids: CaviPlasma Technology

The plasma treatment of liquids, especially water, has been a subject of research effort for more than two decades (Bruggeman and Leys 2009, Bruggeman et al. 2016). The research in this field is driven by the wide spectrum of potential applications. Plasmas in contact with liquids produce complex mixtures of biologically and chemically active species. The most common active species used in plasma treatment of liquids are reactive oxygen and/or nitrogen species, commonly referred to as RONS (Reactive Oxygen and Nitrogen Species), such as hydroxyl radical, singlet oxygen, ozone, hydrogen peroxide and generally the per-oxo compounds, or nitrogen oxides, but also the intense UV radiation (Bruggeman and Leys 2009, Locke et al. 2025, Montalbetti et al. 2025, Šunka et al. 1999, Machala et al. 2019, Gorbanev et al. 2018b). These reactive agents alone, or in combination, have been extensively studied for, e.g., wastewater remediation, as the so-called Advanced Oxidation Processes (AOPs) (Miklos et al. 2018). The great advantage of plasma-liquid systems in comparison to AOPs consists in the synergistic action of all the mentioned agents and also the electric fields, electrons or shockwaves (Bruggeman et al. 2016). Plasma technology brings the benefit of in-situ tailored production of reactive species; however, the efficient transport of produced species is a challenging task (Locke et al. 2025).

Plasma treatment was found effective in the remediation of (waste)water from biological and/or chemical contaminants, especially in low concentrations, i.e., micropollutants (Foster 2017, Topolovec et al. 2022, Magureanu et al. 2021, Jiang et al. 2014, Gerrity et al. 2010). However, the plasma-liquid interactions have a much broader potential, and this field has become highly cross-disciplinary (Rezaei et al. 2019). Biomedical applications (Kaushik et al. 2018, Machala et al. 2019, von Woedtke et al. 2025), agricultural applications (Puač and Škoro 2025, Thirumdas et al. 2018, Graves et al. 2019), plasma-chemical synthesis (Rezaei et al. 2018, Park et al. 2019, Yayci et al. 2020), or nanoparticle synthesis (Mariotti et al. 2012, Liguori et al. 2018) are only excerpts from the extent of this disruptive plasma field.

The industrial demands on plasma-liquid technology remain valid throughout the decades of intensive research, i.e., the energy efficiency (or better the total cost of ownership) in combination with upscaling to industrially relevant (large) volume of treated liquid. The author finds the challenges of application-oriented research in the combination of the complexity of plasma-liquid interactions and the technological demands, i.e., the selection from the pool of plasma sources and tailored treatment conditions, ensuring the plasma-chemical generation of a sufficient quantity of desired active species, often in the direct interaction of the discharge with the liquid, and finally the transport of the active species into the liquid.

The physically interesting approach to the efficient plasma-liquid interactions is the generation of reactive species by electrical discharges in the liquid/water phase (Chauvet et al. 2020). However, the operating conditions of discharges in liquid phase are challenging, considering the high breakdown strength of liquids (>1 MV/cm (Šunka et al. 1999)). The discharge breakdown in a genuinely liquid environment was achieved by ultra-fast high voltage pulses imposed on a highly curved electrode immersed in the liquid (Šimek et al. 2017, Grosse et al. 2019). This approach is scientifically interesting for the achieved exotic discharge conditions, e.g., the pressure on the order of GPa, and the challenging plasma diagnostics of the discharge initiation and propagation (Grosse et al. 2021, Šimek et al. 2020). The hydrogen peroxide production efficiency was reported to be 2 g/kWh for the nanosecond pulsed discharges in water (Chauvet et al. 2020), which is close to the other plasma-liquid systems (Locke and Shih 2011). However, the scalability of this technical solution could represent a challenging task. The large-scale industrial applications will probably not be feasible for these plasma-physically highly interesting discharges in the near future.

The remaining option for the plasma-liquid systems was the utilisation of a subsidiary gas-phase environment, where the electric discharges could be easily sustained and which enables the adoption of a broad spectrum of available plasma sources (Bruggeman et al. 2016). The crucial performance aspect, however, remains: the efficient transport of plasma-produced species into the liquid (Locke et al. 2025, Janda et al. 2025). The gas-phase introduction reduces breakdown strength to technically feasible values ranging typically from 1 to 10 kV/cm. Tuning the gas-phase composition and plasma parameters also enables the tailored production of (re)active species in plasma-treated liquid, according to the application needs (Montalbetti et al. 2025).

The broad overview of the representatives of the gas-phase discharges-to-liquid systems was given in the review by Bruggeman and Leys (2009). The spectrum of setups investigated include plasma jets in contact with the liquid surface or submerged in liquid, discharges generated remotely above the liquid surface (liquid surface does not serve as the electrode) or in direct contact with the liquid surface, where the liquid/electrolyte serves as the electrode and discharges are generated, e.g., against the liquid surface, or in bubbles (Bruggeman and Leys 2009).

However, the efficiency of the plasma systems (Stefan 2017) relies on the efficient transport of active particles into the bulk liquid. These gas-liquid transport processes through the interfacial layer on the gas-liquid boundary (Locke et al. 2025) are generally very complex, and despite the research effort, they are still not fully understood. Diagnostics of the transport processes must be performed on the ns time scale and in a thin micrometre-range liquid layer. The fluxes of neutrals, radicals, and charged species (as well as photon flux, especially UV photons, and also a heat flux) react with or act on the actual state of the liquid surface, being an electrolyte and often a polar one, e.g., water – see, e.g. the reviews (Janda et al. 2025, Locke et al. 2025, Bruggeman et al. 2016, Stefan 2017). Moreover, the interfacial layer cannot be treated as homogeneous, and the complex two-phase environment could be formed on the microscopic level, see, e.g., the

study on the dynamics of micro and nanobubbles in the ns-pulsed discharges (Hoffer et al. 2022). Moreover, even the water properties under discharge conditions are not well understood (Vanraes and Bogaerts 2018).

However, general principles can be assessed even if detailed knowledge of the transport processes is unavailable. Assuming the plasma production of (re)active species in the volume of the gas phase, the produced species have to be transported through the gas-liquid interfacial layer in the volume of liquid (Bruggeman et al. 2016, Locke et al. 2025). We can consider a simple model that could point the way towards more efficient plasma-liquid processing. The flux of plasma-originated species to the gas-liquid boundary will determine the total number of (re)active particles dissolved in the volume of the liquid. Then the concentration of the (re)active particles in the liquid will be proportional to the (gas) particles flux density and the surface area of the boundary. So, to increase the liquid treatment efficiency, we can increase the concentration of plasma-generated particles[12] and/or enlarge the gas-liquid boundary surface area. The latter approach is adopted in discharges in multi-phase environments (Bruggeman et al. 2016). There are two principal approaches to enlarge the surface area of the gas-liquid boundary:

- Systems based on nebulization of the treated liquid: The liquid in the form of mist or small droplets (aerosol) has a significantly increased bulk-to-surface ratio, and the transport efficiency is high (Janda et al. 2025). The total volume of liquid treated per unit time is, however, limited for plasma-aerosol systems, but this could also be seen as the opportunity for controlled micro/nanomaterials and niche applications (Stancampiano et al. 2019, Janda et al. 2025).
- Systems utilising gas bubbles or microbubbles immersed in the water: The discharge is either generated in the bubbles, or the discharge effluent is bubbled through the liquid (Bruggeman and Leys 2009). The gas phase formation in the liquid (bubble) can also be initiated by the high voltage imposed on the electrodes prior the breakdown, see, e.g., (Krčma et al. 2018) for DC pin-hole system, or (Lukes et al. 2013) for capillary/diaphragm discharge. The energy efficiency of the treatment is above average for bubble systems (Locke and Shih 2011). The volume per unit time performance of the bubble systems remained, however, typically in the range 10-100 mL/min (Gao et al. 2022, Wang et al. 2025), and this was the situation in which the CaviPlasma technology **(Čech et al. 2024, 2025)** was invented. Recently, the bubble system was reported (Saedi et al. 2025) with a volume capacity up to 120 L and flow rates up to 16 L/min. The system utilises multiple Venturi tubes in parallel for bubble generation and suction of corona-treated gas. Despite the re-

[12] The effective lifetime of generated species and their transport towards the liquid interface have to be also considered, and the interaction time as well (Janda et al. 2025).

ported volume/flow rate figures being close to the cavitation plasma systems **(Čech et al. 2024)**, the performance measured by RONS concentration in the liquid phase was rather limited, i.e., approx. 0.1 μM of H_2O_2 and 10 μM of NO_3 after 10 min treatment of 1 L of tap water with the plasma input power 25 W, see (Saedi et al. 2025, fig. S6).

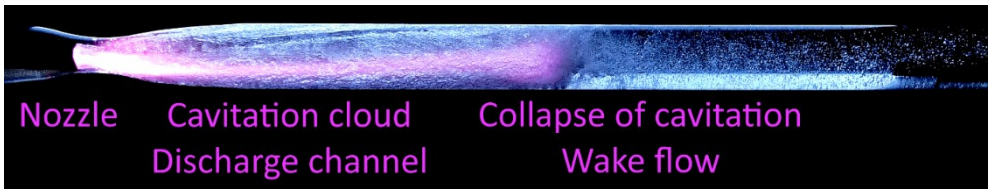

Figure 15: CaviPlasma - 1st generation unbridged regime in tap water. Source: Author

At the origin of the application-oriented research of CaviPlasma was the effort to enhance the efficiency of the cavitation technology investigated at Brno University of Technology and the Institute of Botany, Academy of Sciences of the Czech Republic (Jančula et al. 2014). The cavitation jet water treatment was found effective for the management of cyanobacterial blooms, when the removal of biomass from the water column was successful; however, the metabolic apparatus of cyanobacteria was not affected, and the growth of cavitated biomass was observed (Jančula et al. 2014). The goal of the plasma application effort was the enhancement of the cavitation jet efficiency with the ability to inhibit cyanobacteria's metabolic activity by plasma-produced ROS. The collaboration of research teams on CaviPlasma was based on the previous cooperation of the team at Masaryk University and the Brno University of Technology on the computational evaluation of fluid dynamics in the rotating gliding arc air decontaminator developed at MUNI (Čech et al. 2019).

In 2018, the team at MUNI, led by Assoc. Prof. Sťahel joined the teams led by Assoc. Prof. Rudolf at BUT and Prof. Maršálek at IBOT CAS in the common effort to merge the two worlds – the fluid mechanics with the outstanding cavitation research at BUT and the highly developed proficiency of application-oriented plasma research at MUNI. The research effort at MUNI led to the successful initiation of electric discharge in the water vapour phase inside the liquid, i.e., in the so-called hydrodynamic cavitation cloud, see Fig. 15. After intensive research, the cavitation-plasma treating unit was developed, which combines the best of both fields, boosting the performance of existing plasma-liquid approaches. Its superb efficiency of cyanobacteria decontamination, verified by the IBOT team, paved the way for further joint-research efforts of MUNI, BUT and IBOT teams. The joint patent application was prepared and filled in 2019, and the patent was granted in late 2020 (Rudolf et al. 2019). The technology was later given the name CaviPlasma. Its first implementation could treat 3 L of water at a flow rate of approximately 1.6 m^3/h by the electric discharge with a power input of 0.4 kW **(Maršálek et al. 2020)**. These numbers leverage the plasma-liquid treatment potential at least by an order of magnitude in volume/flow rate performance, while keeping very promising treatment efficiency among other plasma-liquid systems (Locke and Shih 2011, **Čech et al. 2024, Čech et al. 2025**).

The potential of this new technology was recognised at an early stage by the technology transfer experts, awarding CaviPlasma the first place at Transfera Technology Day 2020[13], and also by the expert jury, awarding CaviPlasma the Grand Prix of the Brno International Industrial Fair 2021[14]. In 2023, the first international patent in Israel was granted (IL 293579), and in 2024, the Canadian and European patents followed (CA 3,164,469 and EP 4 073 002 B1). The high societal impact of the CaviPlasma technology was confirmed by the Technology Agency of the Czech Republic (TACR), which awarded the project *Hybrid plasma-chemical oxidation for advanced decontamination of micro-pollutants and waste water disinfection* (TACR SS01020006) the 2024 best applied project prize in the category 'Society', and the project became the absolute winner of the 2024 TACR awards – winning the Czech Idea 2024 prize (orig. *Český nápad 2024*)[15]. The awarded project was based on the CaviPlasma technology.

The promising potential of CaviPlasma was verified in a wide range of decontamination tests on pharmaceuticals, hormones and pesticide residues[16]. The biocidal effects on cyanobacteria and algae were confirmed; see the annotated papers **(Maršálek et al. 2020, Čech et al. 2020)**. However, the superb biocidal effect was also confirmed on the gram-positive and gram-negative bacteria, including the multi-resistant strains of human pathogens[17]. The interesting results were achieved in research focused on the recirculating aquaculture systems, which was led by Dr. Jan Mendel (Institute of Vertebrates of the Czech Academy of Sciences). We have achieved eradication of the Salmonidae bacterial pathogens (*sp. Aeromonas* and *Flavobacterium*) and the *Ichthyophthirius*, the potent fish parasite, that threatens the fish rearing units (two research papers are submitted, or under review process).

The promising results were also achieved in agriculture. The author led the project *Increasing the commercial potential of plasma-treated water technology in the agro-industry by verifying the health safety of such treated plant production* (TACR, MUNI/31/06202105/2021). The project verified the potential of plasma technology in horticulture, especially in recirculating growing systems, see Fig. 16 demonstrating the potential of CaviPlasma on the suppression of microorganisms growth in recirculating growing systems.

[13] See the Transfera.cz web page (in Czech): https://www.transfera.cz/akce/akce/transfera-technology-day/rocnik-2020/

[14] BUT report on the event (in English): https://www.fme.vutbr.cz/en/veda/oceneni/70038

[15] See the report of the Technology Transfer Office of MUNI (in Czech): https://www.ctt.muni.cz/aktualne/aktuality/hlavnim-vitezem-a-drzitelem-ceny-cesky-napad-v-ramci-dne-ta-cr-2024-se-stala-technologie-z-mu

[16] Results on pharmaceuticals presented at CESPC9 conference (Čech et al. 2022a); unpublished data

[17] Results on multi-resistive strains presented at FSO2023 conference (Čech et al. 2022b); unpublished data

The plasma treatment of hydroponic and aquaponic growing solutions resulted in a substantial (15-50%) decrease in the abundance of nitrates in lettuce and basil planted in plasma-treated solutions. Ongoing agri and aquacultural research based on both discoveries is in progress.

The first and second annotated papers in this second part of the thesis **(Maršálek et al. 2020, Čech et al. 2020)** are the very first papers on the CaviPlasma technology and cover the application of CaviPlasma on cyanobacteria and algae.

Figure 16: The cleaning effect of CaviPlasma treatment on a hydroponic recirculating system: no-treatment (left), 60 mg/l H_2O_2 (middle), 90 mg/l H_2O_2 (right). Source: Author

Despite the success of applied research, the physical nature of the new technology remained unclear. The fundamental research of this novel plasma-cavitation source was encompassed by the Czech Science Foundation project: *Exploring fundamental interactions of hydrodynamic cavitation and low-temperature plasma to enhance the disinfection effects* (GA22-11456S). Therefore, the last set of the three annotated papers **(Čech et al. 2024, Čech et al. 2025, Horňák et al. 2025)** covers the results of CaviPlasma diagnostics. The development of CaviPlasma technology starts with the discharge generated in a short cavitation cloud with the metal-to-liquid electrode arrangement (1st generation). Then it continues to utilise an enhanced, prolonged cavitation cloud with the metal-to-metal electrode arrangement (2nd generation), i.e., with the discharge bridging the cavitation cloud in which a pair of metal electrodes is submerged without any water column between the electrodes. The 2nd generation of CaviPlasma became the fundamental configuration in current applied research projects. Diagnostics of the discharge and the generation of the active species are commented on.

4.1 Commentary on the Annotated Scientific Papers: CaviPlasma

This first annotated paper **(Maršálek et al. 2019)** represents the public disclosure of the CaviPlasma technology in a scientific paper. For the newly developed technology, we have introduced the designation *hydrodynamic cavitation plasma jet* (later abandoned), based on the term 'hydraulic cavitation jet' in (Jančula et al. 2014). The image of the earliest phase technology is given in Fig. 17. The discharge was generated in a so-called 'unbridged' regime[18]. The separation of electrodes was approximately 4 cm, and the cavitation cloud was only 2 cm long, i.e., the metal-to-liquid electrode arrangement was formed, and the discharge was in contact with only one metal electrode, the nozzle electrode.

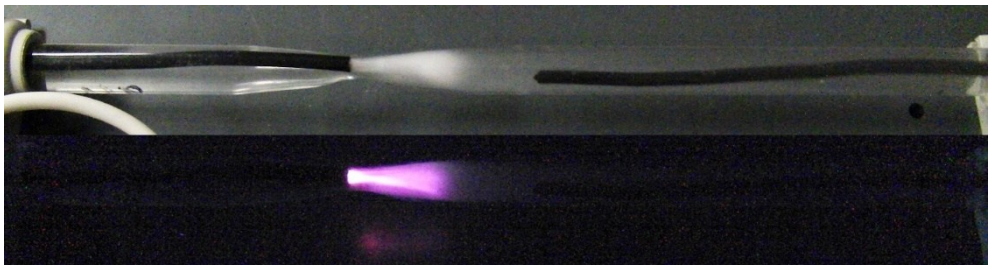

Figure 17: CaviPlasma - the first experiments: (top) Venturi nozzle with cavitation cloud and electrode configuration, (bottom) electric discharge ignited in the cavitation cloud. Source: Jozef Ráheľ

The very first tests of this new technology revealed its outstanding performance in water remediation from the cyanobacteria (*Microcystis Aeruginosa*). The results presented in this paper were the key findings that assured the joint patent application on the CaviPlasma technology by BUT, MUNI and IBOT. The crucial finding was that the electric discharge generated in the cavitation cloud brings a strong synergetic effect, substantially leveraging the performance of the cavitation technology studied by our partners at BUT and IBOT (Jančula et al. 2014). The first CaviPlasma treatment unit was operated at an input power of 0.4 kW. The discharge was sustained using a sine wave high voltage (HV) generator. The frequency of HV was typically between 20 and 65 kHz, and its amplitude was usually 3 to 6 kV (in tap water). The treatment was efficient even at the flow rate of 0.45 L/min, i.e., 1.6 m^3/h, which outperformed contemporary plasma treatment systems by more than one order of magnitude. We have found that even a single cycle of the combined plasma-cavitation treatment of cyanobacteria-contaminated water led to the inhibition of the cyanobacteria's growth with no recovery

[18] This arrangement was used in the first phase of CaviPlasma development. The terms „unbridged" and „bridged", respectively, were introduced after the electrode/cavitation cloud modifications to distinguish between the modifications/development generations.

for more than 192 hours (8 days). Moreover, the cavitation caused the collapse of the gas vesicles of cyanobacteria, which allows for the removal of cyanobacteria using sedimentation. Furthermore, our results proved that the combined effect of cavitation and electric discharge enables the control over the treatment process, preventing the secondary contamination of treated water with the microcystins – the cyanobacteria toxins. We have found that the intensity of the cavitation treatment could be kept at a level sufficient for the collapse of cyanobacteria gas vesicles, but below the level causing cell damage, leading to the release of the cyanotoxins. Moreover, the level of cyanotoxins present in the treated contaminated water was even reduced after the plasma-cavitation combined treatment (by 1/3 of its original value after 3 treatment cycles). The results also show a delayed effect of the combined plasma-cavitation treatment on the cyanobacteria inhibition of approximately 1 day, indicating the presence of mechanisms involving long-lived species. The sole cavitation treatment under the same conditions led to cyanobacteria gas vesicles rupture; however, the growth suppression is limited. Contrary to the combined plasma-cavitation treatment, the photosynthetic activity was not suppressed in the single-pass cavitation-only treatment, and the biomass started to recover approximately 3 days after treatment.

The critical aspect of the experiments was proof of the feasibility of fast, large-volume applications. These results paved the way for the security research project *CaviPlasma: wide-spectrum large-volume decontamination plasma technology for IRS* (SECTECH II, VB02000041) based on the current generation of CaviPlasma technology. Another essential aspect of CaviPlasma efficiency emerges when the effective treatment time of the liquid is assessed. Considering the reaction chamber's dimensions, the plasma-cavitation zone's length and the treated liquid's flow rate, the residence time, i.e., the effective time of action of plasma-cavitation on the liquid, is typically only a few milliseconds. However, the treatment efficiency is at least on par with the state-of-the-art systems.

Only the general principles of operation were discussed in the first published paper. The discharge emission and the treated water were analysed to explain our findings on cyanobacteria. The optical emission spectra revealed the atomization of water vapours inside the cavitation cloud – hydrogen in atomic state and the reactive oxygen species (ROS) were confirmed through Balmer lines (H_α to H_γ), OH radical bands and oxygen atom triplets' emission. The presence of a ROS stable product, the hydrogen peroxide, was quantified using spectrophotometric analysis using the reaction with the titanyl ion.

Further insights into the application potential of CaviPlasma were summarised in the second annotated paper **(Čech et al. 2020)**. In this paper, we have investigated the biocidal effects of water treated by the CaviPlasma unit in the 'unbridged' operation regime. Contrary to the preceding paper, the direct plasma-cavitation action on the cyanobacteria and algae was avoided. Our findings prove that the indirect action of CaviPlasma on the cyanobacteria and algae mediated by the CaviPlasma-treated water (PAW[19]) also brings biocidal effects[20].

The cultivation took place in medium prepared from a 1:1 mixture of PAW and growth medium (the PAW label was adopted for community search reasons). The biological effects were therefore caused only by the long-lived species generated in the water by plasma-cavitation treatment. Three doses of plasma treatment were studied, corresponding to 1, 3 and 5 passes of water through the active plasma-cavitation zone, 9.0 to 9.5 cm long. The HV generator input power was set to 0.4 kW at 65 kHz HV frequency. We have confirmed that the CaviPlasma-treated water has biocidal effects and can inactivate the cyanobacteria and algae. The action on the cells was slower than was observed for directly treated contaminated water in the CaviPlasma unit. The inhibition of cyanobacteria was strongest after 2-3 days of cultivation and was observed for all three PAW treatment doses, see Fig. 18.

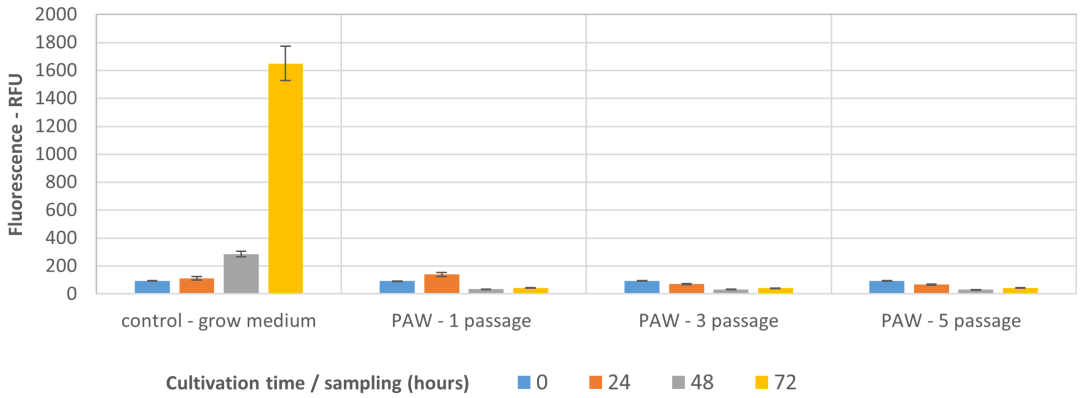

Figure 18: Suppression of Cyanobacteria cultivated in PAW-based medium for three plasma-treatment doses. Data: Blahoslav Maršálek

[19] The PAW is an abbreviation of Plasma Activated Water. Even though the term "activated" is physically incorrect, it was widely adopted in the literature for the water or water-based solutions treated by plasma.

[20] Internal tests conducted by our partners at IBOT confirmed the biocidal activity of prepared CaviPlasma-treated water even after 6 months of storage under standard room conditions.

The algae were also significantly suppressed; however, for the single-pass PAW (lowest treatment dose), we observed the recovery of the fluorescence activity 3 days after the beginning of cultivation. The reduced sensitivity of algae to the PAW can be explained by their cell structure – as eukaryotes, they have more barriers (cellular membrane) than do the evolutionarily simpler cyanobacteria. This result indicates that the selective suppression of cyanobacteria could be feasible when the application of CaviPlasma technology in real biological systems is considered.

The results of further discharge diagnostics were also included in the paper. A high-speed camera (1000 fps) followed the discharge dynamics in the cavitation cloud. The irregularity of the cavitation cloud propagation roughly corresponded to the speed of sound in the cavitation cloud (mixture of liquid and vapour phases) and the velocity field resulting from the numerical simulations performed by our colleagues at BUT. The highly non-equilibrium nature of the discharge in the cavitation cloud was demonstrated on the distribution of reduced population of states of OH (A-X) resulting from the simulation-fitting procedure using massiveOES SW developed at DPPT MUNI by Dr. Jan Voráč and Dr. Petr Synek (Voráč et al. 2017b; 2017a). The distribution shows two-temperature behaviour. The electrical characterisation reveals the absence of current spikes at the onset of the discharge. The current waveforms show a limited rate of discharge resistance changes, as the discharge is stabilised by the resistance of the water column ahead of the downstream electrode. The discharge was therefore in direct contact with the metal electrode only in the throat of the Venturi nozzle. The downstream metal electrode was completely shielded from the direct discharge exposure by the water column, and the discharge is therefore generated against a liquid electrode.

This paper also introduced the technological innovation of the CaviPlasma setup, adopting a vacuum pump in the water reservoir lid. The hydrodynamic cavitation behaviour depends on the pressure difference to the saturated water vapour pressure and the velocity of the water (flow rate), which can be described using the so-called cavitation number (Rudolf et al. 2014). The vacuum pump enabled the controlled manipulation of the hydrodynamic cavitation cloud length by the pressure drop at the discharge tube outlet, allowing a parametric study presented in the following annotated paper.

The first paper dedicated to CaviPlasma diagnostics **(Čech et al. 2024)** summarises plasma research on the first generation of CaviPlasma technology. The discharge and the ROS production were investigated for the 'unbridged' regime of discharge generation, i.e., only a single metal electrode in the throat of the Venturi nozzle is exposed to the discharge. The discharge burns against a liquid electrode and was stabilised by the impedance (resistance) of the water column. A parametric study was conducted for variable flow rate, hydrodynamic cavitation cloud length, and input power of the HV generator (the HV frequency was 65 kHz). The adoption of vacuum subsystem and the modulation of the flow rate and water pump discharge pressure using a variable frequency driver enabled independent selection of flow rate and cavitation length within a specific parametric window (0.5 to 1.5 m^3/h flow rate; 20 to 150 mm cavitation length) given by discharge tube of inner diameter (10 mm) and minimum throat diameter (3.5 mm). The discharge input power up to 0.7 kW was achieved in the described configuration.

The complex characterisation of the discharge and the ROS production was performed using electric measurements (current and voltage), optical imaging using a 1000 fps RGB camera and a gated intensified CCD camera (ICCD), and optical emission spectroscopy. The concentration of hydrogen peroxide in the treated water was followed using colourimetric measurements, i.e., the spectrophotometry of titanyl ions product, and Quantofix peroxide test strips, respectively. In addition, the OH radical concentration measurement was performed using fluorescence spectroscopy of a chemical derivative probe (terephthalic acid) and indirectly also using the phenol oxidation measurements.

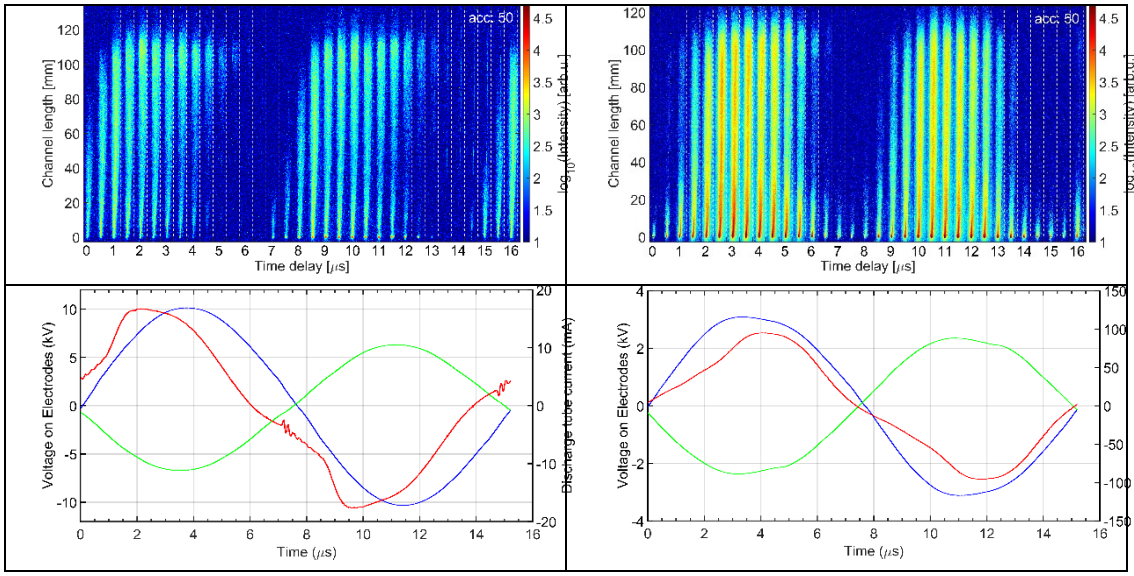

Figure 19: Phase-resolved imaging of CaviPlasma and corresponding current-voltage waveforms, 'unbridged' regime: (left) deionised water, (right) tap water. Temporal resolution 500 ns, 50x accumulations. Source: Author and Pavel Sťahel

The significant outcome of the study concerning the application potential was the ROS generation efficiency of the studied system, expressed in terms of hydrogen peroxide production (standard performance indicator). The measured hydrogen peroxide energy yield of up to 9.5 g/kWh positioned the CaviPlasma technology in the peloton of plasma technologies, next to the discharges in bubbles or aerosol (Locke and Shih 2011). The hydrogen peroxide production rate up to 2.4 g/h also positioned CaviPlasma among the highly ranked plasma-liquid systems (Locke and Shih 2011). The phenol degradation yield of 2.7 g/kWh also proved promising potential for the degradation of chemical pollutants.

What makes CaviPlasma technology unique, however, is its ability to treat huge volumes of liquids – the nominal flow rate of the tested unit was 1.5 m^3/h (the current generation of portable CaviPlasma laboratory unit peaks at 4 m^3/h). This key feature is inherently encoded into its principle of operation, utilising hydrodynamic cavitation flows.

The diagnostics revealed the glow-like nature of the discharge. The ballast resistance of the water column between metal electrodes limits the discharge current. We can describe the discharge dynamics within the half-period of applied HV, which was 8 µs, in several consecutive steps, see Fig. 19: The discharge starts at the nozzle metal electrode, regardless of the polarity. It then evolves on a 1-2 µs scale as the low-emission channel spreading from the nozzle electrode downstream of the cavitation cloud. When the discharge channel reaches the collapsing end of the cavitation cloud, the current rate increases, and the discharge emission peaks for approximately 2 µs and then decays. The emission from the discharge tube does not decay completely in tap water, as the faint emission from the nozzle electrode area was observed between consecutive half-periods of applied HV (considering the 500 ns long acquisition windows).

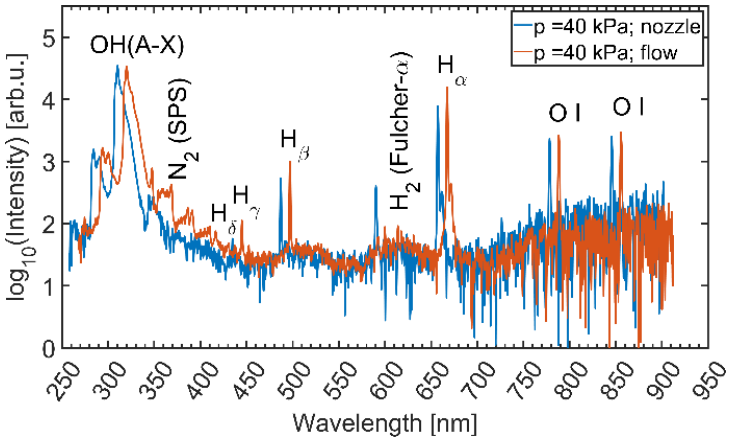

Figure 20: Emission spectrum of CaviPlasma unbridged regime. Comparison of spectra above the nozzle electrode and the cavitation cloud end (intentionally wavelength shifted). SPS of nitrogen present in the cavitation collapse spectrum. Source: Author

The primary spectral components of optical emission spectra, see Fig. 20, are Balmer hydrogen lines in the visible range (dominantly H_α) and OH (A-X) emission band in the UV range. The oxygen atoms' emission (triplets) was observed in the NIR range. Spectroscopic analysis revealed two regimes of the discharge: (a) short cavitation (below 30 mm), and (b) long cavitation (above 30 mm). For short cavitation, the ratio of OH/H measured above the nozzle electrode and the OH/O ratio remains constant and then rises with the increase of cavitation cloud length. The rotational temperature was fitted from the OH (A-X) emission band using massiveOES SW. In the short cavitation regime, the rotational temperature gradually decreases with the prolongation of the channel and remains practically constant once the long cavitation regime is reached. The two-temperature distribution was found in the OH (A-X) population of states. The lower component of rotational temperature is in the range of 1,700 to 2,000 K, while the higher component is in the range of 10,000 to 14,000 K. The vibrational temperature of OH (A-X) is in the 3,000-4,000 K range, following the same trends as the rotational temperature evolution.

The cavitation-discharge dynamics were also studied using the fast-framing RGB camera. The cavitation cloud, as well as the discharge channel, was highly stochastic. The discharge channel does not follow the straight path through the cavitation cloud. The cavitation cloud's local state determines the discharge channel path, following the cavitation cloud disturbances dragged by the flow. The cavitation/discharge channel length at studied conditions is inversely proportional to the square of the pressure in the discharge tube outlet, and the channel oscillates on the hundred-millisecond time scale with the amplitude around 10 mm for a 150 mm long channel.

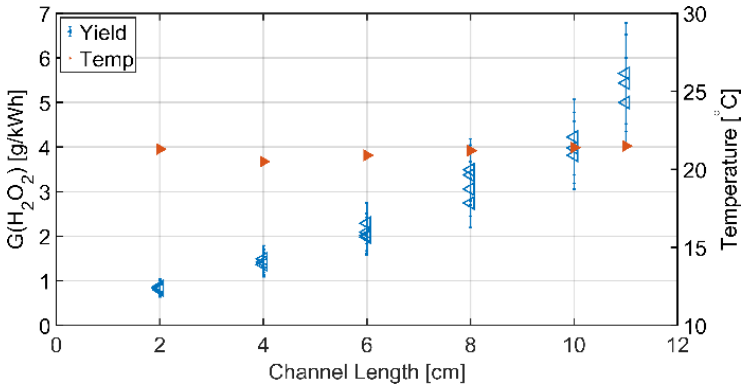

Figure 21: The H_2O_2 yield dependence on the cavitation cloud length, 'unbridged' regime. Source: Author and Lubomír Prokeš

The parametric study of the 'unbridged' regime revealed trends in hydrogen peroxide production concerning process parameters. There is a systematic increase in hydrogen peroxide yield with the prolongation of the cavitation cloud, see Fig. 21. The rise in the treatment's specific input energy (SIE) results in increased hydrogen peroxide concentration. These findings set the course for further development of the technology: to en-

hance the cavitation cloud generation, i.e., increase the cavitation cloud length, and to elevate the energy input into the discharge.

Within the ongoing research, we have found that the system performance measured by the hydrogen peroxide production is limited by the power losses in the water column ahead of the downstream electrode (ballast resistance), as well as in the water pump branch of the hydraulic/electric circuit. The change in the discharge regime from 'unbridged' to 'bridged' significantly reduced these power losses. In the 'bridged' regime, both metal electrodes were exposed to the gas phase of the cavitation cloud and the significant increase of the power input into the discharge was achieved, typically 1-2 kW, but the actual tested limit is beyond 7 kW for a 4 m^3/h unit. Further improvements of the hydraulic circuit resulted in increased cavitation cloud length without the necessity of a vacuum unit, simplifying the system for industrial adoption.

The effect of these changes on CaviPlasma parameters was summarised in the following annotated paper **(Čech et al. 2025)**. The most important technological shift realised in the second generation of CaviPlasma was the deprecation of the vacuum system in favour of a hydraulic setup improvement. The higher-rated specification hydraulic pump (head and flow rates), controlled with a variable-frequency driver and fine-tuning of the nozzle electrode position, allows the length of the cavitation cloud to be set at the desired flow rate. Vacuum system deprecation significantly simplified the industrial adoption challenges and improved the system's reliability. These changes enabled us to keep the discharge tube geometry while increasing the flow rate to 2 m^3/h and prolonging the cavitation cloud above 14 cm. Both metal electrodes were now exposed to the cavitation cloud, and discharge was in direct contact with both electrodes – thus, we called this the 'bridged' regime of operation. The electrodes' separation distance was fixed to 12 cm, based on the system optimisation tests (not covered in the paper). The discharge stability and electrode lifetime were further enhanced using the hollow tube downstream electrode. The changes enabled the system to operate at HV input power up to 2 kW at 32 kHz, utilising the high-power generator developed at DPPT originally for the DCSBD treatment.

The paper summarises the results of the 'bridged' regime diagnostics. A similar set of diagnostics and the manuscript structure were adopted to facilitate the comparison with the 'unbridged' regime described in the previous paper. Therefore, only the key characteristics that differentiate the 'bridged' regime from the 'unbridged' one will be highlighted. The hydrogen peroxide generation yield was enhanced to 12.4 g/kWh and the peak production rate increased nearly 7-fold to 17.6 g/h. The set of experiments was conducted to explore the effects of nozzle electrode material, the conductivity of the liquid and input power on the hydrogen peroxide production efficiency. The pure deionised water was used, except for the conductivity tests.

Let's focus on the electrode material first. The tungsten electrode was tested for its high melting point, ensuring a low electrode erosion rate. However, in practical applications of contaminated water treatment, we have experienced limited long-term discharge stability due to the buildup of electrode deposits. The stainless steel and graphite electrodes were also tested. Against our expectations based on the results of Abramov et al. (2021), the carbon electrode exhibits the lowest treatment efficiency of the tested materials. The deposit prevention was finally resolved with the titanium electrode. We observed only minor differences in the treatment efficiency of tungsten, stainless steel or titanium electrodes.

The second task was the assessment of treatment efficiency concerning water (solution) conductivity, studied in the conductivity range from 5 to 5,000 μS/cm. The tested conductivity ranges from that of deionised water to 10 times higher than that of tap water. We have observed a decreasing trend of efficiency with increasing water conductivity. A deeper analysis revealed that the apparent performance loss was caused by the (ohmic) power losses in the hydraulic pump branch parallel to the discharge tube. Adjusted for the influence of the leakage current, the treatment efficiency does not differ within the error margin. The net power input to the discharge and the power losses in the pump branch were estimated from the current-voltage measurements in both hydraulic/electric branches. This also gave us an estimation of the HV generator's efficiency to be 80 %.

The last set of measurements investigated the dependence of treatment efficiency on the input power, see Fig. 22. When the input power rises from 0.3 to 1.6 kW, the efficiency of the treatment drops from 12.4 to 10.4 g/kWh. However, the production rate increases from 4.3 to 17.6 g/h, favouring high input power for real application despite a slight decrease in energy efficiency. A universal constant for hydrogen peroxide production was assessed for the tested setup. The level of hydrogen peroxide concentration reached using a single pass of the water through the system was found to be 8 mg/L per kW of input power. When sorted according to specific input energy, the highest rate of concentration rise was achieved in the range up to 10 kJ/L for multiple exposure batch treatment.

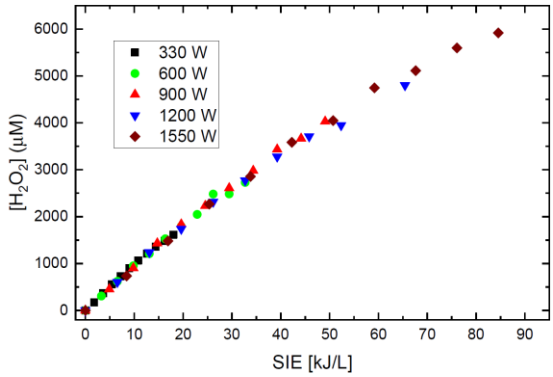

Figure 22: Hydrogen peroxide concentration in deionised water. Dependence on specific input energy (SIE) for repetitive water treatment in the 'bridged' regime with varying input power. Sampled each second pass through the system. Source: Authors collective (Čech et al. 2025)

The discharge configuration evolution results also in the change of the discharge behaviour and characteristics. The complex, phase-resolved diagnostics setup was set to enable characterisation of discharge evolution, see Fig. 23. The semi-automated measurements enabled the correlated acquisitions of discharge emission, using an ICCD camera and an avalanche photodiode, and the current-voltage waveforms, using a digital storage oscilloscope with a pair of voltage and current probes. The discharge in the 'bridged' operation regime evolves stepwise in distinct phases within the 16 μs-long half-periods. It always starts at the nozzle electrode, as in 'unbridged' mode. Then the low-emission channel grows from the nozzle electrode towards the downstream electrode. On voltage-current waveforms, this phase is represented by the increase of gap voltage and progressive rise of current – the discharge tube resistance progressively decreases as the ionisation in the cavitation cloud rises. This low-intensity channel fully develops within a microsecond and bridges the gap between the nozzle and the downstream electrode. When this happens, the voltage suddenly drops and the current peak occurs, about 1 A high and several hundred ns long (the resistance drops to units of kΩ). The bright channel connecting both electrodes appears for several hundred ns and then decays. The decay could be triggered by the combination of the pressure increase due to the shock wave, causing the drop of reduced electric field and ionisation rate, as well as the depletion of energy stored in the HV transformer[21]. This phase resembles transient spark discharge (Janda et al. 2011). After the first (spark) phase, the glow discharge develops in the pre-ionised gas channel. The current slowly rises under stabilised voltage between electrodes. The current reaches the maximum at the end of the duty cycle of the high-frequency generator feeding the HV transformer. At this point, the resistance of the discharge tube is the lowest. The discharge then consumes energy stored in the HV transformer, the current slowly decays and finally the voltage drops and the discharge channel decays. The typical luminous structures observed in the discharge channel during this phase are similar to the low-pressure glow discharge, supporting our discharge mode identification. The discharge cycle then repeats at the opposite voltage polarity.

[21] Rigorously speaking, the energy is not stored in the HV circuit components, but in the generated (variable) electromagnetic fields.

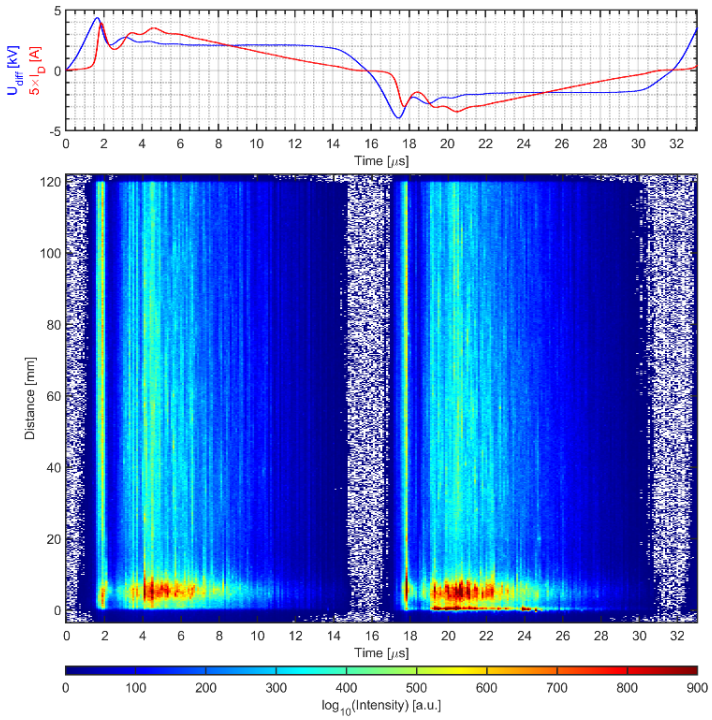

Figure 23 Spatio-temporal evolution of CaviPlasma in 'bridged' regime for deionised water. The visualisation in streak-camera representation with corresponding current-voltage waveforms. Source: Author and Radek Horňák, Adapted from (Čech et al. 2025)

Between the discharge half-periods, the measured current does not follow the voltage polarity reversal, and a positive offset was observed on current waveforms of the 'bridged' regime of CaviPlasma. We have investigated this phenomenon with a pair of Pearson current probes around the discharge tube. The positive current offset was observed when the current probes were positioned at the active discharge region, or a few centimetres behind the downstream electrode. The positive offset current decayed on the microsecond time scale, when the HV generator was halted. The positive current offset disappeared when the current probe was positioned further downstream behind the downstream electrode. This positive current offset, sensed at the downstream electrode, was also not observed when the cavitation cloud length was halved, changing the operation regime to 'unbridged'. This indicates that the observed phenomenon is probably not the current probe artefact[22]. The CaviPlasma utilises a fast flow of liquid passing through the discharge tube, which carries the dissolved particles. The origin of the measured current could be caused by the drift of charged particles in the discharge tube,

[22] Observations in another experiment caused the described verification. The negative offset on current waveforms was observed using the same current probe in the atomiser experiment, where the pulsed discharge with no liquid involved was investigated. In that particular experiment, the current offset was found to be an artefact caused by the current probe characteristics and pulsed-dc operation, as no offset was confirmed using a shunt resistor probe, which could be utilised in that experiment.

presumably the positively charged ones, considering the sign of the current offset and the flow direction. The decay of the measured current offset shares the same time scale as the decay of the luminescence signal caused by ROS, measured in the last annotated paper **(Horňák et al. 2025)**. This correlation further supports the feasibility of the observed current offset interpretation.

The still open question remains, which of the discharge phases contributes predominantly to the active species production and the overall excellent efficiency of this plasma system. The phase-resolved optical emission spectrometry investigation is in progress. The temporal development of spectral components will indicate the active species dynamics and enable the comparison of spark and glow phases. The assessment of the plasma-chemical kinetic model could finally suggest the relative abundance of generated ROS in respective phases, based on the assumptions from the phase-resolved OES.

The ROS production and their lifetime are the determining factors of the CaviPlasma efficiency of micropollutants removal. Especially for liquid (water) decontamination, the active species in contact with the liquid surface and dissolved in the liquid are essential. In the multidisciplinary research team, we have investigated the dissolved ROS produced by CaviPlasma treatment (Odehnalová et al. 2024). The EPR spectrometry, fluorescence spectrometry and colourimetric measurements were based on the chemical derivative probes/spin trapping technique and colourimetric assays . The measurements confirmed the presence of the following ROS in CaviPlasma-treated liquid: OH radical and singlet oxygen ($^1O_2$) as the short-lived species and ozone (O_3) and hydrogen peroxide (H_2O_2) as the long-lived species. The hydrogen peroxide was the most abundant product, with the liquid-phase concentration about 270 times higher than ozone. Even though the OH radical is the primary precursor of the hydrogen peroxide molecule, we have found that the hydrogen peroxide concentration outpaces OH radicals by more than 100-fold. This strongly correlates with Gorbanev et al. (2018a) findings, who concluded that hydrogen peroxide is dominantly produced in the gas phase and then dissolved into the liquid.

The findings above (Odehnalová et al. 2024) disclosed the main oxidising species responsible for the mechanisms of CaviPlasma action on micropollutants. However, the ROS presence was investigated only post-treatment, and the information on the dynamics of their production cannot be disclosed using the adopted diagnostics. Among all the ROS detected in CaviPlasma-treated water, the OH radical was the most potent oxidant produced. Therefore, we have investigated the possibilities of mapping OH radicals during the active phase of CaviPlasma treatment.

Finally, we have adopted the chemiluminescence probe to visualise the OH radicals, and the results are summarised in the last of the selected annotated papers **(Horňák et al. 2025)**, which will conclude the CaviPlasma part of the thesis.

The OH radical plays an essential role in plasma-liquid chemical reactions due to its high reactivity (Graves 2012), making it an efficient agent against organic pollutants. Mapping the OH radicals in the liquid phase could give a fundamental insight into the action of (not only) plasma technologies on water pollution remediation. The widely adopted OH detection technique in discharge diagnostics is the laser-induced fluorescence (LIF) (Bruggeman et al. 2016). LIF is an excellent tool for direct OH probing in the gas phase, capable of absolute concentration estimation after calibration. Unfortunately, the optically highly non-homogeneous and stochastic nature of cavitation-based treatment systems effectively restrains the adoption of the LIF detection method in CaviPlasma. The indirect techniques utilising chemical probes were developed for OH detection in the liquid phase (Bruggeman et al. 2016), but predominantly ex-situ.

In the literature, the luminol chemical probe method was reported to investigate the presence of OH radicals in the liquid phase of liquid-treatment systems, including the pure hydrodynamic cavitation (Perrin et al. 2021) and atmospheric pressure discharges in contact with liquid (Schüttler et al. 2024). In this annotated paper **(Horňák et al. 2025)**, we have reported on the OH radical mapping in a plasma-cavitation system for the first time, utilising the luminol chemiluminescence.

We followed the emission of the radiative state of luminol derivative in the active discharge phase of CaviPlasma and the post-discharge phase. According to the literature (Wasselin-Trupin et al. 2000), the luminol chemiluminescence is a two-step process involving: (1) oxidation of luminol dianion by OH radical, and (2) subsequent reaction with the superoxide anion radical ($O_2^{\bullet -}$), resulting in an excited state that relaxes as the broad peak of chemiluminescence radiation with the maximum around 425 nm. This puts OH mapping using luminol chemiluminescence in question regarding the process selectivity, because the superoxide is the chemiluminescence triggering molecule. In (Shirai et al. 2019) the authors concluded that for the luminescence process occurring in the liquid phase, the OH radical is the superoxide anion precursor for plasma-treated liquid. Thus, the luminescence signal can be utilised to map the presence of OH radicals in CaviPlasma-treated liquid. Moreover, the lifetime of OH-induced chemiluminescence of luminol was reported to be hundreds of nanoseconds for the plasma-liquid system (Shirai et al. 2019) or water radiolysis (Wasselin-Trupin et al. 2000). This allows for the investigation of the dynamics of the OH radicals in CaviPlasma.

Specifically, we have investigated the 'unbridged' regime of CaviPlasma **(Čech et al. 2024)**, because this regime enables the simultaneous observation of the luminescence in the active plasma-cavitation zone and the post-discharge zone after cavitation collapse. Moreover, the processes at the cavitation collapse zone are not influenced by the presence of a metal electrode in the 'unbridged' regime.

In our previous OH measurement in the study **(Čech et al. 2024)**, we encountered problems with the temporal stability of the chemical derivative probe (terephthalic acid) present directly in the treated liquid. Fortunately, the strong chemiluminescence signal was observable for the luminol probe even after 5 minutes of plasma-treatment of the luminol solution. This time was sufficient to conduct the luminescence mapping by fast-framing sequences using an RGB camera and spectrally filtered imaging using an ICCD camera. This enabled the estimation of spatial and temporal luminescence dynamics proportional to the relative quantity of OH radicals.

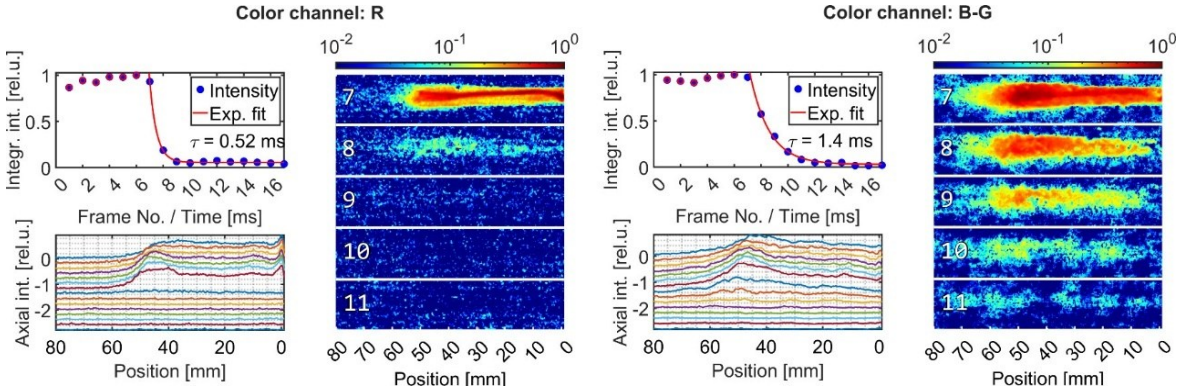

Figure 224: Sequence of 2D (post)-discharge emission/luminescence acquired in 1-ms steps. Graphs showing corresponding integral emission decay sequences and axial intensity profiles were intentionally shifted down for better visibility. Red channel (R) represents the H_α. The differential blue-green channel (B-G) represents the luminescence. The flow direction was from the right to the left. Source: Authors collective (Horňák et al. 2025)

In the first experiment, the RGB fast framing camera was used to acquire 2D resolved emission from the discharge and the chemiluminescence along the discharge tube, see Fig. 24. The emission was followed before and after the discharge switch-off in a 1000 fps image sequence (the camera's limit). The red image channel followed the discharge emission distribution, as this channel was susceptible to the H_α discharge emission. The spectral sensitivities of blue and green image channels overlap at approximately the H_β position. The blue channel was much more sensitive to the chemiluminescence signal, and the differential signal of the blue minus green channel was assessed to follow the temporal luminescence evolution in 2D. We have realised that the chemiluminescence signal was the strongest in the active discharge zone, specifically in the cavitation cloud close to its collapsing end. Post-discharge, the luminescence signal exponentially decays. The effective lifetime of the luminescence was 1.4 ms, which was an order of magnitude longer than for atmospheric pressure plasma jet impinging water surface (Shirai et al. 2019), indicating the effective lifetime of OH radicals is considerably longer for CaviPlasma than for atmospheric pressure discharges. We have also observed the chemiluminescence signal decay behind the cavitation collapse in the wake. However, the sensitivity and dynamic range of the RGB camera were not sufficient to evaluate the luminescence dynamics in this region. For highly resolved, high-dynamic-range meas-

urement of the luminescence behind the active discharge zone, the ICCD camera equipped with an interference filter centred at 420 nm was used. We have observed a complex 2D structured emission pattern of the luminescence, visualising the presence of OH radicals in a 2D section along the discharge tube axis. The lower liquid flow rate stabilised the 2-3 cm long cavitation, allowing an unobstructed view of approximately 8 cm long wake flow behind cavitation collapse. The luminescence signal (and thus the OH radicals) was detected more than 5 cm behind the cavitation collapse, and the luminescence pattern followed the locally asymmetric flow. The luminescence decay patterns were similar, varying the HV input power from 0.6 to 1.5 kW.

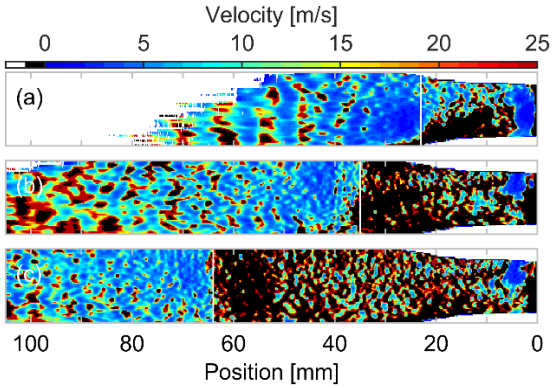

Figure 235 Reconstruction of stream velocity after HCC collapse based on the assumed luminescence decay rate constant τ = 1.4 ms. The comparison is given for 3 HCC lengths indicated by white lines. Source: Authors collective (Horňák et al. 2025)

Finally, we have hypothesised that the long span of the luminescence signal was caused by the drag of the OH radicals by the fast flow of the liquid in the discharge tube. So, we wanted to determine whether the local stream velocity could be assessed from the observed luminescence decay. The axial drift velocity model was proposed for the flow after the cavitation collapse (wake). The model described the luminescence emission decay outside the active discharge zone, which was considered a constant source of OH radicals. Under the assumption of constant effective luminescence lifetime, the temporal variation of luminescence was transformed to spatial variation using the axial drift velocity approximation. The spatial derivative of the luminescence signal was estimated using a smoothing cubic spline. The resulting reconstruction of the stream velocity (axial drift velocity) showed good agreement with the plug-flow estimation for the given discharge tube geometry. The 2D maps of the velocity field were assessed, see Fig. 25, representing the reconstruction of local drift velocity. The maps were calculated for three different water flow rates, resulting in three cavitation cloud lengths. The 2D velocity field maps helped distinguish between the active discharge zone and decay zone behind the cavitation cloud. The maps were also helpful in visualising the local stream inhomogeneities in the wake. These inhomogeneities could result from the local density variations, see supplement material to the **(Čech et al. 2024)**, or shockwaves, that could result from the gas-liquid phase transition behind the cavitation cloud collapse.

We can conclude that the mapping of OH radicals revealed two domains, where the direct reactions of OH radicals with the micropollutants presumably occur. Besides the active discharge zone alone, there is probably a prolonged interaction zone in the cavitation collapse zone and the wake behind it, which effectively enhances the efficiency of the water treatment using the CaviPlasma technology.

4.2 Conclusion to the CaviPlasma Part

The discovery of CaviPlasma technology represents a novel approach to the large-volume plasma treatment of liquids. The treatment performance measured by the hydrogen peroxide generation positioned CaviPlasma among the top of current systems in terms of energy efficiency (yield) and production rate, however, at unprecedented flow rates of several m^3/h. The systematic investigation revealed the basic characteristics of bridged and unbridged regimes of CaviPlasma in terms of spatio-temporal discharge development, its spectral characteristics, and the dynamics of reactive oxygen species. The parametric study revealed the hydrogen peroxide generation efficiency with respect to processing parameters, e.g., flow rate, electrode configuration and composition, specific input energy, or water conductivity.

The last remark goes to the society-wide benefit of the technology. In the past seven years of research and development effort, the patent-protected CaviPlasma technology has matured, and its application potential has been growing with each new collaboration. The water remediation from micropollutants and biological threats, or the agriculture and aquaculture applications, have already been investigated in applied research projects. Moreover, the two licences have been awarded to the Czech companies, and one of them already presented a commercial prototype of the professional CaviPlasma treater at the EXPO 2025 in Osaka in July 2025. But the CaviPlasma potential has not been drained at the moment. Recently, the 3rd generation of CaviPlasma technology was developed at MUNI, which opened a new window of opportunities by controlling the discharge atmosphere composition. This innovation has probably paved the way for large-volume plasma-induced chemistry in liquids and new cross-disciplinary collaborations. And the author looks forward to new experimental challenges and discoveries in the future.

Summary

The habilitation thesis summarises the author's research at the Department of Plasma Physics and Technology (Department of Physical Electronics), Masaryk University. The commentary to the annotated papers covers his contribution to the application-oriented research of two plasma technologies: the Diffuse Coplanar Surface Barrier Discharge (DCSBD) and the CaviPlasma®. The author utilises the intensified CCD cameras (ICCD) for the phase-resolved and spatially resolved diagnostics, i.e., imaging, optical emission spectroscopy, or correlated optical/electric measurements. The acquired data were analysed using custom processing codes. The simplified models were developed for numerical simulations supporting the analysis of observed phenomena.

The first part is focused on the development and applications of the DCSBD. The coplanar discharge test bed reactor (The Box) was designed to enable the flexibility in the geometry of the electrodes, dielectrics and discharge atmosphere, which is technically and economically challenging for the DCSBD design. The Box enabled a parametric study on the influence of electrode geometry, temperature and discharge conditions on the parameters and behaviour of the coplanar discharge and the microdischarges it consists of. The results served for the focused development of the DCSBD. Moreover, two phenomena in coplanar discharges were described: (i) the role of residual heat on the spatial stabilisation of microdischarges, and (ii) the ultra-low intensity Charge Relaxation Event, preceding Townsend avalanching phase in the homogeneous regime in helium. The utilisation of DCSBD in a hydrogen atmosphere was described, as well as the properties of a laminated small-footprint variation of DCSBD in low-pressure conditions (wide pressure range), investigated for plasma decontaminator applications.

The second part presents the story of CaviPlasma® technology, a system for plasma treatment of liquids developed jointly by Masaryk University, Brno University of Technology, and the Institute of Botany of the Czech Academy of Sciences in 2018. The author contributed to the development and diagnostics of this plasma system, which exploits the synergy of hydrodynamic cavitation and electric discharge in the low-pressure gaseous environment of the cavitation cloud. The diagnostics described two discharge regimes (with/without liquid electrode). The parametric studies quantified the production of reactive oxygen species (ROS), particularly hydrogen peroxide, in both regimes. The measured hydrogen peroxide energy yield (>10 g/kWh) and production rates (>17 g/h) positioned CaviPlasma among the high-performance plasma-liquid systems. However, what makes the CaviPlasma unique is the unprecedented flow rate of several cubic metres per hour at which these performance figures are achieved. The efficiency of CaviPlasma and its international patent protection make it well-suited to real-scale applications, which are currently under investigation with our industrial partners.

Bibliography

ABOLMASOV, Sergey N., Rei ABO, Tatsuru SHIRAFUJI and Kunihide TACHIBANA, 2006. Spatiotemporal Surface Charge Measurement in Two Types of Dielectric Barrier Discharges Using Pockels Effect. *Japanese Journal of Applied Physics* [online]. **45**(10B), 8255–8259. ISSN 0021-4922. Available at: doi:10.1143/JJAP.45.8255

ABRAMOV, Vladimir O., Anna V. ABRAMOVA, Giancarlo CRAVOTTO, Roman V. NIKONOV, Igor S. FEDULOV and Vladimir K. IVANOV, 2021. Flow-mode water treatment under simultaneous hydrodynamic cavitation and plasma. *Ultrasonics Sonochemistry* [online]. **70**(September 2020), 105323. ISSN 1873-2828. Available at: doi:10.1016/j.ultsonch.2020.105323

ADAMOVICH, I., S. AGARWAL, E. AHEDO, L. L. ALVES, S. BAALRUD, N. BABAEVA, A. BOGAERTS, A. BOURDON, P. J. BRUGGEMAN, C. CANAL, E. H. CHOI, S. COULOMBE, Z. DONKÓ, D. B. GRAVES, S. HAMAGUCHI, D. HEGEMANN, M. HORI, H. H. KIM, G. M.W. KROESEN, M. J. KUSHNER, A. LARICCHIUTA, X. LI, T. E. MAGIN, S. MEDEDOVIC THAGARD, V. MILLER, A. B. MURPHY, G. S. OEHRLEIN, N. PUAC, R. M. SANKARAN, S. SAMUKAWA, M. SHIRATANI, M. ŠIMEK, N. TARASENKO, K. TERASHIMA, E. THOMAS, J. TRIESCHMANN, S. TSIKATA, M. M. TURNER, I. J. VAN DER WALT, M. C.M. VAN DE SANDEN and T. VON WOEDTKE, 2022. The 2022 Plasma Roadmap: low temperature plasma science and technology. *Journal of Physics D: Applied Physics* [online]. **55**(37), 373001. ISSN 1361-6463. Available at: doi:10.1088/1361-6463/ac5e1c

AKISHEV, Yuri, Gregory APONIN, Anton BALAKIREV, Mikhail GRUSHIN, Vladimir KARALNIK, Alexander PETRYAKOV and Nikolay TRUSHKIN, 2011. 'Memory' and sustention of microdischarges in a steady-state DBD: volume plasma or surface charge? *Plasma Sources Science and Technology* [online]. **20**(2), 024005. ISSN 0963-0252. Available at: doi:10.1088/0963-0252/20/2/024005

BOEUF, J. P. and L. C. PITCHFORD, 2005. Electrohydrodynamic force and aerodynamic flow acceleration in surface dielectric barrier discharge. *Journal of Applied Physics* [online]. **97**(10), 103307. ISSN 0021-8979. Available at: doi:10.1063/1.1901841

BOGAERTS, Annemie, Erik NEYTS, Renaat GIJBELS and Joost VAN DER MULLEN, 2002. Gas discharge plasmas and their applications. *Spectrochimica Acta Part B: Atomic Spectroscopy* [online]. **57**(4), 609–658. ISSN 0584-8547. Available at: doi:10.1016/S0584-8547(01)00406-2

BRANDENBURG, R., Z. NAVRÁTIL, J. JÁNSKÝ, P. ST'AHEL, D. TRUNEC and H. E. WAGNER, 2009. The transition between different modes of barrier discharges at atmospheric pressure. *Journal of Physics D: Applied Physics* [online]. **42**(8), 085208. ISSN 0022-3727. Available at: doi:10.1088/0022-3727/42/8/085208

BRANDENBURG, Ronny, 2017. Dielectric barrier discharges: progress on plasma sources and on the understanding of regimes and single filaments. *Plasma Sources Science and Technology* [online]. **26**(5), 053001. ISSN 1361-6595. Available at: doi:10.1088/1361-6595/aa6426

BRUGGEMAN, P. J., M. J. KUSHNER, B. R. LOCKE, J. G.E. GARDENIERS, W. G. GRAHAM, D. B. GRAVES, R. C.H.M. HOFMAN-CARIS, D. MARIC, J. P. REID, E. CERIANI, D. FERNANDEZ RIVAS, J. E. FOSTER, S. C. GARRICK, Y. GORBANEV, S. HAMAGUCHI, F. IZA, H. JABLONOWSKI, E. KLIMOVA, J. KOLB, F. KRCMA, P. LUKES, Z. MACHALA, I. MARINOV, D. MARIOTTI, S. MEDEDOVIC THAGARD, D. MINAKATA, E. C. NEYTS, J. PAWLAT, Z. Lj PETROVIC, R. PFLIEGER, S. REUTER, D. C. SCHRAM, S. SCHRÖTER, M. SHIRAIWA, B. TARABOVÁ, P. A. TSAI, J. R.R. VERLET, T. VON WOEDTKE, K. R. WILSON, K. YASUI and G. ZVEREVA, 2016. Plasma-liquid interactions: A review and roadmap. *Plasma Sources Science and Technology* [online]. **25**(5), 0–125. ISSN 1361-6595. Available at: doi:10.1088/0963-0252/25/5/053002

BRUGGEMAN, Peter J., Felipe IZA and Ronny BRANDENBURG, 2017. Foundations of atmospheric pressure non-equilibrium plasmas. *Plasma Sources Science and Technology* [online]. **26**(12), 123002. ISSN 1361-6595. Available at: doi:10.1088/1361-6595/aa97af

BRUGGEMAN, Peter and Christophe LEYS, 2009. Non-thermal plasmas in and in contact with liquids. *Journal of Physics D: Applied Physics* [online]. **42**(5), 053001. ISSN 0022-3727. Available at: doi:10.1088/0022-3727/42/5/053001

ČECH, J., L. PROKEŠ, M. ZEMÁNEK, L. DOSTÁL, D. ŠIMEK, J. VALENTA, R. ŽEBRÁK, L. ZÁPOTOCKÝ and P. SŤAHEL, 2019. Rotating Gliding Arc: Innovative Source for VOC Remediation. *PLASMA PHYSICS AND TECHNOLOGY* [online]. **6**(2), 156–160. ISSN 2336-2634. Available at: doi:10.14311/ppt.2019.2.156

ČECH, Jan, Pavel SŤAHEL, Lubomír PROKEŠ, Jozef RÁHEĽ, Pavel RUDOLF, Eliška MARŠÁLKOVÁ, Blahoslav MARŠÁLEK, Luděk BLÁHA, Petr LUKEŠ, Aleksandra LAVRIKOVA, Zdenko MACHALA and Jaroslav LEV, 2022a. CaviPlasma: A large-throughput technology for plasma treatment of contaminated water using peroxide chemistry. In: *9th Central European Symposium on Plasma Chemistry (CESPC9)*.

ČECH, Jan, Pavel SŤAHEL, Lubomír PROKEŠ, Jozef RÁHEĽ, Pavel RUDOLF, Eliška MARŠÁLKOVÁ, Blahoslav MARŠÁLEK, Jan FLODR, Filip RŮŽIČKA, Ivana PAPEŽÍKOVÁ and Jan MENDEL, 2022b. CaviPlasma: A plasma source capable of application-scale generation of plasma treated water for agriculture, aquaculture, and medicine. In: *Workshop COST Action CA19110 Plasma Applications for Smart and Sustainable Agriculture (PlAgri)*.

ČERNÁK, M., L'. ČERNÁKOVÁ, I HUDEC, D. KOVÁČIK and A. ZAHORANOVÁ, 2009. Diffuse Coplanar Surface Barrier Discharge and its applications for in-line processing of low-added-value materials. *The European Physical Journal Applied Physics* [online]. **47**(2), 22806. ISSN 1286-0042. Available at: doi:10.1051/epjap/2009131

CHAUVET, Laura, Chaiyasit NENBANGKAEO, Katharina GROSSE and Achim VON KEUDELL, 2020. Chemistry in nanosecond plasmas in water. *Plasma Processes and Polymers* [online]. **17**(6), 1900192. ISSN 1612-8869. Available at: doi:10.1002/ppap.201900192

CHIROKOV, Alexandre, Alexander GUTSOL, Alexander FRIDMAN, Kurt D. SIEBER, Jeremy M. GRACE and Kelly S. ROBINSON, 2006. A Study of Two-Dimensional Microdischarge Pattern Formation in Dielectric Barrier Discharges. *Plasma Chemistry and Plasma Processing* [online]. **26**(2), 127–135. ISSN 0272-4324. Available at: doi:10.1007/s11090-006-9007-5

CVELBAR, Uroš, James L. WALSH, Mirko ČERNÁK, Hindrik W. DE VRIES, Stephan REUTER, Thierry BELMONTE, Carles CORBELLA, Camelia MIRON, Nataša HOJNIK, Andrea JUROV, Harinarayanan PULIYALIL, Marija GORJANC, Sabine PORTAL, Romolo LAURITA, Vittorio COLOMBO, Jan SCHÄFER, Anton NIKIFOROV, Martina MODIC, Ondrej KYLIAN, Martin POLAK, Cedric LABAY, Jose M. CANAL, Cristina CANAL, Matteo GHERARDI, Kateryna BAZAKA, Prashant SONAR, Kostya K. OSTRIKOV, David CAMERON, Sabu THOMAS and Klaus Dieter WELTMANN, 2019. White paper on the future of plasma science and technology in plastics and textiles. *Plasma Processes and Polymers* [online]. **16**(1), 1–37. ISSN 1612-8869. Available at: doi:10.1002/ppap.201700228

DVONC, Lukas and Mario JANDA, 2015. Study of Transient Spark Discharge Properties Using Kinetic Modeling. *IEEE Transactions on Plasma Science* [online]. **43**(8), 2562–2570. ISSN 0093-3813. Available at: doi:10.1109/TPS.2015.2452947

ELIASSON, B, M HIRTH and U KOGELSCHATZ, 1987. Ozone synthesis from oxygen in dielectric barrier discharges. *Journal of Physics D: Applied Physics* [online]. **20**(11), 1421–1437. ISSN 0022-3727. Available at: doi:10.1088/0022-3727/20/11/010

ELIASSON, Baldur and Ulrich KOGELSCHATZ, 1991. Nonequilibrium volume plasma chemical processing. *IEEE Transactions on Plasma Science* [online]. **19**(6), 1063–1077. ISSN 0093-3813. Available at: doi:10.1109/27.125031

FOSTER, John E., 2017. Plasma-based water purification: Challenges and prospects for the future. *Physics of Plasmas* [online]. **24**(5), 055501. ISSN 1070-664X. Available at: doi:10.1063/1.4977921

FRIDMAN, A., A. CHIROKOV and A. GUTSOL, 2005. Non-thermal atmospheric pressure discharges. *Journal of Physics D: Applied Physics* [online]. **38**(2), R1–R24. ISSN 0022-3727. Available at: doi:10.1088/0022-3727/38/2/R01

GAO, Yawen, Mingbo LI, Chao SUN and Xuehua ZHANG, 2022. Microbubble-enhanced water activation by cold plasma. *Chemical Engineering Journal* [online]. **446**(P4), 137318. ISSN 1385-8947. Available at: doi:10.1016/j.cej.2022.137318

GERRITY, Daniel, Benjamin D. STANFORD, Rebecca A. TRENHOLM and Shane A. SNYDER, 2010. An evaluation of a pilot-scale nonthermal plasma advanced oxidation process for trace organic compound degradation. *Water Research* [online]. **44**(2), 493–504. ISSN 0043-1354. Available at: doi:10.1016/j.watres.2009.09.029

GIBALOV, Valentin I and Gerhard J PIETSCH, 2004a. Dynamics of dielectric barrier discharges in coplanar arrangements. *Journal of Physics D: Applied Physics* [online]. **37**(15), 2082–2092. ISSN 0022-3727. Available at: doi:10.1088/0022-3727/37/15/006

GIBALOV, Valentin I and Gerhard J PIETSCH, 2004b. Properties of dielectric barrier discharges in extended coplanar electrode systems. *Journal of Physics D: Applied Physics* [online]. **37**(15), 2093–2100. ISSN 0022-3727. Available at: doi:10.1088/0022-3727/37/15/007

GIBALOV, Valentin I and Gerhard J PIETSCH, 2012. Dynamics of dielectric barrier discharges in different arrangements. *Plasma Sources Science and Technology* [online]. **21**(2), 024010. ISSN 0963-0252. Available at: doi:10.1088/0963-0252/21/2/024010

GORBANEV, Y., C. C. W. VERLACKT, S. TINCK, E. TUENTER, K. FOUBERT, P. COS and A. BOGAERTS, 2018a. Combining experimental and modelling approaches to study the sources of reactive species induced in water by the COST RF plasma jet. *Physical Chemistry Chemical Physics* [online]. **20**(4), 2797–2808. ISSN 1463-9076. Available at: doi:10.1039/C7CP07616A

GORBANEV, Yury, Angela PRIVAT-MALDONADO and Annemie BOGAERTS, 2018b. Analysis of Short-Lived Reactive Species in Plasma–Air–Water Systems: The Dos and the Do Nots. *Analytical Chemistry* [online]. **90**(22), 13151–13158. ISSN 0003-2700. Available at: doi:10.1021/acs.analchem.8b03336

GRAVES, David B., 2012. The emerging role of reactive oxygen and nitrogen species in redox biology and some implications for plasma applications to medicine and biology. *Journal of Physics D: Applied Physics* [online]. **45**(26). ISSN 0022-3727. Available at: doi:10.1088/0022-3727/45/26/263001

GRAVES, David B., Lars B. BAKKEN, Morten B. JENSEN and Rune INGELS, 2019. Plasma Activated Organic Fertilizer. *Plasma Chemistry and Plasma Processing* [online]. **39**(1), 1–19. ISSN 0272-4324. Available at: doi:10.1007/s11090-018-9944-9

GROSSE, K., M. FALKE and A. VON KEUDELL, 2021. Ignition and propagation of nanosecond pulsed plasmas in distilled water - Negative vs positive polarity applied to a pin electrode. *Journal of Applied Physics* [online]. **129**(21), 213302. ISSN 1089-7550. Available at: doi:10.1063/5.0045697

GROSSE, K., J. HELD, M. KAI and A. VON KEUDELL, 2019. Nanosecond plasmas in water: Ignition, cavitation and plasma parameters. *Plasma Sources Science and Technology* [online]. **28**(8), 085003. ISSN 1361-6595. Available at: doi:10.1088/1361-6595/ab26fc

HEGEMANN, Dirk and Sandra GAISER, 2022. Plasma surface engineering for manmade soft materials: a review. *Journal of Physics D: Applied Physics* [online]. **55**(17), 173002. ISSN 0022-3727. Available at: doi:10.1088/1361-6463/ac4539

HODER, T., M. ŠÍRA, K. V. KOZLOV and H.-E. WAGNER, 2009. 3D Imaging of the Single Microdischarge Development in Coplanar Barrier Discharges in Synthetic Air at Atmospheric Pressure. *Contributions to Plasma Physics* [online]. **49**(6), 381–387. ISSN 1521-3986. Available at: doi:10.1002/ctpp.200910035

HODER, T, P SYNEK, D CHORVÁT, J RÁHEL', R BRANDENBURG and M ČERNÁK, 2017. Complex interaction of subsequent surface streamers via deposited charge: a high-resolution experimental study. *Plasma Physics and Controlled Fusion* [online]. **59**(7), 074001. ISSN 0741-3335. Available at: doi:10.1088/1361-6587/aa6ea2

HODER, Tomáš. *High-resolution Spectroscopy of Transient Micro-Plasmas: Discharge Mechanisms and Electric Field Determination*. [online]. Habilitation thesis. Brno: Masaryk University. 2017. Available from: https://www.muni.cz/inet-doc/1363591

HOFFER, Petr, Petr BÍLEK, Václav PRUKNER, Zdeněk BONAVENTURA and Milan ŠIMEK, 2022. Dynamics of macro- and micro-bubbles induced by nanosecond discharge in liquid water. *Plasma Sources Science and Technology* [online]. **31**(1). ISSN 1361-6595. Available at: doi:10.1088/1361-6595/ac3bd6

IVKOVIĆ, Saša S, Goran B. SRETENOVIĆ, Bratislav M. OBRADOVIĆ, Nikola CVETANOVIĆ and Milorad M. KURAICA, 2014. On the use of the intensity ratio of He lines for electric field measurements in atmospheric pressure dielectric barrier discharge. *Journal of Physics D: Applied Physics* [online]. **47**(5), 055204. ISSN 0022-3727. Available at: doi:10.1088/0022-3727/47/5/055204

JANČULA, Daniel, Přemysl MIKULA, Blahoslav MARŠÁLEK, Pavel RUDOLF and František POCHYLÝ, 2014. Selective method for cyanobacterial bloom removal: hydraulic jet cavitation experience. *Aquaculture International* [online]. **22**(2), 509–521. ISSN 0967-6120. Available at: doi:10.1007/s10499-013-9660-7

JANDA, Mario, Viktor MARTIŠOVITŠ and Zdenko MACHALA, 2011. Transient spark: a dc-driven repetitively pulsed discharge and its control by electric circuit parameters. *Plasma Sources Science and Technology* [online]. **20**(3), 035015. ISSN 0963-0252. Available at: doi:10.1088/0963-0252/20/3/035015

JANDA, Mario, Augusto STANCAMPIANO, Francesco DI NATALE and Zdenko MACHALA, 2025. Short Review on Plasma–Aerosol Interactions. *Plasma Processes and Polymers* [online]. **22**(1). ISSN 1612-8850. Available at: doi:10.1002/ppap.202400275

JIANG, Bo, Jingtang ZHENG, Shi QIU, Mingbo WU, Qinhui ZHANG, Zifeng YAN and Qingzhong XUE, 2014. Review on electrical discharge plasma technology for wastewater remediation. *Chemical Engineering Journal* [online]. **236**, 348–368. ISSN 1385-8947. Available at: doi:10.1016/j.cej.2013.09.090

KAUSHIK, Nagendra Kumar, Bhagirath GHIMIRE, Ying LI, Manish ADHIKARI, Mayura VEERANA, Neha KAUSHIK, Nayansi JHA, Bhawana ADHIKARI, Su-Jae LEE, Kai MASUR, Thomas VON WOEDTKE, Klaus-Dieter WELTMANN and Eun Ha CHOI, 2018. Biological and medical applications of plasma-activated media, water and solutions. *Biological Chemistry* [online]. **400**(1), 39–62. ISSN 1437-4315. Available at: doi:10.1515/hsz-2018-0226

KOGELSCHATZ, U, 2010. Collective phenomena in volume and surface barrier discharges. *Journal of Physics: Conference Series* [online]. **257**, 012015. ISSN 1742-6596. Available at: doi:10.1088/1742-6596/257/1/012015

KOGELSCHATZ, U, B ELIASSON and W EGLI, 1997. Dielectric-Barrier Discharges. Principle and Applications. *Le Journal de Physique IV* [online]. **07**(C4), C4-47-C4-66. ISSN 1155-4339. Available at: doi:10.1051/jp4:1997405

KOGELSCHATZ, Ulrich, 2003. Dielectric-Barrier Discharges: Their History, Discharge Physics, and Industrial Applications. *Plasma Chemistry and Plasma Processing* [online]. **23**(1), 1–46. ISSN 0272-4324. Available at: doi:10.1023/A:1022470901385

KOZLOV, K V, R BRANDENBURG, H-E WAGNER, a M MOROZOV and P MICHEL, 2005. Investigation of the filamentary and diffuse mode of barrier discharges in N 2 /O 2 mixtures at atmospheric pressure by cross-correlation spectroscopy. *Journal of Physics D: Applied Physics* [online]. **38**(4), 518–529. ISSN 0022-3727. Available at: doi:10.1088/0022-3727/38/4/003

KRČMA, F., Z. KOZÁKOVÁ, V. MAZÁNKOVÁ, J. HORÁK, L. DOSTÁL, B. OBRADOVIĆ, A. NIKIFOROV and T. BELMONTE, 2018. Characterization of novel pin-hole based plasma source for generation of discharge in liquids supplied by DC non-pulsing voltage. *Plasma Sources Science and Technology* [online]. **27**(6), 065001. ISSN 1361-6595. Available at: doi:10.1088/1361-6595/aac521

LIGUORI, Anna, Tommaso GALLINGANI, Dilli Babu PADMANABAN, Romolo LAURITA, Tamilselvan VELUSAMY, Gunisha JAIN, Manuel MACIAS-MONTERO, Davide MARIOTTI and Matteo GHERARDI, 2018. Synthesis of Copper-Based Nanostructures in Liquid Environments by Means of a Non-equilibrium Atmospheric Pressure Nanopulsed Plasma Jet. *Plasma Chemistry and Plasma Processing* [online]. **38**(6), 1209–1222. ISSN 0272-4324. Available at: doi:10.1007/s11090-018-9924-0

LOCKE, Bruce R. and Kai-Yuan SHIH, 2011. Review of the methods to form hydrogen peroxide in electrical discharge plasma with liquid water. *Plasma Sources Science and Technology* [online]. **20**(3), 034006. ISSN 0963-0252. Available at: doi:10.1088/0963-0252/20/3/034006

LOCKE, Bruce R., Selma Mededovic THAGARD and Petr LUKES, 2025. Recent Insights Into Interfacial Transport and Chemical Reactions of Plasma-Generated Species in Liquid. *Plasma Processes and Polymers* [online]. **22**(1). ISSN 1612-8850. Available at: doi:10.1002/ppap.202400207

LUKES, P., M. CLUPEK, V. BABICKY, E. SPETLIKOVA, I. SISROVA, E. MARSALKOVA and B. MARSALEK, 2013. High power DC diaphragm discharge excited in a vapor bubble for the treatment of water. *Plasma Chemistry and Plasma Processing* [online]. **33**(1), 83–95. ISSN 0272-4324. Available at: doi:10.1007/s11090-012-9432-6

MACHALA, Z., B. TARABOVÁ, D. SERSENOVÁ, M. JANDA and K. HENSEL, 2019. Chemical and antibacterial effects of plasma activated water: correlation with gaseous and aqueous reactive oxygen and nitrogen species, plasma sources and air flow conditions. *Journal of Physics D: Applied Physics* [online]. **52**(3), 034002. ISSN 0022-3727. Available at: doi:10.1088/1361-6463/aae807

MAGUREANU, M., F. BILEA, C. BRADU and D. HONG, 2021. A review on non-thermal plasma treatment of water contaminated with antibiotics. *Journal of Hazardous Materials* [online]. **417**(December 2020), 125481. ISSN 1873-3336. Available at: doi:10.1016/j.jhazmat.2021.125481

MARIOTTI, Davide, Jenish PATEL, Vladimir ŠVRČEK and Paul MAGUIRE, 2012. Plasma–Liquid Interactions at Atmospheric Pressure for Nanomaterials Synthesis and Surface Engineering. *Plasma Processes and Polymers* [online]. **9**(11–12), 1074–1085. ISSN 1612-8850. Available at: doi:10.1002/ppap.201200007

MASSINES, F., N. GHERARDI, N. NAUDÉ and P. SÉGUR, 2009. Recent advances in the understanding of homogeneous dielectric barrier discharges. *The European Physical Journal Applied Physics* [online]. **47**(02), 22805. ISSN 1286-0042. Available at: doi:10.1051/epjap/2009064

MIKLOS, David B., Christian REMY, Martin JEKEL, Karl G. LINDEN, Jörg E. DREWES and Uwe HÜBNER, 2018. Evaluation of advanced oxidation processes for water and wastewater treatment – A critical review. *Water Research* [online]. **139**, 118–131. ISSN 0043-1354. Available at: doi:10.1016/j.watres.2018.03.042

MONTALBETTI, Roberto, Zdenko MACHALA, Matteo GHERARDI and Romolo LAURITA, 2025. "Production and Chemical Composition of Plasma Activated Water: A Systematic Review and Meta-Analysis." *Plasma Processes and Polymers* [online]. **22**(1). ISSN 1612-8850. Available at: doi:10.1002/ppap.202400249

MOREAU, Eric, 2007. Airflow control by non-thermal plasma actuators. *Journal of Physics D: Applied Physics* [online]. **40**(3), 605–636. ISSN 0022-3727. Available at: doi:10.1088/0022-3727/40/3/S01

ODEHNALOVÁ, Klára, Jan ČECH, Eliška MARŠÁLKOVÁ, Pavel SŤAHEL, Barbora MAYER, Vinicius Tadeu SANTANA, Pavel RUDOLF and Blahoslav MARŠÁLEK, 2024. Exploring the dynamics of reactive oxygen species from CaviPlasma and their disinfection and degradation potential — the case of cyanobacteria and cyanotoxins. *Environmental Science and Pollution Research* [online]. **32**(2), 849–863. ISSN 1614-7499. Available at: doi:10.1007/s11356-024-35803-4

PARK, Hyunjae, Seungryul YOO and Kangil KIM, 2019. Synthesis of Carbon-Coated TiO 2 by Underwater Discharge With Capillary Carbon Electrode. *IEEE Transactions on Plasma Science* [online]. **47**(2), 1482–1486. ISSN 0093-3813. Available at: doi:10.1109/TPS.2019.2892456

PERRIN, L., D. COLOMBET and F. AYELA, 2021. Comparative study of luminescence and chemiluminescence in hydrodynamic cavitating flows and quantitative determination of hydroxyl radicals production. *Ultrasonics Sonochemistry* [online]. **70**(June 2020), 105277. ISSN 1873-2828. Available at: doi:10.1016/j.ultsonch.2020.105277

PUAČ, N. and N. ŠKORO, 2025. Plasma–Liquid Interaction for Agriculture—A Focused Review. *Plasma Processes and Polymers* [online]. **22**(1), 1–17. ISSN 1612-8850. Available at: doi:10.1002/ppap.202400208

RÁHEL', Jozef and Daniel M. SHERMAN, 2005. The transition from a filamentary dielectric barrier discharge to a diffuse barrier discharge in air at atmospheric pressure. *Journal of Physics D: Applied Physics* [online]. **38**(4), 547–554. ISSN 0022-3727. Available at: doi:10.1088/0022-3727/38/4/006

RAHEL, Josef, Jan CECH and Tomas MORAVEK, 2016b. A Treatise on the Diffusiveness of Diffuse Coplanar Surface Barrier Discharge. In: M CERNAK and T HODER, eds. *HAKONE XV: INTERNATIONAL SYMPOSIUM ON HIGH PRESSURE LOW TEMPERATURE PLASMA CHEMISTRY: WITH JOINT COST TD1208 WORKSHOP: NON-EQUILIBRIUM PLASMAS WITH LIQUIDS FOR WATER AND SURFACE TREATMENT*. pp. 92–96. ISBN 978-80-210-8318-9.

RAN, Junxia, Caixia LI, Dong MA, Haiyun LUO and Xiaowei LI, 2018. Homogeneous dielectric barrier discharges in atmospheric air and its influencing factor. *Physics of Plasmas* [online]. **25**(3). ISSN 1070-664X. Available at: doi:10.1063/1.5019989

REZAEI, Fatemeh, Anton NIKIFOROV, Rino MORENT and Nathalie DE GEYTER, 2018. Plasma Modification of Poly Lactic Acid Solutions to Generate High Quality Electrospun PLA Nanofibers. *Scientific Reports* [online]. **8**(1), 2241. ISSN 2045-2322. Available at: doi:10.1038/s41598-018-20714-5

REZAEI, Fatemeh, Patrick VANRAES, Anton NIKIFOROV, Rino MORENT and Nathalie DE GEYTER, 2019. Applications of Plasma-Liquid Systems: A Review. *Materials* [online]. **12**(17), 2751. ISSN 1996-1944. Available at: doi:10.3390/ma12172751

RUDOLF, Pavel, Martin HUDEC, Milan GRÍGER and David ŠTEFAN, 2014. Characterization of the cavitating flow in converging-diverging nozzle based on experimental investigations. *EPJ Web of Conferences* [online]. **67**. ISSN 2100-014X. Available at: doi:10.1051/epjconf/20146702101

RUDOLF, Pavel, František POCHYLÝ, Pavel ST'AHEL, Jozef RÁHEL, Jan ČECH and Blahoslav MARŠÁLEK, 2019. Apparatus for purifying liquids and a method for purifying liquids using this apparatus. [online]. Czech Republic, CZ 308 532. 2019. Available at: https://isdv.upv.cz/webapp/resdb.print_detail.det?pspis=PT/2019-772&plang=CS

SAEDI, Ziya, Deepak PANCHAL, Qiuyun LU, Muzammil KUDDUSHI, Sina Esfandiar POUR and Xuehua ZHANG, 2025. Integrating multiple cold plasma generators and Bernoulli-driven microbubble formation for large-volume water treatment. *Sustainable Materials and Technologies* [online]. **44**(February), e01300. ISSN 2214-9937. Available at: doi:10.1016/j.susmat.2025.e01300

SAMUKAWA, Seiji, Masaru HORI, Shahid RAUF, Kunihide TACHIBANA, Peter BRUGGEMAN, Gerrit KROESEN, J Christopher WHITEHEAD, Anthony B MURPHY, Alexander F GUTSOL, Svetlana STARIKOVSKAIA, Uwe KORTSHAGEN, Jean-Pierre BOEUF, Timothy J SOMMERER, Mark J KUSHNER, Uwe CZARNETZKI and Nigel MASON, 2012. The 2012 Plasma Roadmap. *Journal of Physics D: Applied Physics* [online]. **45**(25), 253001. ISSN 0022-3727. Available at: doi:10.1088/0022-3727/45/25/253001

SCHÜTTLER, Steffen, Ludwig JOLMES, Emanuel JESS, Kristina TSCHULIK and Judith GOLDA, 2024. Validation of in situ diagnostics for the detection of OH and H 2 O 2 in liquids treated by a humid atmospheric pressure plasma jet. *Plasma Processes and Polymers* [online]. **21**(2). ISSN 1612-8850. Available at: doi:10.1002/ppap.202300079

SHIRAI, Naoki, Goju SUGA and Koichi SASAKI, 2019. Correlation between gas-phase OH density and intensity of luminol chemiluminescence in liquid interacting with atmospheric-pressure plasma. *Journal of Physics D: Applied Physics* [online]. **52**(39), 39LT02. ISSN 1361-6463. Available at: doi:10.1088/1361-6463/ab2ff2

ŠIMEK, M, P F AMBRICO and V PRUKNER, 2011. ICCD microscopic imaging of a single micro-discharge in surface coplanar DBD geometry: determination of the luminous diameter of N2 and Ar streamers. *Plasma Sources Science and Technology* [online]. **20**(2), 025010. ISSN 0963-0252. Available at: doi:10.1088/0963-0252/20/2/025010

ŠIMEK, Milan, Petr HOFFER, Václav PRUKNER and Jiří SCHMIDT, 2020. Disentangling dark and luminous phases of nanosecond discharges developing in liquid water. *Plasma Sources Science and Technology* [online]. **29**(9). ISSN 1361-6595. Available at: doi:10.1088/1361-6595/abac49

ŠIMEK, Milan, Branislav PONGRÁC, Václav BABICKÝ, Martin ČLUPEK and Petr LUKEŠ, 2017. Luminous phase of nanosecond discharge in deionized water: Morphology, propagation velocity and optical emission. *Plasma Sources Science and Technology* [online]. **26**(7), 07LT01. ISSN 1361-6595. Available at: doi:10.1088/1361-6595/aa758d

ŠIMOR, Marcel, Jozef RÁHEL', Pavel VOJTEK, Mirko ČERNÁK and Antonín BRABLEC, 2002. Atmospheric-pressure diffuse coplanar surface discharge for surface treatments. *Applied Physics Letters* [online]. **81**(15), 2716. ISSN 0003-6951. Available at: doi:10.1063/1.1513185

STANCAMPIANO, Augusto, Tommaso GALLINGANI, Matteo GHERARDI, Zdenko MACHALA, Paul MAGUIRE, Vittorio COLOMBO, Jean-Michel POUVESLE and Eric ROBERT, 2019. Plasma and Aerosols: Challenges, Opportunities and Perspectives. *Applied Sciences* [online]. **9**(18), 3861. ISSN 2076-3417. Available at: doi:10.3390/app9183861

STEFAN, Mihaela I., 2017. Advanced Oxidation Processes for Water Treatment - Fundamentals and Applications. *Water Intelligence Online* [online]. **16**. ISSN 1476-1777. Available at: doi:10.2166/9781780407197

ŠTIPL, Michal. *Studium mobility mikrovýbojů dielektrického bariérového výboje* [online]. Master's thesis. Brno: Masaryk University, Faculty of Science. 2019. Available from: https://is.muni.cz/th/vpau3/

ŠUNKA, P., V. BABICKÝ, M. ČLUPEK, P. LUKEŠ, M. ŠIMEK, J. SCHMIDT and M. ČERNÁK, 1999. Generation of chemically active species by electrical discharges in water. *Plasma Sources Science and Technology* [online]. **8**(2), 258–265. ISSN 0963-0252. Available at: doi:10.1088/0963-0252/8/2/006

THIRUMDAS, Rohit, Anjinelyulu KOTHAKOTA, Uday ANNAPURE, Kaliramesh SILIVERU, Renald BLUNDELL, Ruben GATT and Vasilis P. VALDRAMIDIS, 2018. Plasma activated water (PAW): Chemistry, physico-chemical properties, applications in food and agriculture. *Trends in Food Science and Technology* [online]. **77**(September 2017), 21–31. ISSN 0924-2244. Available at: doi:10.1016/j.tifs.2018.05.007

TOPOLOVEC, Barbara, Nikola ŠKORO, Nevena PUAČ and Mira PETROVIC, 2022. Pathways of organic micropollutants degradation in atmospheric pressure plasma processing – A review. *Chemosphere* [online]. **294**, 1–56. ISSN 1879-1298. Available at: doi:10.1016/j.chemosphere.2022.133606

TSCHIERSCH, R, S NEMSCHOKMICHAL, M BOGACZYK and J MEICHSNER, 2017. Surface charge measurements on different dielectrics in diffuse and filamentary barrier discharges. *Journal of Physics D: Applied Physics* [online]. **50**(10), 105207. ISSN 0022-3727. Available at: doi:10.1088/1361-6463/aa5605

VANRAES, Patrick and Annemie BOGAERTS, 2018. Plasma physics of liquids - A focused review. *Applied Physics Reviews* [online]. **5**(3). ISSN 1931-9401. Available at: doi:10.1063/1.5020511

VON WOEDTKE, Thomas, Sander BEKESCHUS, Klaus-Dieter WELTMANN and Kristian WENDE, 2025. Plasma-Treated Liquids for Medicine: A Narrative Review on State and Perspectives. *Plasma Processes and Polymers* [online]. **22**(1). ISSN 1612-8850. Available at: doi:10.1002/ppap.202400255

VORÁČ, Jan, Petr SYNEK, Lucia POTOČŇÁKOVÁ, Jaroslav HNILICA and Vít KUDRLE, 2017a. Batch processing of overlapping molecular spectra as a tool for spatio-temporal diagnostics of power modulated microwave plasma jet. *Plasma Sources Science and Technology* [online]. **26**(2), 025010. ISSN 1361-6595. Available at: doi:10.1088/1361-6595/aa51f0

VORÁČ, Jan, Petr SYNEK, Vojtěch PROCHÁZKA and Tomáš HODER, 2017b. State-by-state emission spectra fitting for non-equilibrium plasmas: OH spectra of surface barrier discharge at argon/water interface. *Journal of Physics D: Applied Physics* [online]. **50**(29), 294002. ISSN 1361-6463. Available at: doi:10.1088/1361-6463/aa7570

VOZÁROVÁ, Lenka. *Studium slabých optických signálů pomocí statistického zpracování dat z ICCD kamery* [online]. Bachelor's thesis. Brno: Masaryk University, Faculty of Science. 2020. Available from: https://is.muni.cz/th/ynsyh/

WAGNER, H.-E., R. BRANDENBURG, K.V. KOZLOV, a. SONNENFELD, P. MICHEL and J.F. BEHNKE, 2003. The barrier discharge: basic properties and applications to surface treatment. *Vacuum* [online]. **71**(3), 417–436. ISSN 0042-207X. Available at: doi:10.1016/S0042-207X(02)00765-0

WANG, Sitao, Zhijie LIU, Xin LI, Hezhi GUO, Zekai ZHANG, Bolun PANG, Yuting GAO, Patrick J. CULLEN and Renwu ZHOU, 2025. Development of pilot-scale plasma bubble reactors for efficient antibiotics removal in wastewater. *Environmental Research* [online]. **264**(P1), 120310. ISSN 1096-0953. Available at: doi:10.1016/j.envres.2024.120310

WASSELIN-TRUPIN, V., G. BALDACCHINO, S. BOUFFARD, E. BALANZAT, M. GARDÈS-ALBERT, Z. ABEDINZADEH, D. JORE, S. DEYCARD and B. HICKEL, 2000. A New Method for the Measurement of Low Concentrations of OH/O 2 - Radical Species in Water by High-LET Pulse Radiolysis. A Time-Resolved Chemiluminescence Study. *The Journal of Physical Chemistry A* [online]. **104**(38), 8709–8714. ISSN 1089-5639. Available at: doi:10.1021/jp000462z

WELTMANN, Klaus-Dieter, Juergen F. KOLB, Marcin HOLUB, Dirk UHRLANDT, Milan ŠIMEK, Kostya (Ken) OSTRIKOV, Satoshi HAMAGUCHI, Uroš CVELBAR, Mirko ČERNÁK, Bruce LOCKE, Alexander FRIDMAN, Pietro FAVIA and Kurt BECKER, 2019. The future for plasma science and technology. *Plasma Processes and Polymers* [online]. **16**(1), 1800118. ISSN 1612-8850. Available at: doi:10.1002/ppap.201800118

WELTMANN, Klaus Dieter, Eckhard KINDEL, Thomas VON WOEDTKE, Marcel HÄHNEL, Manfred STIEBER and Ronny BRANDENBURG, 2010. Atmospheric-pressure plasma sources: Prospective tools for plasma medicine. *Pure and Applied Chemistry* [online]. **82**(6), 1223–1237. ISSN 0033-4545. Available at: doi:10.1351/PAC-CON-09-10-35

YAYCI, Abdulkadir, Álvaro Gómez BARAIBAR, Marco KREWING, Elena Fernandez FUEYO, Frank HOLLMANN, Miguel ALCALDE, Robert KOURIST and Julia E. BANDOW, 2020. Plasma-Driven in Situ Production of Hydrogen Peroxide for Biocatalysis. *ChemSusChem* [online]. **13**(8), 2072–2079. ISSN 1864-5631. Available at: doi:10.1002/cssc.201903438

Bibliography: List of Annotated Papers

Sorted organically in order of appearance in the thesis.

CECH, Jan*(corresponding author)*, Pavel STAHEL, Zdenek NAVRATIL and Mirko CERNAK, 2008. Space and Time Resolved Optical Emission Spectroscopy of Diffuse Coplanar Barrier Discharge in Nitrogen. *Chemicke Listy*. **102**(S4), S1348-S1351. ISSN 1213-7103.

CECH, J.*(corresponding author)*, P. STAHEL and Z. NAVRATIL, 2009. The influence of electrode gap width on plasma properties of diffuse coplanar surface barrier discharge in nitrogen. *European Physical Journal D* [online]. **54**(2), 259–264. ISSN 1434-6079. Available at: doi:10.1140/epjd/e2009-00013-1

CECH, Jan*(corresponding author)*, Jana HANUSOVA, Pavel ST'AHEL and Mirko CERNAK, 2015. Diffuse Coplanar Surface Barrier Discharge in Artificial Air: Statistical Behaviour of Microdischarges. *Open Chemistry* [online]. **13**(1), 528–540. ISSN 2391-5420. Available at: doi:10.1515/chem-2015-0062

RAHEL, Jozef, Zsolt SZALAY, **Jan CECH** and Tomas MORAVEK, 2016. On spatial stabilization of dielectric barrier discharge microfilaments by residual heat build-up in air. *European Physical Journal D* [online]. **70**(4, Article 92). ISSN 1434-6079. Available at: doi:10.1140/epjd/e2016-70061-5

MORAVEK, Tomas, **Jan CECH**, Zdenek NAVRATIL and Jozef RAHEL, 2016. Pre-breakdown phase of coplanar dielectric barrier discharge in helium. *European Physical Journal-Applied Physics* [online]. **75**(2, Article 24706). ISSN 1286-0050. Available at: doi:10.1051/epjap/2016150538

NAVRATIL, Zdenek, Tomas MORAVEK, Jozef RAHEL, **Jan CECH**, Ondrej LALINSKY and David TRUNEC, 2017. Diagnostics of pre-breakdown light emission in a helium coplanar barrier discharge: the presence of neutral bremsstrahlung. *Plasma Sources Science & Technology* [online]. **26**(5, Article 055025). ISSN 1361-6595. Available at: doi:10.1088/1361-6595/aa66b5

CECH, Jan*(corresponding author)*, Zdenek NAVRATIL, Michal STIPL, Tomas MORAVEK and Jozef RAHEL, 2018. 2D-resolved electric field development in helium coplanar DBD: spectrally filtered ICCD camera approach. *Plasma Sources Science & Technology* [online]. **27**(10, Article 105002). ISSN 1361-6595. Available at: doi:10.1088/1361-6595/aade41

PRYSIAZHNYI, V., A. BRABLEC, **J. CECH**, M. STUPAVSKA and M. CERNAK, 2014. Generation of Large-Area Highly-Nonequlibrium Plasma in Pure Hydrogen at Atmospheric Pressure. *Contributions to Plasma Physics* [online]. **54**(2), 138–144. ISSN 1521-3986. Available at: doi:10.1002/ctpp.201310060

KROMKA, Alexander, **Jan CECH**, Halyna KOZAK, Anna ARTEMENKO, Tibor IZAK, Jan CERMAK, Bohuslav REZEK and Mirko CERNAK, 2015. Low-temperature hydrogenation of diamond nanoparticles using diffuse coplanar surface barrier discharge at atmospheric pressure. *Physica Status Solidi B-Basic Solid State Physics* [online]. **252**(11), 2602–2607. ISSN 1521-3951. Available at: doi:10.1002/pssb.201552232

CECH, J.*(corresponding author)*, Z. BONAVENTURA, P. STAHEL, M. ZEMANEK, H. DVORAKOVA and M. CERNAK, 2017. Wide-pressure-range coplanar dielectric barrier discharge: Operational characterisation of a versatile plasma source. *Physics of Plasmas* [online]. **24**(1, Article 013504). ISSN 1089-7674. Available at: doi:10.1063/1.4973442

MARSALEK, Blahoslav, Eliska MARSALKOVA, Klara ODEHNALOVA, Frantisek POCHYLY, Pavel RUDOLF, Pavel STAHEL, Jozef RAHEL, **Jan CECH**, Simona FIALOVA and Stepan ZEZULKA, 2020. Removal of Microcystis aeruginosa through the Combined Effect of Plasma Discharge and Hydrodynamic Cavitation. *Water* [online]. **12**(1, Article 8). ISSN 2073-4441. Available at: doi:10.3390/w12010008

CECH, Jan*(corresponding author)*, Pavel STAHEL, Jozef RAHEL, Lubomir PROKES, Pavel RUDOLF, Eliska MARSALKOVA and Blahoslav MARSALEK, 2020. Mass Production of Plasma Activated Water: Case Studies of Its Biocidal Effect on Algae and Cyanobacteria. *Water* [online]. **12**(11, Article 3167). ISSN 2073-4441. Available at: doi:10.3390/w12113167

CECH, J.*(corresponding author)*, P. STAHEL, L. PROKES, D. TRUNEC, R. HORNAK, P. RUDOLF, B. MARSALEK, E. MARSALKOVA, P. LUKES, A. LAVRIKOVA and Z. MACHALA, 2024. CaviPlasma: parametric study of discharge parameters of high-throughput water plasma treatment technology in glow-like discharge regime. *Plasma Sources Science & Technology* [online]. **33**(11, Article 115005). ISSN 1361-6595. Available at: doi:10.1088/1361-6595/ad7e4e

CECH, J., P. STAHEL, L. PROKES, D. TRUNEC, R. HORNAK, P. RUDOLF, B. MARSALEK, E. MARSALKOVA and P. LUKES, 2025. Glow discharge in water cavitation cloud with improved efficiency for hydrogen peroxide production. *Plasma Sources Science & Technology* [online]. **34**(6, Article 065009). ISSN 1361-6595. Available at: doi:10.1088/1361-6595/addf79

HORNAK, Radek, **Jan CECH*(corresponding author)***, Pavel ST'AHEL, Lubomir PROKES, David TRUNEC, Pavel RUDOLF and Blahoslav MARSALEK, 2025. Spatial Mapping of OH Radicals Produced by Electric Discharge in Hydrodynamic Cavitation Cloud. *Journal of Physical Chemistry Letters* [online]. **16**(25), 6279–6285. ISSN 1948-7185. Available at: doi:10.1021/acs.jpclett.5c00979

List of Author's Publications Without Annotated Papers

Sorted chronologically, newest first

ODEHNALOVÁ, Klára, **Jan ČECH**, Eliška MARŠÁLKOVÁ, Pavel SŤAHEL, Barbora MAYER, Vinicius Tadeu SANTANA, Pavel RUDOLF and Blahoslav MARŠÁLEK, 2025. Exploring the dynamics of reactive oxygen species from CaviPlasma and their disinfection and degradation potential — the case of cyanobacteria and cyanotoxins. *Environmental Science and Pollution Research* [online]. **32**(2), 849–863. ISSN 0944-1344. Available at: doi:10.1007/s11356-024-35803-4

MAZANKOVA, Vera, Pavel STAHEL, Petra MATOUSKOVA, Antonin BRABLEC, **Jan CECH**, Lubomir PROKES, Vilma BURSIKOVA, Monika STUPAVSKA, Marian LEHOCKY, Kadir OZALTIN, Petr HUMPOLICEK and David TRUNEC, 2020. Atmospheric Pressure Plasma Polymerized 2-Ethyl-2-oxazoline Based Thin Films for Biomedical Purposes. *Polymers* [online]. **12**(11, Article 2679). ISSN 2073-4360. Available at: doi:10.3390/polym12112679

DVORAKOVA, Hana, **Jan CECH*(corresponding author)***, Monika STUPAVSKA, Lubomir PROKES, Jana JURMANOVA, Vilma BURSIKOVA, Jozef RAHEL' and Pavel ST'AHEL, 2019. Fast Surface Hydrophilization via Atmospheric Pressure Plasma Polymerization for Biological and Technical Applications. *Polymers* [online]. **11**(10, Article 1613). ISSN 2073-4360. Available at: doi:10.3390/polym11101613

KRUMPOLEC, Richard, **Jan CECH**, Jana JURRRIANOVA, Pavol DURINA and Mirko CERNAK, 2017. Atmospheric pressure plasma etching of silicon dioxide using diffuse coplanar surface barrier discharge generated in pure hydrogen. *Surface & Coatings Technology* [online]. **309**, 301–308. ISSN 0257-8972. Available at: doi:10.1016/j.surfcoat.2016.11.036

CECH, Jan, Antonin BRABLEC, Mirko CERNAK, Nevena PUAC, Nenad SELAKOVIC and Zoran Lj. PETROVIC, 2017. Mass spectrometry of diffuse coplanar surface barrier discharge: influence of discharge frequency and oxygen content in N2/O2 mixture. *European Physical Journal D* [online]. **71**(2, Article 27). ISSN 1434-6079. Available at: doi:10.1140/epjd/e2016-70607-5

JIRASEK, Vit, **Jan CECH**, Halyna KOZAK, Anna ARTEMENKO, Mirko CERNAK and Alexander KROMKA, 2016. Plasma treatment of detonation and HPHT nanodiamonds in diffuse coplanar surface barrier discharge in H2/N2 flow. *Physica Status Solidi A-Applications and Materials Science* [online]. **213**(10), 2680–2686. ISSN 1862-6319. Available at: doi:10.1002/pssa.201600184

KELAR, Jakub, **Jan CECH** and Pavel SLAVICEK, 2015. Energy Efficiency of Planar Discharge for Industrial Applications. *Acta Polytechnica* [online]. **55**(2), 109–112. ISSN 1805-2363. Available at: doi:10.14311/Ap.2015.55.0109

CECH, Jan*(corresponding author)*, Miroslav ZEMANEK, Pavel STAHEL, Hana DVORAKOVA and Mirko CERNAK, 2014. Influence of Substrate Thickness on Diffuse Coplanar Surface Barrier Discharge Properties. *Acta Polytechnica* [online]. **54**(6), 383–388. ISSN 1805-2363. Available at: doi:10.14311/Ap.2014.54.0383

PAVLINAK, D., O. GALMIZ, M. ZEMANEK, A. BRABLEC, **J. CECH** and M. CERNAK, 2014. Permanent hydrophilization of outer and inner surfaces of polytetrafluoroethylene tubes using ambient air plasma generated by surface dielectric barrier discharges. *Applied Physics Letters* [online]. **105**(15, Article 154102). ISSN 1077-3118. Available at: doi:10.1063/1.4898134

CECH, Jan*(corresponding author)*, Jana HANUSOVA, Pavel STAHEL and Pavel SLAVICEK, 2013. Diffuse Coplanar Surface Barrier Discharge in Nitrogen: Microdischarges Statistical Behavior. *Acta Polytechnica*. **53**(2), 127–130. ISSN 1805-2363.

CECH, Jan*(corresponding author)*, Jana HANUSOVA and Pavel STAHEL, 2012. Diagnostics of Diffuse Coplanar Surface Barrier Discharge Operated in Artificial Air Working Gas: Basic Results. *Chemicke Listy*. **106**(S5), S1435-S1438. ISSN 0009-2770.

STAHEL, Pavel, Vilma BURSIKOVA, **Jan CECH**, Zdenek NAVRATIL and Petr KLOC, 2011. Deposition and Characterization of Thin Hydrophobic Layers Using Atmospheric-Pressure Surface Barrier Discharge. *Chemicke Listy*. **105**(S2), S129-S131. ISSN 1213-7103.

LEHOCKY, Marian, Pavel ST'AHEL, Marek KOUTNY, **Jan CECH**, Jakub INSTITORIS and Ales MRACEK, 2009. Adhesion of Rhodococcus sp S3E2 and Rhodococcus sp S3E3 to plasma prepared Teflon-like and organosilicon surfaces. *Journal of Materials Processing Technology* [online]. **209**(6), 2871–2875. ISSN 0924-0136. Available at: doi:10.1016/j.jmatprotec.2008.06.042

VRAJOVA, J., L. CHALUPOVA, O. NOVOTNY, **J. CECH**, F. KRCMA and P. STAHEL, 2009. Removal of paper microbial contamination by atmospheric pressure DBD discharge. *European Physical Journal D* [online]. **54**(2), 233–237. ISSN 1434-6060. Available at: doi:10.1140/epjd/e2009-00127-4

STAHEL, P., V. BURSIKOVA, J. BURSIK, **J. CECH**, J. JANCA and M. CERNAK, 2008. Hydrophylisation of non-woven polypropylene textiles using atmospheric pressure surface barrier discharge. *Journal of Optoelectronics and Advanced Materials*. **10**(1), 213–218. ISSN 1841-7132.

VRAJOVA, J., L. CHALUPOVA, **J. CECH**, F. KRCMA and P. STAHEL, 2008. Paper Sterilization by Atmospheric Pressure DBD Discharge. *Chemicke Listy*. **102**(S4), S1445-S1449. ISSN 0009-2770.

CECH, J.*(corresponding author)*, A. BRABLEC, P. STAHEL and M. CERNAK, 2006. The influence of dielectric layer on the plasma parameters of atmospheric pressure coplanar discharge. *Czechoslovak Journal of Physics* [online]. **56**(6), B1074-B1078. ISSN 0011-4626. Available at: doi:10.1007/s10582-006-0329-6

TRUNEC, D., Z NAVRÁTIL, P. STAHEL, L. ZAJÍCKOVÁ, V. BURSÍKOVÁ and **J. CECH**, 2004. Deposition of thin organosilicon polymer films in atmospheric pressure glow discharge. *Journal of Physics D-Applied Physics* [online]. **37**(15), 2112–2120. ISSN 1361-6463. Available at: doi:10.1088/0022-3727/37/15/010

CECH, J., P. STAHEL, M. SÍRA, V. BURSÍKOVÁ, Z. NAVRÁTIL, D. TRUNEC and A. BRABLEC, 2004. Thermal stability of coatings prepared in atmospheric pressure glow discharge. *Czechoslovak Journal of Physics*. **54**(5), C872-C876. ISSN 0011-4626.

Book chapter:

SKÁCELOVÁ, Dana, Dušan KOVÁČIK, Tomáš HOMOLA, **Jan ČECH** and Mirko ČERNÁK, 2016. Surface Modification of Paper and Paperboards Using Atmospheric Pressure Plasma. In: PARKER, Margaret. *Atmospheric pressure plasmas: Processes, technology and applications*. New York: Nova Science Publishers, Inc., p. 227-236. ISBN 978-1-63485-180-0.

Appendix – Full Texts of the Annotated Articles

The content of this Appendix is not included in the public version of the thesis due to the copyright restrictions on the annotated articles.